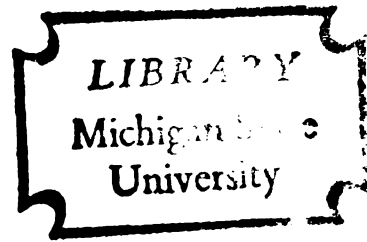


MICROENVIRONMENTAL MODIFICATION BY SMALL
WATER DROPLET EVAPORATION

Thesis for the Degree of Ph. D.
MICHIGAN STATE UNIVERSITY
FRED VERNON NURNBERGER
1972



This is to certify that the
thesis entitled
MICROENVIRONMENTAL MODIFICATION BY
SMALL WATER DROPLET EVAPORATION
presented by
FRED VERNON NURNBERGER

has been accepted towards fulfillment
of the requirements for

Ph.D. degree in Agricultural Engineering

George E. Meria
major professor

Date Nov 8, 1972

~~5500~~ 072

~~192~~

R-274

~~2980~~ 06

ABSTRACT

MICROENVIRONMENTAL MODIFICATION BY SMALL WATER DROPLET EVAPORATION

By

Fred Vernon Nurnberger

The relief of heat and moisture stress on actively growing plants is a major concern to agriculturists and horticulturists. To date, sprinkler irrigation has been the primary mode of stress condition relief. The current investigation proposes a different method whereby small water droplets are sprayed into the air and allowed to evaporate before reaching the lower surface.

The objectives of this investigation were to:

(1) develop a mathematical model for the droplet evaporation modification process; (2) experimentally verify the model; and (3) use the model to predict modifications for various atmospheric conditions and spray rates. The model was developed for modification over bare soil conditions to facilitate experimental verification over known lower boundary conditions.

An evaporation coefficient was developed from the literature to provide liquid water evaporation proportional to the saturated water vapor concentration deficit. The

exponential wind profile law, Swinbank (1964), and similarity profiles of temperature and water vapor concentration were used.

The numerical solution technique utilized was the miniature control volume integral equation method proposed by Spalding and Patankar (1968).

Experimental verification was performed over a bared strip of land at the Michigan State University Experimental Muck Farm. Water droplets were sprayed into the air from a 300 m long elevated line at a height of 1 m. Measurements of the profiles of wind speed, and dry and wet bulb temperatures were made upstream and downstream from the spray line. Other measurements included net radiation, wind direction, soil heat flux, and soil temperature.

The Swinbank profile for wind speed was found to be appropriate but the similarity initial profiles for temperature and water vapor concentration exhibited some error. The agreement between the measured and model results was very good for the ratio of turbulent diffusivities suggested by Leichtman and Ponomareva (1969).

The maximum predicted cooling for the various atmospheric conditions and spray rates investigated was -14.5°C . The method proposed does warrant further investigation with the influence of a plant canopy included.

References

Leichtman, D. L. and Ponomareva, S. M., (1969). On the ratio of the Turbulent Transfer Coefficients for Heat and Momentum in the Surface Layer of the Atmosphere, *Izves., Atmos. and Ocean. Phys.*, Vol. 5, No. 12, 1245-1250.

Spalding, D. B. and Patankar, S. V., (1968). Heat and Mass Transfer in Boundary Layers, 138 pp., C. R. C. Press, Cleveland.

Swinbank, W. C., (1964). The Exponential Wind Profile, *Quart. Jour. Roy. Meteor. Soc.*, Vol. 90, No. 384, 119-135.

Approved George E. Merva
Major Professor

Approved B A Stout
Department Chairman

MICROENVIRONMENTAL MODIFICATION BY
SMALL WATER DROPLET EVAPORATION

By

Fred Vernon Nurnberger

A THESIS

Submitted to
Michigan State University
in partial fulfillment of the requirements
for the degree of

DOCTOR OF PHILOSOPHY

Department of Agricultural Engineering

1972

© 1994

To Hazle

ACKNOWLEDGMENTS

The author wishes to thank Dr. James B. Harrington, Jr. under whose guidance this project was conceived and developed. A special thanks to Dr. George E. Merva (Agricultural Engineering) for serving as the guidance committee chairman and for his many hours of invaluable Russian translation.

Thanks to Dr. A. M. Dhanak (Mechanical Engineering), Dr. R. C. Hamelink (Mathematics), and Prof. E. H. Kidder (Agricultural Engineering) for serving on the guidance committee.

A final thank you to all my fellow graduate students, family and friends who "volunteered" to help with the many tasks of the field experiment.

TABLE OF CONTENTS

	Page
DEDICATION	ii
ACKNOWLEDGMENTS	iii
LIST OF TABLES	vi
LIST OF FIGURES	viii
LIST OF APPENDICES	xi
LIST OF SYMBOLS	xii
 Chapter	
1. INTRODUCTION	1
2. LITERATURE REVIEW	4
2.1 Scope of Literature Review	4
2.2 Selection of Technique	4
2.3 Relevant Parameters	5
2.4 Atmospheric Diffusion Models	10
2.5 Evaporation Models	13
3. THEORETICAL MODEL DEVELOPMENT	22
3.1 Diffusion Equation	22
3.2 Initial Conditions	24
3.3 Source Terms	27
3.4 Boundary Conditions	31
3.4.1 Lower Boundary Conditions	31
3.4.2 Upper Boundary Conditions	32
4. SOLUTION TECHNIQUE	33
4.1 Method	33
4.2 Development of the Finite Difference Equations	36
4.3 Parameter Evaluation	43
4.4 Solution Procedure	55

Chapter	Page
5. EXPERIMENTAL PROCEDURE.	57
5.1 Site Selection	57
5.2 Water Supply System	58
5.3 Instrumentation.	59
5.3.1 Profile Measurements	59
5.3.2 Other Measurements.	66
6. EXPERIMENTAL RESULTS	68
6.1 Test Conditions.	68
6.2 Wind Speed and Direction.	68
6.3 Net Radiation, Soil Heat Flux, and Sensible Heat Flux	72
6.4 Temperature and Moisture Measurements	72
6.4.1 Initial Conditions.	72
6.4.2 Modified Conditions	76
7. MODEL PREDICTION.	100
8. DISCUSSION.	111
9. CONCLUSIONS	116
APPENDICES	117
LIST OF REFERENCES.	173

LIST OF TABLES

Table	Page
2.5.1 Constants for the evaporation kinetics of water drops, (cgs units)	19
3.3.1 A comparison of values calculated from Equation (3.3.3) and the volume formula for a sphere for various droplet radii, a. . . .	29
4.3.1 A summary of the general Spalding-Patankar symbols and the specific symbols of the equations to be solved.	44
4.3.2 A summary of the variability in the moist air parameters for the temperature and moisture range pertinent to the model being developed and for P=1000 mb	47
6.2.1 The 30 minute average wind direction and mast positions relative to the spray line	69
6.4.2.1 Sum of the squared errors using Swinbanks similarity profiles as initial conditions	87
6.4.2.2 Sum of the squared errors using linearized initial conditions	98
7.1 A summary of the values of L , T_i , u_i , and the spray rate used in the prediction model	100
A1 A comparison of saturation times and cloud lifetimes for the Maxwell and Fuchs-Okuyama-Zung relationships with cloud radius, $R=10$ m, degree of dilution, $b/a=20$, and $T=25^\circ\text{C}$	122
A2 Cloud lifetimes for the Maxwell relationship for various cloud radii and with $a=100$ μ , $b/a=20$ and $T=25^\circ\text{C}$	122

Table	Page	
A3	A comparison of saturation radii, saturation times, and cloud lifetimes for the Maxwell and Fuchs-Okuyama-Zung relationships for various degrees of dilution, b/a , with $a=10\mu$, $R=1$ m, and $T=25^{\circ}\text{C}$	123
A4	A comparison of cloud lifetimes for the continuum and cellular models for various degrees of dilution with $a=10\mu$, $R_0=1.0$ m, and $T=25^{\circ}\text{C}$	126
A5	A comparison of saturation radii, saturation times, and cloud lifetimes for various degrees of dilution for Zung's generalized model with $a=10\mu$, $R=1$ m, and $T=25^{\circ}\text{C}$	127
A6	A comparison of cloud lifetimes for the cellular model for fixed and turbulent clouds for various degrees of dilution with $a_0=10\mu$, $R_0=1$ m, $T=25^{\circ}\text{C}$, $v_t=1$ cm/sec, and Maxwellian evaporation assumed	129
A7	A comparison of evaporation rates for the continuum model for fixed and turbulent clouds for various degrees of dilution with $a_0=10\mu$, $R_0=1$ m, $T=25^{\circ}\text{C}$, $v_t=1$ cm/sec, and Maxwellian evaporation assumed	131
A8	A comparison of the evaporation rates for various average cloud lifetimes using Equation (A22) with $a_0=10\mu$, $R_0=1$ m, $T=25^{\circ}\text{C}$, $v_t=1$ cm/sec, $c_{\infty}=0$, $m_2 c_s=2.33 \times 10^{-5}$ g/cm ³ , $D=0.249$ cm ² /sec, and $b/a=18.0$	132
B1	30 min mean wind speed data, m/sec.	136
B2	30 min mean initial conditions (mast 1)	136
B3	30 min mean temperature and moisture values.	137
B4	A summary of the assigned constants used in the theoretical model	138
B5	Values of the constants used in the prediction model.	139
B6	Prediction model results	140

LIST OF FIGURES

Figure	Page
3.2.1 Initial liquid water profile.	26
4.1.1 Grid nomenclature and control volume to be used in the numerical solution scheme.	35
5.2.1 Schematic diagram of the experimental site	60
5.3.1.1 Psychrometer unit	62
5.3.1.2 Bottom view of the psychrometer's radiation shielding and sensing unit	62
5.3.1.3 Cross sectional schematic diagram of the psychrometer sensing unit and radiation shielding	63
5.3.1.4 Instrumentation arrangement on masts 1 and 2 with the elevated spray line in the background.	64
5.3.1.5 A close up view of the anemometer and psychrometer arrangement	64
5.3.1.6 Data acquisition system	65
5.3.2.1 Schematic diagram of the instrumentation and spray line	67
6.2.1 Wind speed profiles.	70
6.4.1.1 Initial temperature profiles.	74
6.4.1.2 Initial moisture concentration profiles	75
6.4.2.1 Operational spray line for small water droplets	77
6.4.2.2 Droplet dispersion and disappearance between masts 2 and 3.	77

Figure	Page
6.4.2.3 Temperature profiles at mast 2 with Swinbank initial conditions	79
6.4.2.4 Temperature profiles at mast 3 with Swinbank initial conditions	80
6.4.2.5 Temperature profiles at mast 4 with Swinbank initial conditions	81
6.4.2.6 Temperature profiles at mast 5 with Swinbank initial conditions	82
6.4.2.7 Moisture concentration profiles at mast 2 with Swinbank initial conditions	83
6.4.2.8 Moisture concentration profiles at mast 3 with Swinbank initial conditions	84
6.4.2.9 Moisture concentration profiles at mast 4 with Swinbank initial conditions	85
6.4.2.10 Moisture concentration profiles at mast 5 with Swinbank initial conditions	86
6.4.2.11 Initial linearized temperature profile	88
6.4.2.12 Temperature profiles at mast 2 with the linearized initial conditions	89
6.4.2.13 Temperature profiles at mast 3 with the linearized initial conditions	90
6.4.2.14 Temperature profiles at mast 4 with the linearized initial conditions	91
6.4.2.15 Temperature profiles at mast 5 with the linearized initial conditions	92
6.4.2.16 Initial linearized moisture concentration profile.	93
6.4.2.17 Moisture concentration profiles at mast 2 with the linearized initial conditions	94
6.4.2.18 Moisture concentration profiles at mast 3 with the linearized initial conditions	95
6.4.2.19 Moisture concentration profiles at mast 4 with the linearized initial conditions	96

Figure	Page
6.4.2.20 Moisture concentration profiles at mast 5 with the linearized initial conditions . . .	97
7.1 Predicted temperature profiles with $T_i=$ 30.0°C	103
7.2 Predicted moisture concentration profiles for $T_i=30.0^{\circ}\text{C}$ and $\text{R.H.}_i=25\%$	104
7.3 Predicted temperature profiles with $T_i=40.0^{\circ}\text{C}$	105
7.4 Predicted moisture concentration profiles for $T_i=40.0^{\circ}\text{C}$ and $\text{R.H.}_i=25\%$	106
7.5 Maximum cooling with $u_i=0.5$ m/sec and three spray rates	107
7.6 Maximum cooling with $u_i=1.0$ m/sec and three spray rates	108
7.7 Maximum cooling with $u_i=2.0$ m/sec and three spray rates	109
7.8 Maximum cooling with $u_i=4.0$ m/sec and three spray rates	110

LIST OF APPENDICES

Appendix	Page
A. Detailed Review of Cloud Droplet Evaporation Models	118
B. Field Data and Prediction Model Results	135
C. FORTRAN IV Program for Theoretical Model.	142

LIST OF SYMBOLS

Chapter 2 and Appendix A

Symbol	Meaning
a	= Droplet radius
a_0	= Initial droplet radius
a_s	= Droplet radius at cellular saturation
$\alpha(a)$	= Evaporation-condensation coefficient
α'	= $4\pi D (3/4\pi\rho_w)^{1/3}$
α_H	= Ratio of turbulent diffusivity of sensible heat to the turbulent diffusivity of momentum
α_0	= α_H at the ground surface
$\alpha_{-\infty}$	= α_H at large ζ
b	= Cell radius
$\bar{b}(t)$	= Average cell radius at time t
$B(a)$	= Gas phase resistance for the droplet
β	= $\alpha'[c(r,t) - c_0]m_2$
c	= Water vapor concentration not near the drop's surface
c_0	= Water vapor concentration at the drop's surface
c_p	= Isobaric specific heat
c_∞	= Water vapor concentration far from the drop
c_s	= Saturated vapor concentration at the surface of the drops
$C(a)$	= Surface resistance of the droplet

Symbol	Meaning
$c(t)$	= Average liquid molecule concentration
D	= Diffusivity of water vapor through air
D'	= New diffusion coefficient $\equiv D/(1-E)$
\mathcal{D}	= Differential operator, $\frac{\partial}{\partial T} - KV^2$
∂	= Partial differential
δ	= Free angle ratio
Δ	= Fuchs' concentration jump distance
∇^2	= Laplacian Operator
E	= Void fraction
$E_i(x)$	= Integrated error function
\exp	= Exponential function
ζ	= z/L
g	= Acceleration of gravity
H	= Sensible heat flux
I_{FOZ}	= Fuchs'-Okuyama-Zung evaporation rate per drop
I_M	= Maxwellian evaporation rate per drop
j	= Moisture flux
k	= Von Karman's constant
k_B	= Boltzman constant
K_H	= Turbulent diffusivity for sensible heat
K_M	= Turbulent diffusivity for momentum
K_χ	= Turbulent diffusivity for moisture vapor
L	= Monin-Obukhov scale length
L'	= Modified Monin-Obukhov scale length

Symbol	Meaning
\ln	= Natural logarithm
m	= Droplet mass
m_2	= Molecular mass of the evaporating liquid
m_v	= Mass of a vapor molecule
M	= Total cloud mass
μ	= Micron
n	= Droplet density in the cloud
ν	= Kinematic viscosity of air
π	= 3.14159
Q_c	= Steady state continuum model evaporation rate in a turbulent cloud
Q_{NS}	= Nonstationary rate of evaporation in the cloud
Q_{ss}	= Steady state rate of evaporation in the fixed cloud
r	= Position in a spherical cloud
R_0	= Initial cloud radius
$R(t)$	= Cloud radius at time t
ρ	= Ambient air density
ρ_w	= Liquid water density
σ	= Dimensionless coefficient in the KEYPS equation
σ'	= Modified σ
σ_s	= Liquid surface tension
t	= Time
t_{cloud}	= Total cloud lifetime
t_e	= Cloud lifetime after saturation

Symbol	Meaning
t_j	= Lifetime of outer droplets after cellular saturation
t_{outer}	= Lifetime of outer droplets before cellular saturation
t_s	= Time required for inner cloud cells to become saturated
t_u	= Cloud lifetime for the unsaturated case
T	= Ambient temperature
T_A	= Absolute temperature
T_C	= Functional relationship of t used in Zung's continuum model
T_0	= Temperature at the height z_0
T_*	= Similarity temperature profile coefficient
τ	= Shear stress
τ_0	= Shear stress at the ground surface
$u(z)$	= Wind speed in the direction of mean flow
u_*	= Friction velocity
v	= Volume of a single liquid molecule
$\bar{v}_t(t)$	= Average turbulent relative velocity
ϕ	= Droplet evaporation size coefficient
ϕ_0	= $\phi(a_0)$
ϕ_{FOZ}	= Fuchs'-Okuyama-Zung evaporation rate per unit droplet surface area
ϕ_M	= Maxwellian evaporation rate per unit droplet surface area
χ	= Ambient water vapor concentration
χ_0	= Water vapor concentration at the height z_0
χ_*	= Similarity water vapor concentration profile coefficient

Symbol	Meaning
ψ	= Dimensionless wind speed gradient used in the KEYPS equation
z	= Height
z_0	= Surface roughness height
Z	= $3 v \sigma_s / k_B T_A$
ζ	= Dimensionless height ratio, z/L

Chapter 3

Symbol	Meaning
C	= Contaminant (liquid water) concentration
C_i	= Initial liquid water concentration profile
C_0	= Average initial liquid water concentration
c_1	= Evaporation source term coefficient
d	= Total differential
K_C	= Turbulent diffusivity for liquid water drops
$K(x)$	= Turbulent diffusivity in the x-direction
$K(y)$	= Turbulent diffusivity in the y-direction
$K(z)$	= Turbulent diffusivity in the Z-direction
L_v	= Latent heat of vaporization
N	= Average droplet concentration
Q_E	= Latent heat flux
Q_G	= Soil heat flux
Q_H	= Sensible atmospheric heat flux
Q_N	= Net all wavelength radiation
S	= Spray rate per meter of line

Symbol	Meaning
\bar{u}	= Mean wind speed in the x-direction
\bar{v}	= Mean wind speed in the y-direction
\bar{w}	= Mean wind speed in the z-direction
ϕ	= Contaminant source term
ϕ_1	= Liquid water concentration source term
ϕ_2	= Sensible heat source term
ϕ_3	= Water vapor concentration source term
x	= Direction along the mean wind
y	= Direction transverse to the mean wind
z	= Vertical direction
z_2	= Bottom vertex of initial liquid water concentration profile
z_3	= Top vertex of initial liquid water concentration profile
z_{\max}	= Maximum height of solution
z_{MS}	= Location of the maximum initial liquid water concentration

Other symbols as previously defined

Chapter 4

Symbols	Meaning
A, A'	= Spalding-Patankar solution coefficients
A_1, A_2, A_3	= Intermediate source term Parameters
B, B'	= Spalding-Patankar solution coefficients
C	= Spalding-Patankar solution coefficient
C_f	= Compressibility factor

Symbol	Meaning
$C(\omega)$	= General turbulent diffusivity
Δc_p	= Isobaric specific heat residual
d	= Generalized source term
D	= Downstream solution node
DD	= Midpoint between vertically adjacent downstream nodes
e_s	= Saturated vapor pressure
ϵ	= Ratio of the molecular weight of water to the molecular weight of dry air
G_1, \dots, G_4	= Intermediate solution parameters
I_s	= Simpsons integration
P	= Ambient atmospheric pressure
P_1, P_2, \dots, P_6	= Intermediate solution parameters
R_{da}	= Dry air gas constant
R_v	= Water vapor gas constant
$R.H.$	= Relative humidity
T_v	= Virtual temperature
U	= Upstream solution node
UU	= Midpoint between vertically adjacent upstream nodes
w	= Mixing ratio
w_s	= Saturated mixing ratio
Δx	= Solution increment in the x-direction
ϕ	= General diffusing property
χ_s	= Saturated water vapor concentration
ω	= Dimensionless vertical axis = $-\zeta$
$\Delta \omega$	= Solution increment in the ω -direction

Subscripts

- + = Adjacent node above the solution point
- = Adjacent node below the solution point
- Others as previously defined

Chapter 8

Symbols

Meaning

- | | |
|--------|--|
| η | = Dynamic viscosity of air |
| v_T | = Terminal velocity of falling water droplets in still air |
| z_1 | = The solution point closest to the ground surface |

1. INTRODUCTION

The injurious effects of the commonly known problems of heat and moisture stress on plants have been of major concern to agriculturists and horticulturists for many years. The results of these stresses are to reduce the crop yield in quantity and/or quality and may even prove fatal to the plants under extreme conditions.

The two stresses are not independent. Moisture stress can occur in the presence of a low soil moisture content. The root system cannot obtain the water required for the plant's normal development. Moisture stress can also occur during periods of high evapotranspiration rates. Under such conditions water is lost from the above ground portions of the plant, primarily the leaves, faster than the below ground root system can supply the water. Evaporation is the principal means of cooling the plant during the day. When evaporation is restricted, leaf temperatures rise and the plant is subjected to heat stress. It is obvious that the most severe conditions are low soil moisture and high potential evapotranspiration rates.

The widely accepted practices of supplemental and total irrigation have been used many years to reduce

the stress caused by low soil moisture. Methods for the reduction of high evapotranspiration rate induced moisture and heat stress are not as well developed.

Some of the factors affecting the evapotranspiration rates are: (1) wind speed resulting in transport of the water vapor from the plant canopy; (2) low ambient moisture conditions which results in an increase in the water vapor diffusion rates from the leaf stomates; and (3) high plant temperatures, due to high insolation rates, which increase the evaporative cooling demands. The wind speed is largely uncontrollable, except where wind breaks are used e.g. Geiger (1965), Brown and Rosenberg (1971). Reduced wind speed can have a reverse affect, though, if an ample supply of soil moisture is available. The reduced wind flow lowers the evaporation rate thereby decreasing the evaporative cooling and increasing the heat stress. Ambient temperature and moisture conditions, however, can be modified.

Carolus, Erickson, Kidder, and Wheaton (1965), Carolus and Van Den Brink (1965), and Carolus (1965,1969), have investigated and demonstrated the affects of low rate sprinkler irrigation to provide a source of water for evaporative cooling exterior to the plant. A disadvantage of the sprinkling approach is that the plant environment remains nearly saturated thus possibly increasing

disease susceptibility. A different approach would be to modify and cool the air before it reaches the plants. Thus the plant canopy would not be continuously wet.

The method proposed herein for modifying and cooling the air is the complete evaporation of small water droplets. The cooling will be provided by the latent heat energy required for evaporation of the droplets.

Before any practical engineering applications of this technique can be designed more knowledge of the relevant parameters is needed so that a mathematical model of the problem can be developed.

The current investigation will be limited to the development and testing of a suitable model for describing the affects of the evaporation of small water droplets on the downwind microclimatic temperature, humidity, and wind profiles. The model will be restricted to a two-dimensional problem for an elevated line source of water droplets above a bare soil surface.

2. LITERATURE REVIEW

2.1 Scope of Literature Review

The review of the pertinent literature included in this chapter will be limited to the establishment of sufficient background information for the subsequent development of the model. Literature citations directly pertinent to the model itself will be deferred until the appropriate section. A more detailed review of evaporation models is included in Appendix A.

2.2 Selection of Technique

The region of the atmosphere to be considered in this model is within the surface boundary layer of the earth. The environmental study of this region involves a study of the microclimate and is commonly referred to as micro-meteorology. Many investigators have studied the various aspects of the microclimate. The investigations have been either in the form of a statistical analysis of the turbulent characteristics or in the form of profile gradients. Excellent reviews of the statistical and profile gradient relationships are given by Sutton (1953), Pasquill (1962), Lumley and Panofsky (1964), Harrington (1965), Waggoner (1965), Monin and Yaglom (1971), and others. The profile

gradient techniques were the ones chosen for this investigation. This choice implicitly neglects the turbulent kinetic energy exchange discussed by Lumley and Panofsky (1964), Zilitinkevich, Leichtmann and Monin (1967), and others.

2.3 Relevant Parameters

The atmospheric parameters of importance in this investigation are: the shear stress; the wind speed, temperature and humidity profiles; the net radiation; the surface heat and moisture fluxes; and the stability. Many investigators, e.g. Calder (1939), Sutton (1953), Monin and Obukhov (1954) have shown that for normal atmospheric conditions within the region up to an average height of 50 meters, the turbulent shear stress, τ , is constant and equal to that at the ground surface, τ_0 . Additional substantiation was provided in the work reported by Lettau and Davidson (1957) for the O'Neal, Nebraska Project Prairie Grass.

The various expressions for the wind speed profile have been thoroughly reviewed by Harrington (1965). Harrington (1965, p. 123) concluded that the Swinbank (1964) exponential-law profile is "the most appropriate expression for the wind profile near the ground". Swinbank's model for the wind profile is:

$$u(z) = \frac{u_*}{k} \ln \left\{ \frac{\exp(\frac{z}{L}) - 1}{\exp(\frac{z_0}{L}) - 1} \right\} . \quad (2.3.1)$$

The corresponding momentum diffusivity is:

$$K_M(z) = k u_* L [1 - \exp(-\frac{z}{L})] , \quad (2.3.2)$$

where u_* = the friction velocity, (m/sec),

k = Von Karman's constant ≈ 0.4 ,

z_0 = roughness height, (m)

L = Monin-Obukhov (1954) scale height, (m),

$$= \frac{-u_*^3}{kgH/\rho c_p T} ,$$

with g = acceleration of gravity, (m/sec²),

H = sensible surface heat flux, (cal/m²-sec),

ρ = ambient air density, (g/m³),

c_p = specific heat of the air, (cal/g-°K)

and T = absolute temperature, (°K).

The friction velocity, u_* , as defined by Sutton (1953) is:

$$u_*^2 = \left| \frac{\tau}{\rho} \right|$$

Since the shear stress, $\tau = \tau_0$ as noted above, $u_* = \sqrt{|\tau_0/\rho|}$, and is customarily assumed constant for given flow and stability conditions. The roughness height, z_0 , is the dynamic roughness parameter at which the velocity is zero.

The Monin-Obukhov scale height is in fact a stability parameter arrived at through dimensional analysis. The sign of L is chosen such that for a positive sensible heat flux, i.e. $H > 0$ and unstable conditions, $L < 0$ and for a negative sensible heat flux, i.e. $H < 0$ and stable conditions, $L > 0$.

The theory of similarity developed by Monin and Obukhov (1954) and used by Lumley & Panofsky (1964), Swinbank (1964), Harrington (1965), Monin and Yaglom (1971) and others is assumed to hold. Under the similarity theory, the initial temperature and moisture vapor profiles have a form mathematically similar to the wind velocity profile. The initial temperature profile thus becomes:

$$T = T_0 - T_* \left[\ln \left(\frac{\exp(z/L) - 1}{\exp(z_0/L) - 1} \right) \right], \quad (2.3.3)$$

where T_0 = temperature at z_0 , ($^{\circ}\text{C}$),

and $T_* = -\frac{1}{ku_*} \frac{H}{\rho c_p}$, ($^{\circ}\text{C}$).

The initial moisture concentration profile is:

$$\chi = \chi_0 - \chi_* \left[\ln \left(\frac{\exp(z/L) - 1}{\exp(z_0/L) - 1} \right) \right], \quad (2.3.4)$$

where χ_0 = moisture concentration at z_0 , (g/m^3),

$$\chi_* = -j/ku_*, \quad (\text{g}/\text{m}^3)$$

j = moisture flux, ($\text{g}/\text{m}^2\text{-sec}$),

and the others as previously defined.

The relationships of the turbulent diffusivities for momentum, heat and moisture have not been well established.

The most common assumption is

$$\alpha_i(\zeta) = K_i/K_M = 1,$$

where $\zeta = z/L$,

K_M = momentum diffusivity,

K_i = diffusivity for parameter i .

Sutton (1953, p. 319) deduced that:

$K_M = K_\chi < K_H$ in unstable conditions,

$K_H = K_\chi > K_M$ in stable conditions,

where K_H = diffusivity of heat

K_χ = diffusivity of any contaminant

Swinbank (1968) suggested

$$\alpha_H = 2.7|\zeta|^{0.24}.$$

Stewart and Lemon (1969) proposed

$$\alpha_H = -1.4 \exp(1.5\zeta) + 3.0.$$

Leichtmann & Ponomareva (1969) indicated that

$$\alpha_H = \begin{cases} 0.8 & -.03 < \zeta \leq +.10 \\ 3.2|\zeta|^{.35} & -.8 < \zeta \leq -.03 \\ 3.0 & \zeta \leq -.8 \end{cases}$$

Monin and Yaglom (1971, p. 490-494) reviewed the estimates of α attempted in more than fifteen investigators' different sets of data reported in the literature from Australia, the United States and the U.S.S.R. The results were so widely scattered that only rough conclusions could be drawn. "On the whole the existing data show only that $\alpha(0)=\alpha_0$ is close to unity; with increase of instability, the ratio α increases and with increase of stability it seems to be slightly decreasing. However, the estimates of the limiting value α_{∞} are presently quite uncertain: the Australian observations imply the value $\alpha_{\infty} \approx 3$ to 3.5. Nevertheless, some investigators are inclined to use considerably lower estimates (close to 2 or even between 1 and 1.5)". "At present we can say only that all existing data on the humidity profiles are in agreement with the assumption that $K_{\chi}/K_H = \text{constant}$ [and even with the assumption that $K_{\chi}/K_H = 1$]." The relationships can thus be summarized as:

$$K_H \approx K_{\chi} > K_M \quad \text{in unstable conditions, i.e. } L < 0,$$

$$K_H \approx K_{\chi} < K_M \quad \text{in stable conditions, i.e. } L > 0,$$

which is almost completely opposite to Sutton's earlier suggestion.

Panofsky, Blackadar, and McVehil (1960), Webb (1960), Panofsky (1963), Lumley and Panofsky (1964) and Monin and Yaglom (1971) discuss an alternate approach by defining a new scale factor $L' = \alpha_H L$.

The various derivations by Kazanski and Monin (1956), Ellison (1957), Yamamoto (1959), Panofsky (1961) and Sellers (1962), satisfies an equation of the form:

$$\psi^4 - \sigma \frac{z}{L_T} \psi^3 = 1 \quad (2.3.5)$$

where $\psi \left(\frac{z}{L_T} \right) = \frac{kz}{u_*} \frac{\partial u}{\partial z}$

Equation (2.3.5) is known as the KEYPS equation. The value of σ is not definitely determined. Monin and Yaglom (1971) report values ranging in size from 4 to 14 that were proposed by Panofsky, Blackadar and McVehil (1960), and Charnock (1967) respectively. Likewise the value of $\sigma' = \alpha_{\infty} \sigma$ has not been definitely determined. Monin and Yaglom (1971) report a range of values between 10 and 20. A comparison of the values for σ and σ' , however, indicates that $\alpha_{\infty} > 1$, and is consistent with the previously stated conclusions.

2.4 Atmospheric Diffusion Models

The diffusion of substances in the atmosphere near the ground have been of interest to micrometeorologists for many years. Sutton (1953) presents the solution to various diffusion models for both instantaneous and continuous point, line, and plane sources. He first used the Fickian diffusion equation which required the diffusivities to be constant and assumed the wind speed was also a constant value. For

the diffusion of heat, Sutton (1953, p. 145) states: "As yet, there is no generally accepted formulation of the problems of heat transfer by atmospheric turbulence."

Sutton reviewed the theories presented by G. I. Taylor, Brunt, L. F. Richardson, Calder, and Priestley & Swinbank, and concluded in agreement with Deacon that the wind speed and diffusivity profiles were simple power functions of height under diabatic conditions. He resolved the diffusion equation using the power law profiles. The results have proved to be valid only in the limited near neutral stability situation but were an important first step in understanding the atmospheric diffusion process.

For an elevated source, Sutton (1953, p. 139) introduced the method of images to conveniently handle the assumed impervious boundary condition. This method utilizes a mirror image technique whereby a virtual source, corresponding to the actual source, is located below the zero plane. Thus, no net flux occurs across the boundary.

Philip (1959) included advection into the diffusion model but retained the power law profiles, and $\alpha_H=1$. Rider, Philip and Bradley (1964) reviewed the work done by Timofeev (1954), deVries (1959), and Philip (1959) to develop a model for a freely evaporating soil surface. They retained the power law profile and $\alpha_H=1$.

Yordanov (1966) developed a two layer analytical model for continuous diffusion from an elevated point source, in which he used the Lagrangian correlation coefficients. The wind speed was assumed constant with height while the turbulent diffusivity was that of Monin and Obukhov (1954) i.e. $K(z) = k u_* L f(\zeta)$. An implicit assumption of $\alpha_H = 1$ was made. The two layers employed were those indicated by the results of Priestley (1955), Deacon (1959) and Gurvich (1965) to be the thermal sublayer and the dynamic sublayer. The transition region from the dynamic to the thermal sublayer was indicated to be for ζ in the range from -0.03 to -0.05. (See also Waggoner (1959) and Monin and Yaglom (1971)). Yordanov (1968) extended his model to an infinite elevated line source. His results, though agreeing with other researcher's data, were much too complicated mathematically to be of practical use in the current investigation.

Jaffe (1967) used the results of Monin and Obukhov (1954), Priestly (1959) and Lumley and Panofsky (1964) to develop a three layer diffusion model. The diffusivities for the layers were:

- (1) "log + linear" of Monin & Obukhov for $|\zeta| < 0.03$
- (2) $K_M \propto (z)^{4/3}$ of Priestly for $0.03 < |\zeta| \leq 1$ to 1
- (3) $K_M \propto z^2$ of Lumley and Panofsky for $|\zeta| > 1$

The common assumption of $\alpha_H=1$ was retained, "because of the confusion surrounding the K_H/K_M ratio--and for convenience." [Jaffe (1967) p. 302]. The numerical solution of the two-dimensional steady state diffusion equation provided results consistent with the Project Prairie Grass data reported by Lettau and Davidson (1957).

The adoption of Swinbank's exponential law profile in Section 2.3 above and the fact that the thermal sublayer exists where $|\zeta| > 0.05$ leads to the adoption of a single layer model as the current diffusion model.

2.5 Evaporation Models

Models for the atmospheric evaporation of water droplets have not been widely developed. This is in contrast to the evaporation studies conducted in enclosed chambers for combustion and food drying processes.

Milburn (1957) developed a model for non-turbulent, homogeneous cloud evaporation restricted by the following assumptions: (1) "The individual cloud droplets are sufficiently far apart for the average vapor pressure and temperature in the immediately surrounding medium into which they evaporate to be described by simple scalar 'field' functions of space and time." (2) "The individual droplets will be able to reach a steady-state condition with respect to their immediate surroundings in a time short

compared with the duration of processes affecting the cloud as a whole." (3) "The individual water droplets remain fixed in space so that the number of such drops in a unit volume is constant." The last assumption is to presume non-turbulent idealized conditions.

Assumption (2) was verified by demonstrating that the evaporation of about 2% of the droplet's mass would reduce the cell temperature to the wet-bulb value. The resulting equation for droplet mass transfer was:

$$\frac{\partial}{\partial t} m(r,t) = 4\pi D (3m/4\pi\rho_w)^{1/3} [c(r,t) - c_o(r,t)], \quad (2.5.1)$$

where;

$m(r,t)$ = droplet mass at (r,t) , (g),

D = diffusivity of water vapor through air, (cm^2/sec),

m = initial mass of individual droplets, (g),

ρ_w = density of water, (g/cm^3),

$c(r,t)$ = water vapor concentration at (r,t) , not near drop surface, (g/cm^3),

and $c_o(r,t)$ = same as c above but at the drop surface, (g/cm^3).

The inclusion of the bulk vapor and heat diffusion equations, and the droplet heat transfer equation yielded the relationship:

$$-n \frac{\partial m}{\partial t} = \left(\frac{3}{8\pi D}\right) \left(\frac{4\pi\rho_w}{3}\right)^{1/3} \left(\frac{\partial}{\partial t} - D\nabla^2\right)m^{-1/3} \frac{\partial m}{\partial t}, \quad (2.5.2)$$

[with the incorporation of a correction noted by Zung (1967, b, p. 3579)], where n = droplet density in the cloud, (No./cm³), and ∇^2 = the Laplacian operator. Equation (2.5.2) was not solved until a linearizing assumption was applied to the dimensionless form and its applicability was reduced to the very early stages of evaporation i.e. small t and evaporation of less than 20% of the mass of the droplets.

Milburn (1958) extended the previous model to turbulent clouds, thereby relaxing assumption (3) above, but retaining the first two. In addition, he assumed that the evaporation of individual droplets was describable by "quasistatic" or equilibrium-flow equations. The quasistatic assumption implied that the transient terms had been damped out, and the droplets were able to attain equilibrium temperatures before saturation was reached. The individual droplet evaporation was assumed to be governed by Equation (2.5.1) which neglects the effect of turbulence since the laminar boundary layer around the droplet was estimated to be more than 2 orders of magnitude larger than the droplet radius. "It may be argued . . . that diffusion in a temperature gradient is more accurately represented by an equation in partial vapor pressures than by one in vapor concentration. At practical temperatures there is but little difference,

however." (Milburn, 1958, p. 116). The diffusivities of heat, momentum, and vapor were assumed to be the same.

The resulting unsolved equation was:

$$\mathcal{D} n(m, r, t) = (3\alpha/2) \left\{ \frac{\partial}{\partial m} m^{1/3} n(m, r, t) \right\} \cdot \left\{ \int_0^{\infty} dm \cdot m \cdot n(m, r, t) + c(r, t) - \psi(r, t) \right\}, \quad (2.5.3)$$

where;

$$\mathcal{D} = \frac{\partial}{\partial t} - K \nabla^2,$$

$n(m, r, t)$ = number density of droplets in a unit mass interval at (r, t) ,

K = turbulent diffusivity, (cm^2/sec) ,

$$\alpha = \left(\frac{8\pi D}{3} \right) \left(\frac{3}{4\pi\rho_w} \right)^{1/3}, \quad (1/\text{cm}),$$

and $\psi(r, t) = c(r, t) + \int_0^{\infty} dm \, m \, n(m, r, t)$, (g/cm^3) .

Okuyama and Zung (1967) noted that Maxwell's derivation for the stationary evaporation of a spherical drop in a motionless media has the form:

$$\phi_M = \frac{c_s - c_\infty}{a/D}, \quad (2.5.4)$$

where;

ϕ_M = Maxwell rate of evaporation per drop per unit surface, $(\text{g}/\text{sec}\text{-cm}^2\text{-drop})$,

c_s = saturated vapor concentration at the drop surface, (g/cm^3) ,

c_∞ = vapor concentration at an infinite distance from the drop, (g/cm^3) ,

D = molecular diffusion coefficient of the vapor in air, (cm^2/sec),

and a = droplet radius, (cm).

"Equation (2.5.4) is valid only for drops larger than 10^{-2} cm radius (200 μ diameter), becomes less accurate for smaller drops, and includes only properties of the vapor phase."

Okuyamam and Zung demonstrated that the formulations of Fuchs, and of Monchick and Reiss were essentially the same, but did include both liquid and vapor properties. The derivation of the evaporation-condensation coefficient for very small droplets was made in the form $\alpha(a) = \delta \cdot \phi(a)$;

where;

δ = free-angle ratio,

and ϕ = size coefficient.

The coefficient was found to be:

$$\alpha(a) = \delta \exp(-3v\sigma/ak_B T_A) \quad (2.5.5)$$

where;

v = volume of a single liquid molecule, (cm^3),

σ_s = surface tension of the liquid, (ergs/cm^2),

k_B = the Boltzman constant, ($\text{ergs}/^\circ\text{K}$),

and T_A = absolute temperature, ($^\circ\text{K}$).

The inclusion of Equation (2.5.5) into Fuchs' equation leads to the more general rate equation:

$$\phi_{\text{FOZ}} = \frac{(c_0 - c_\infty)}{(a/D)[a/(a+\Delta)] + (1/\nu\delta\phi)} \quad (2.5.6)$$

where;

ϕ_{FOZ} = the generalized Fuchs-Okuyama-Zung evaporation rate per drop per unit surface, (g/sec-cm²-drop),

Δ = Fuchs' concentration jump distance, and is the distance from the drop surface at which the steady concentration is maintained, (cm),

and $\nu = \frac{1}{4} \left(\frac{8k_B T_A}{\pi m_v} \right)^{1/2}$, (cm/sec),

m_v = mass of a vapor molecule, (g).

Equation (2.5.6) includes properties of the liquid, vapor, and liquid-vapor interface. The values reported by Okuyama and Zung (1967, p. 1582) for the above parameters are given in Table 2.5.1. The denominator of Equation (2.5.6) can be redefined as $B(a) + C(a)$, where;

$B(a) = (a/D)[a/(a+\Delta)] \equiv$ gas phase resistance,

and $C(a) = 1/\nu\delta\phi \equiv$ surface resistance.

It can be seen that for large a , ϕ_{FOZ} reduces to the Maxwell equation and is diffusion controlled. When $a \rightarrow 0$, the process is governed by $\phi(a)$, the size coefficient, and Δ is completely eliminated. By examining $B(a)$ and $C(a)$, Okuyama & Zung discovered that B increases with increasing radius while C increases with decreasing radius for

TABLE 2.5.1.--Constants for the evaporation kinetics of water drops, (cgs units).

Parameter	T (°K)		cgs units
	373	273	
property of the liquid phase, v	3.11×10^{-23}	2.98×10^{-23}	cm^3
properties of the gas-liquid interface, σ_s	58.8	75.6	ergs/cm^2
$a_\phi = .5$	1.5×10^{-7}	3×10^{-7}	cm
δ	0.042	0.039	
properties of the gas phase, C_s	5.98×10^{-4}	4.87×10^{-6}	g/cm^3
v	1.65×10^4	1.42×10^4	cm/sec
D	3.60×10^{-1}	1.98×10^{-1}	cm^2/sec
Δ	1.09×10^{-5}	7.0×10^{-6}	cm

$a < 10^{-4}$ cm (i.e. 1μ). This is due to $\phi(a)$ decreasing very rapidly with decreasing radius below about $a = 10^{-5}$ cm. Thus $\phi_{\text{FOZ}}(a)$ has a maximum value at some value of a . For evaporation in air at 0°C , $\phi_{\text{FOZ,MAX}}(a)$ was shown to be for a 10^{-5} cm (i.e. 0.1μ). The range of maximum values was for radii between 1 and 0.01μ .

The above derivations are valid only for individual droplets. Zung (1967,a) extended the results to droplet assemblages in air by use of a modified cellular model. The cellular model has been used primarily for enclosed systems for combustion and spray drying. As such the model is not directly applicable to cloud evaporation.

For the modified cellular model, Zung limited his considerations to monodisperse systems evaporating into a motionless medium. The cells are assumed spherical with radius b containing one droplet with radius a per cell. The inner cell's droplets will cease to evaporate after cellular saturation has occurred while the outer cell layers will continue to evaporate.

The Maxwell expression, Equation (2.5.4) which was for evaporation in g/sec-cm^2 , can be rewritten as,

$$I_M = 4\pi a D m_2 (c_s - c_\infty), \quad (2.5.7)$$

where; I_M = Maxwell evaporation, (g/sec-drop),
 m_2 = molecular mass of the evaporating liquid,
 (g),

and the other parameters are as previously noted.

In a similar manner, the general expression of Fuchs-Okuyama-Zung, (i.e. Equation 2.5.6) which is valid for $a > 10^{-8}$ cm, is

$$I_{\text{FOZ}} = \frac{4\pi a D m_2 (c_s - c_\infty)}{(D/av\alpha\phi) + a/(a+\Delta)}, \quad (2.5.8)$$

where I_{FOZ} = evaporation rate per drop, (g/sec-drop),

$$\phi = \exp\left(\frac{-3v\sigma}{a k_B T_A}\right),$$

$$v = (k_B T_A / 2\pi m_2)^{1/2}$$

$$\Delta = D/2v$$

$$\alpha = \text{evaporation coefficient} = \delta,$$

and the other parameters as noted previously.

For a more detailed review of the modified cellular and continuum models developed by Zung for both still and turbulent clouds, see Appendix A.

For the problem in question in this thesis the models reviewed fall short of the ideal in several respects.

(1) The diffusivity was assumed constant with position and only a function of time. The models for fixed clouds assumed the diffusivity was constant and equal to the molecular diffusivity of water vapor in air. (2) In the continuum model development, the assumption was made in the derivation of the new diffusion coefficient that "The radius, a , of the droplet does not vary much". This is not true when it is permitted to go from $a=a_0$ to $a=0$. It would be true only during the initial stages of evaporation. (3) The continuum model is valid only in the saturated and near saturated cases while the cellular model is valid in the unsaturated case. (4) None of the models have been experimentally verified and can be therefore used only as a guide to the evaporation process.

3. THEORETICAL MODEL DEVELOPMENT

3.1 Diffusion Equation

The problem under investigation is an active contaminant diffusion problem. The mathematical description of the general three dimensional, unsteady, incompressible, diffusion problem [Sutton (1953), Pasquill (1962), and Harrington (1965)] is:

$$\frac{dC}{dt} = \frac{\partial}{\partial x}(K(x) \frac{\partial C}{\partial x}) + \frac{\partial}{\partial y}(K(y) \frac{\partial C}{\partial y}) + \frac{\partial}{\partial z}(K(z) \frac{\partial C}{\partial z}) + \phi, \quad (3.1.1)$$

where; $\frac{dC}{dt} = \frac{\partial C}{\partial t} + \bar{u}(z) \frac{\partial C}{\partial x} + \bar{v}(z) \frac{\partial C}{\partial y} + \bar{w}(z) \frac{\partial C}{\partial z},$

C = contaminant concentration, (mass/vol),

t = time, (sec),

x = direction along the mean wind,

y = direction transverse to the mean wind,

z = vertical direction,

K(i) = turbulent diffusivity in direction i,

ϕ = contaminant source term,

and $\bar{u}, \bar{v}, \bar{w}$ = mean wind velocities in the x, y & z directions respectively.

The solution of Equation (3.1.1) would require an excessive amount of computer space, time and methodology not presently available. Therefore, several simplifying assumptions must be made. The first will be to reduce it to a two dimensional problem by eliminating variations in the transverse (y) direction, thus $\partial C/\partial y = 0$. The second will be to assume a steady-state condition, thus $\partial C/\partial t = 0$. From the choice of a coordinate system x is in the direction of the mean wind, thus $\bar{v}=\bar{w}=0$. It has been demonstrated by an order of magnitude analysis, by Sutton (1953), Monin (1956), Harrington (1965) Yordanov (1967), and others, that the diffusion in the direction of the mean wind (x-direction) is much less than the transport by the wind and also much less than the diffusion in the vertical (z) direction. $\frac{\partial}{\partial x}(K(x)\frac{\partial C}{\partial x})$ can therefore be neglected. By substituting the above assumptions into Equation (3.1.1), the water droplet diffusion equation becomes:

$$\bar{u}(z) \frac{\partial C}{\partial x} = \frac{\partial}{\partial z}(K_C(z)\frac{\partial C}{\partial z}) + \phi_1(z,x). \quad (3.1.2)$$

A check of the units reveals that ϕ_1 must have the units $ML^{-3}T^{-1}$.

The diffusion of the water vapor will be governed by the same turbulent conditions as the liquid water droplets. Thus, the water vapor diffusion equation will have the same form as Equation (3.1.2):

$$\bar{u}(z) \frac{\partial \chi}{\partial x} = \frac{\partial}{\partial z} (K_{\chi}(z) \frac{\partial \chi}{\partial z}) + \phi_3(z, x), \quad (3.1.3)$$

where;

χ = water vapor concentration, (g/m³),

and ϕ_3 = water vapor source term, (g/m³-sec),

The energy diffusion equation will be of the same general form with additional parameters for homogeneity of energy units, [Sutton (1953), Crank (1956),]:

$$\rho c_p (\bar{u}(z) \frac{\partial T}{\partial x}) = \rho c_p \frac{\partial}{\partial z} (K_H(z) \frac{\partial T}{\partial z}) + \phi_2(z, x), \quad (3.1.4)$$

where;

T = temperature, (°C),

ρ = ambient air density, (g/m³),

c_p = isobaric specific heat of moist air, (cal/g-°C),

and ϕ_2 = energy source term, (cal/m³-sec).
For evaporation it will be a negative source, i.e. a sink.

The coupling of Equations (3.1.2), (3.1.3), and (3.1.4) is through the source term. With the general problem defined above, the forms of the wind speed profile, diffusivities, initial conditions, source terms and boundary conditions must now be specified.

3.2 Initial Conditions

The selection of the Swinbank similarity profiles in Section 2.3 specifies the wind speed profile by Equation

(2.3.1), the momentum diffusivity by Equation (2.3.2), the initial temperature profile by Equation (2.3.3) and the initial moisture vapor concentration by Equation (2.3.4). The initial solutions of the present problem will be made for $\alpha_H=1$. Other α_H relationships will be tested for comparison. The profiles of wind and diffusivities will be assumed to remain unchanged by the introduction of the evaporating mist.

The initial liquid water droplet concentration at the spray line will be assumed to have a triangular profile. The location of the vertices will be adjusted to the observed spray pattern. The average uniform spray concentration is determined by the following formula:

$$c_o = \frac{S}{\int_{z_2}^{z_3} u(z) dz} , \quad (3.2.1)$$

where;

c_o = mean liquid water concentration, (g/m^3),

S = mean rate of liquid sprayed into the air, (g/m_y -sec),

$\int_{z_2}^{z_3} u(z) dz$ = total wind flow past the spray line between the heights z_2 & z_3 , ($m_z m_x$ /sec),

and z_2 & z_3 = lower and upper bounds respectively of the droplet distribution, (m).

For a triangular profile, the same concept can be utilized, but restricted to each node in question and multiplied by an appropriate weighting function so that a continuity check will yield the same amount of water per unit area for the initial profile, i.e. $\int_{z_2}^{z_3} C_i(z) dz = \text{constant}$. $C_i(z)$ is the initial liquid water concentration profile and is equal to zero below z_2 and above z_3 . For the average uniform concentration the continuity value would be $c_o(z_3 - z_2)$.

The initial triangular profile is shown in Figure 3.2.1. where $z_{MS} = z$ for maximum spray, and $z_2 < z_{MS} < z_3$.

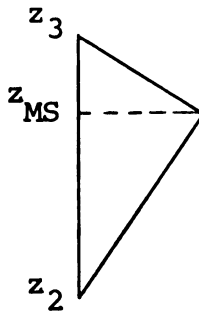


FIGURE 3.2.1.--Initial liquid water profile.

The weighting function must be such that $\int_{z_2}^{z_3} \text{wt. } f(z) dz = 1$. It can be shown that the following function satisfies the above conditions:

$$\text{wt.f}(z) = \begin{cases} \frac{2(\Delta z)(z-z_2)}{(z_{MS}-z_2)(z_3-z_2)}, & \text{for } z_2 < z_{MS} < z_3 \\ & z_2 < z < z_{MS}, \\ \frac{2(\Delta z)(z_3-z)}{(z_3-z_{MS})(z_3-z_2)}, & \text{for } z_2 < z_{MS} < z_3 \\ & z_{MS} < z < z_3, \end{cases} \quad (3.2.2)$$

where Δz = vertical node spacing,

and z is the midpoint of Δz .

The initial liquid water concentration profile is:

$$C_i(z) = \frac{\text{wt.funct.} \times S}{u(z) \times \Delta z}. \quad (3.2.3)$$

3.3 Source Terms

The form of the source terms will be modified versions of the Fuchs-Okuyama-Zung expression, Equation (2.5.8), since it is valid for much smaller droplets than the Maxwell relationship, Equation (2.5.7). The solution technique herein will be numerical and not analytical. Therefore, the individual solution nodes will be assumed fixed during the evaporation process as required by the Fuchs-Okuyama-Zung equation but diffusion will be allowed between nodal solutions. In addition, instead of using $m_2(c_s - c_\infty)$ as the evaporation potential, the actual saturated vapor concentration deficit $(c_s - c)$ in g/m^3 will be used. Thus the rapidly changing vapor concentration near the ground surface will be included. The form of the source term will be:

$$\phi_1 = \left[\frac{4\pi aDN}{(D/av\delta\phi) + [a/(a+\Delta)]} \right] (c_s - c), \quad (\text{g/sec-m}^3) \quad (3.3.1)$$

where;

$$N = \text{average number of drops/cm}^3,$$

$$\text{or} \quad \phi_1 = c_1 (c_s - c), \quad (3.3.2)$$

where;

$$c_1 = \text{the term in brackets in Equation (3.3.1).}$$

The diffusivity immediately adjacent to the drop will be molecular so D will be retained in the coefficient c_1 . For $T = 25^\circ\text{C}$ and the previously reported values for D, v , δ , and Δ , c_1 becomes:

$$c_1 = 3.13 \left[\frac{aN}{\left(\frac{4.20 \times 10^{-4}}{a\phi} \right) + \left(\frac{a}{a+\Delta} \right)} \right], \quad (3.3.3)$$

$$\text{where;} \quad \phi = \exp \left(\frac{1.55 \times 10^{-7}}{a} \right).$$

Table 3.3.1 contains the results from calculations using Equation (3.3.3) and the spherical droplet volume for various values of the droplet radius, a.

In the model currently under development, an average value of c_1 will be chosen for the range of the most significant water vapor producing droplets, i.e. the droplets whose mass will contribute the most cooling upon evaporation. The initial droplet size distribution will be assumed to have

TABLE 3.3.1.1.--A comparison of values calculated from Equation (3.3.3) and the volume formula for a sphere for various droplet radii, a.

μ	a cm	$\frac{V}{\frac{4}{3}\pi\text{cm}^3}$	$\phi(a)$	$a+\Delta$ (cm)	$a\phi$ (cm)	$\frac{a}{a+\Delta}$	$c_{1/N}$ (1/sec)
1000	10^{-1}	10^{-3}	1	1.0×10^{-1}	1.0×10^{-1}	1	0.313
100	10^{-2}	10^{-6}	1	1.0×10^{-2}	1.0×10^{-2}	1	0.03
10	10^{-3}	10^{-9}	1	1.008×10^{-3}	1.0×10^{-3}	1	2.20×10^{-3}
1	10^{-4}	10^{-12}	1.00155	1.08×10^{-4}	1.00156×10^{-4}	0.994	6.03×10^{-5}
.1	10^{-5}	10^{-15}	1.0156	1.8×10^{-5}	1.0156×10^{-5}	0.555	7.48×10^{-7}
.01	10^{-6}	10^{-18}	1.1675	9.0×10^{-6}	1.1675×10^{-6}	0.111	8.70×10^{-9}

a mean radius in the 10 to 100 μ range. From the comparison of droplet volumes¹ in Table 3.3.1, it can be easily seen that the evaporation of droplets larger than 10 μ radius would affect the environmental cooling more than those less than 10 μ radius, by several orders of magnitude. Hence, the value of $\bar{c}_{1/N}$ to be chosen should be between 0.0022 and 0.03. The average value will be several orders of magnitude too large when the droplets become very small, but their negligible contribution to the cooling process will not introduce any significant error.

The sink term for energy removal will be the corresponding latent energy required for the evaporation source term. Thus,

$$\phi_2 = \frac{L_v}{\rho c_p} \phi_1, \quad (3.3.4)$$

where;

L_v = latent heat of vaporization, (cal/g), and the other symbols are as previously defined.

The increase in water vapor will be the negative of the evaporation source term so that the total mass of liquid plus water vapor remains constant. Thus,

$$\phi_3 = -\phi_1 \quad (3.3.5)$$

¹Since ρ_w is very nearly = 1 g/cm³ at ambient temperatures, the numerical values of the droplet mass and volume are the same.

3.4 Boundary Conditions

3.4.1 Lower Boundary Conditions

The problem being considered is one for a bare vegetationless surface. As demonstrated by Sutton (1953), pp. 139-140), the method of images can be used to establish a lower boundary condition of zero flux across the surface. For the liquid water droplets and the vapor concentration, the technique of images will be employed. It must be modified when a crop canopy is introduced, since the zero flux assumption is not applicable in the presence of evapotranspiration.

The lower boundary condition for heat flux will be determined by the energy balance at the surface. From Munn (1966),

$$Q_N = Q_G + Q_H + Q_E, \quad (3.4.1.1)$$

where;

Q_N = net all wavelength radiation, + → energy gained by the surface,

Q_G = heat transfer through the ground, + → downward flow,

Q_H = turbulent transfer of sensible heat to the atmosphere, + → upward flow,

and Q_E = latent heat flow, + → upward flow.

Q_E is identical to H in Section 2.3.

For zero flux of moisture across the surface,
 $Q_E = 0$. Therefore, after rearrangement Equation (3.4.1)
 becomes:

$$Q_H = Q_N - Q_G. \quad (3.4.1.2)$$

3.4.2 Upper Boundary Conditions

The upper boundary conditions for all three profiles will be ones of constancy. Since above a given level the modification process will have no affect, the values for temperature, moisture concentration, and liquid water concentration will remain equal to the initial conditions at that level.

$$T(x, z_{\max}) = T(0, z_{\max})$$

$$C(x, z_{\max}) = C(0, z_{\max}) \quad (3.4.2.1)$$

$$\chi(x, z_{\max}) = \chi(0, z_{\max})$$

4. SOLUTION TECHNIQUE

4.1 Method

The solution of Equations (3.1.2), (3.1.3) and (3.1.4) with the initial conditions, Equations (2.3.1), (2.3.3), (2.3.4) and (3.2.3), and boundary conditions, Equations (3.4.1.2) and (3.4.2.1), must be by numerical means. The method proposed by Richtmyer and Morton (1967, pp. 185-201) for the solution of equations with variable coefficients was rejected because the transformation of variables led to inconsistent boundary conditions. The methods reviewed by Harrington (1965), and the basic Crank-Nicolson method proposed therein would have required large amounts of computer space and time, since matrix inversions would have been necessary. The much faster and simpler form proposed by Spalding and Patankar (1968) has been adopted herein.

The solution technique is a marching-integration procedure whereby the values for the unknown variables will be evaluated in a stepwise manner downstream for all vertical nodes at each step. Thus no matrix inversions are required. The general Spalding-Patankar method has the additional advantages that uniform grid spacing is not required,

variable coefficients may be included, variable forward step increments are permitted and all forms of boundary conditions are permitted, i.e. constant values, constant gradients or entrainments along free boundaries.

The equations to be solved have the general form

$$\frac{\partial \phi}{\partial x} = \frac{1}{u(\omega)} \frac{\partial}{\partial \omega} (c(\omega) \frac{\partial \phi}{\partial \omega}) + d, \quad (4.1.1)$$

where;

ϕ = dependent variable,

x = distance along the mean horizontal direction
of flow,

ω = vertical axis,

u = vertical wind profile,

c = turbulent diffusivity,

and d = source term not containing terms of the
form $\partial \phi / \partial \omega$.

The variables used in the development of the solution technique correspond to those of Spalding and Patankar. The symbols previously used in this paper will be reintroduced upon actual solution.

The finite-difference equation to be derived from Equation (4.1.1) will not be by the use of Taylor-series expansion as is commonly done, e.g. Harrington (1965), Smith (1965), Richtmyer and Morton (1967), or any standard numerical analysis text. Instead, a miniature integral equation over a chosen control volume is used coupled with

an assumption regarding the nature of the variation of ϕ between the grid points. "In other words, the finite-difference equation is obtained by expressing each term in the parent differential equation as an integrated average over a small control volume. The advantage of this procedure is that, unlike the conventional method, it ensures that the conservation equation will be satisfied over any part of the boundary layer" (Spalding & Patankar, 1968, p. 35).

The grid and control volume used is shown in Figure 4.1.1,

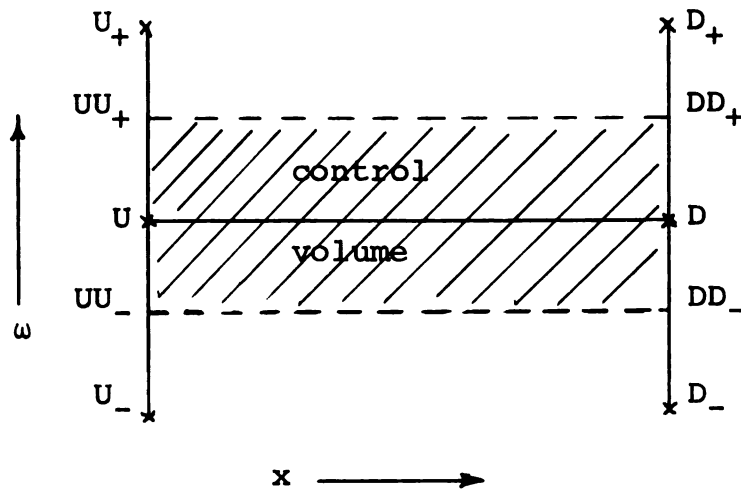


FIGURE 4.1.1.--Grid nomenclature and control volume to be used in the numerical solution scheme.

where;

U & D represent the upstream and downstream nodes respectively at a given ω ,

U_+ , U_- , D_+ , D_- represent corresponding adjacent points to U & D for adjacent ω values,

and UU_+ , UU_- , DD_+ , DD_- represent the midpoints that define the control volume between the indicated U's & D's.

The evaluation of the $\partial\phi/\partial\omega$ terms can be at x_U or x_D . As noted by Spalding and Patankar, since it can be shown that the use of the downstream station values are more accurate for large values of the forward step, yield stable solutions and are more convenient, the downstream evaluation will be the procedure adopted. To obtain equations linear in ϕ , any coefficients will always be evaluated from the known upstream values of ϕ . It is assumed that, in the ω direction, ϕ varies linearly with ω between grid points while in the x direction, the variation is considered to be stepwise. The values of ϕ for the interval $x_U < x < x_D$, therefore, will be uniform and equal to those at x_D . This is consistent with the decision to evaluate the $\partial/\partial\omega$ terms at x_D .

4.2 Development of the Finite Difference Equations

To obtain the finite difference equations, each term in Equation (4.1.1) must be expressed as an integrated average over the indicated control volume. Thus the expression to be evaluated for the first term is:

$$\frac{\partial\phi}{\partial x} \approx \left\{ \int_{x_U}^{x_D} \int_{\omega_{DD-}}^{\omega_{DD+}} \left(\frac{\partial\phi}{\partial x} \right) d\omega dx \right\} / \left\{ (x_D - x_U) (\omega_{DD+} - \omega_{DD-}) \right\} .$$

(4.2.1)

This is identical to Spalding & Patankar's Equation (2.4.1).

The results are:

$$\frac{\partial \phi}{\partial x} \approx P_1 (\phi_{D+} - \phi_{U+}) + P_2 (\phi_D - \phi_U) + P_3 (\phi_{D-} - \phi_{U-}), \quad (4.2.2)$$

where;

$$P_1 \equiv \frac{(\omega_{D+} - \omega_D)}{4(\omega_{D+} - \omega_{D-})(x_D - x_U)}; \quad P_2 \equiv \frac{3}{4(x_D - x_U)},$$

and

$$P_3 \equiv \frac{\omega_D - \omega_{D-}}{4(\omega_{D+} - \omega_{D-})(x_D - x_U)}.$$

(Note: a typographical error in the expression for P_1 reported by Spalding and Patankar has been corrected). The expression for the flux term is:

$$\frac{1}{u(\omega)} \frac{\partial}{\partial \omega} (c(\omega) \frac{\partial \phi}{\partial \omega}) \approx \left\{ \int_{x_U}^{x_D} \int_{\omega_{DD-}}^{\omega_{DD+}} \frac{1}{u(\omega)} \frac{\partial}{\partial \omega} (c(\omega) \frac{\partial \phi}{\partial \omega}) d\omega dx \right\} /$$

$$\{ (x_D - x_U) (\omega_{DD+} - \omega_{DD-}) \}. \quad (4.2.3)$$

Since $u(\omega) \neq f(x)$ and $\partial/\partial\omega$ are to be evaluated at x_D , Equation (4.2.3) reduces immediately to:

$$\frac{1}{u(\omega)} \frac{\partial}{\partial \omega} (c(\omega) \frac{\partial \phi}{\partial \omega}) \approx \left\{ \int_{\omega_{DD-}}^{\omega_{DD+}} \frac{1}{u(\omega)} \frac{\partial}{\partial \omega} (c(\omega) \frac{\partial \phi}{\partial \omega}) d\omega \right\} /$$

$$(\omega_{DD+} - \omega_{DD-}). \quad (4.2.4)$$

The integration must be performed by parts,

$$\int u dv = uv - \int v du.$$

Let $u = 1/u(\omega)$ and $dv = \frac{\partial}{\partial \omega} (c(\omega) \frac{\partial \phi}{\partial \omega}) d\omega$,

then $du = -\frac{1}{u^2(\omega)} \frac{\partial u}{\partial \omega} d\omega$ and $v = c(\omega) \frac{\partial \phi}{\partial \omega}$.

Equation (4.2.4) becomes:

$$\begin{aligned} \frac{1}{u(\omega)} \frac{\partial}{\partial \omega} (c(\omega) \frac{\partial \phi}{\partial \omega}) &\approx \left\{ \frac{1}{u(\omega)} (c(\omega) \frac{\partial \phi}{\partial \omega}) \Big|_{\omega_{DD-}}^{\omega_{DD+}} - \int_{\omega_{DD-}}^{\omega_{DD+}} [c(\omega) \frac{\partial \phi}{\partial \omega}] \left[\frac{-1}{u^2(\omega)} \frac{\partial u}{\partial \omega} \right] d\omega \right\} / \\ &\quad (\omega_{DD+} - \omega_{DD-}) \\ &= \left\{ \frac{1}{u_{DD+}} c_{DD+} \left(\frac{\partial \phi}{\partial \omega} \right)_{DD+} - \frac{1}{u_{DD-}} c_{DD-} \left(\frac{\partial \phi}{\partial \omega} \right)_{DD-} + \int_{\omega_{DD-}}^{\omega_{DD+}} [c(\omega) \frac{\partial \phi}{\partial \omega}] \right. \\ &\quad \left. \left[\frac{-1}{u^2(\omega)} \frac{\partial u}{\partial \omega} \right] d\omega \right\} / (\omega_{DD+} - \omega_{DD-}) \end{aligned} \quad (4.2.5)$$

Since in this problem, functional forms of $u(\omega)$ and $c(\omega)$ are known, the midpoint calculations can be made. The evaluation of the partial derivatives must be made in conjunction with the assumed linearity of ϕ with ω between nodes. Thus

$$\left(\frac{\partial \phi}{\partial \omega} \right)_{DD+} = \frac{\phi_{D+} - \phi_D}{\omega_{D+} - \omega_D}; \quad \left(\frac{\partial \phi}{\partial \omega} \right)_{DD-} = \frac{\phi_D - \phi_{D-}}{\omega_D - \omega_{D-}}$$

and $(\omega_{DD+} - \omega_{DD-}) = \left(\frac{\omega_{D+} - \omega_{D-}}{2} \right).$ (4.2.6)

The integration is performed using Simpson's rule:

$$I_S = \int_{x_0}^{x_0+2\Delta x} y(x) dx \approx \frac{\Delta x}{3} (y_0 + 4y_1 + y_2). \quad (4.2.7)$$

This technique requires that Δx be constant. Thus the general Spalding-Patankar technique has become modified by requiring $\Delta \omega$ to be uniform or at least a very slowly changing value between nodes.

For this case $x_0 = \omega_{DD-}$, $x_0 + 2\Delta x = \omega_{DD+}$, and therefore $\Delta x = \frac{1}{4}(\omega_{D+} - \omega_{D-})$.

Since the ω increment is now required to be constant, let

$$\omega_{D+} - \omega_{D-} = \omega_D - \omega_{D-} = \Delta \omega$$

Now $\Delta x = \frac{1}{4}(2\Delta \omega) = \frac{\Delta \omega}{2}$ and Equation (4.2.7) is:

$$\begin{aligned} I_S = \int_{\omega_{DD-}}^{\omega_{DD+}} (c(\omega) \frac{\partial \phi}{\partial \omega}) \left(\frac{1}{u^2(\omega)} \frac{\partial u}{\partial \omega} \right) d\omega \approx \frac{\Delta \omega}{2(3)} [(c(\omega) \frac{\partial \phi}{\partial \omega}) \left(\frac{1}{u^2(\omega)} \right) \left(\frac{\partial u}{\partial \omega} \right) \Big|_{DD-} \\ + 4 (c(\omega) \frac{\partial \phi}{\partial \omega}) \left(\frac{1}{u^2(\omega)} \right) \left(\frac{\partial u}{\partial \omega} \right) \Big|_D \\ + (c(\omega) \frac{\partial \phi}{\partial \omega}) \left(\frac{1}{u^2(\omega)} \right) \left(\frac{\partial u}{\partial \omega} \right) \Big|_{DD+}]. \end{aligned} \quad (4.2.8)$$

If one uses the results of Equations (4.2.6) in Equation (4.2.8) and notes that

$$\left(\frac{\partial \phi}{\partial \omega} \right)_D \approx \left(\frac{\phi_{D+} - \phi_{D-}}{\omega_{D+} - \omega_{D-}} \right), \quad (4.2.9)$$

the integral becomes:

$$\begin{aligned}
I_S \approx & \frac{\Delta\omega}{2(3)} \left\{ c_{DD-} \left(\frac{\phi_{D+} - \phi_{D-}}{\omega_{D+} - \omega_{D-}} \right) \left(\frac{1}{u_{DD-}} \right) \left(\frac{\partial u}{\partial \omega} \right)_{DD-} \right. \\
& + 4 \left[c_D \left(\frac{\phi_{D+} - \phi_{D-}}{\omega_{D+} - \omega_{D-}} \right) \left(\frac{1}{u_D} \right) \left(\frac{\partial u}{\partial \omega} \right)_D \right] \\
& \left. + c_{DD+} \left(\frac{\phi_{D+} - \phi_{D-}}{\omega_{D+} - \omega_{D-}} \right) \left(\frac{1}{u_{DD+}} \right) \left(\frac{\partial u}{\partial \omega} \right)_{DD+} \right\}. \quad (4.2.10)
\end{aligned}$$

After substituting the above expressions into Equation (4.2.5), rearranging and collecting like terms, the general expression for the flux term is found to be:

$$\frac{1}{u(\omega)} \frac{\partial}{\partial \omega} (c(\omega) \frac{\partial \phi}{\partial \omega}) \approx (P_4 + P_5) \phi_{D+} + (P_6 - P_4) \phi_D - (P_5 + P_6) \phi_{D-}, \quad (4.2.11)$$

where;

$$P_4 = \left(\frac{2}{\omega_{D+} - \omega_{D-}} \right) \left\{ \frac{1}{\omega_{D+} - \omega_D} \frac{c_{DD+}}{u_{DD+}} \left[1 + \frac{\Delta\omega}{2(3)u_{DD+}} \left(\frac{\partial u}{\partial \omega} \right)_{DD+} \right] \right\},$$

$$P_5 = \left(\frac{1}{\omega_{D+} - \omega_{D-}} \right) \left(\frac{4\Delta\omega}{3u_D(\omega_{D+} - \omega_{D-})} \right) \left(\frac{c_D}{u_D} \right) \left(\frac{\partial u}{\partial \omega} \right)_D,$$

and

$$P_6 = \left(\frac{2}{\omega_{D+} - \omega_{D-}} \right) \left\{ \frac{1}{(\omega_D - \omega_{D-})} \left(\frac{c_{DD-}}{u_{DD-}} \right) \left[\left(\frac{\Delta\omega}{2(3)u_{DD-}} \right) \left(\frac{\partial u}{\partial \omega} \right)_{DD-} - 1 \right] \right\}.$$

Under the restriction of the uniform grid spacing, the expressions for the P's become:

$$P_1 = P_3 = 1/8\Delta x, \quad (4.2.12)$$

$$P_2 = 3/4\Delta x,$$

$$P_4 = \frac{1}{(\Delta\omega)^2} \left(\frac{c}{u}\right)_{DD+} \left[1 + \frac{\Delta\omega}{6u_{DD+}} \left(\frac{\partial u}{\partial \omega}\right)_{DD+}\right],$$

$$P_5 = \frac{1}{3\Delta\omega u_D} \left(\frac{c}{u}\right)_D \left(\frac{\partial u}{\partial \omega}\right)_D,$$

$$\text{and } P_6 = \frac{1}{(\Delta\omega)^2} \left(\frac{c}{u}\right)_{DD-} \left[\frac{\Delta\omega}{6u_{DD-}} \left(\frac{\partial u}{\partial \omega}\right)_{DD-} - 1\right].$$

The source term must now be included in the finite difference equation. The value of d will be assumed uniform over the control volume and equal to that at D . Since d may not be linear with ϕ , it can be approximated by

$$d_D \approx d_U + \left(\frac{\partial d}{\partial \phi}\right)_U (\phi_D - \phi_U). \quad (4.2.13)$$

The expression to be evaluated becomes

$$d \approx \int_{\omega_{DD-}}^{\omega_{DD+}} (d)_{x=x_D} d\omega / (\omega_{DD+} - \omega_{DD-}). \quad (4.2.14)$$

If one assumes d is linear with ω between grid points, Equation (4.2.14) can be broken into two parts and evaluated from ω_{DD-} to ω_D and from ω_D to ω_{DD+} . Since d is assumed linear in these intervals, it can be easily shown that the average value of d for the interval is $\bar{d} = \frac{1}{4}(3d_D + d_{Di})$, where i is $-$ or $+$ for the respective interval. By performing the indicated operations with equations (4.2.13) and

and (4.2.14) and employing the definitions of the P's, one obtains

$$d \approx G_1 \phi_{D+} + G_2 \phi_D + G_3 \phi_{D-} + G_4, \quad (4.2.15)$$

where;

$$G_1 = P_1 \left(\frac{\partial d}{\partial \phi} \right)_{U+} (x_D - x_U),$$

$$G_2 = P_2 \left(\frac{\partial d}{\partial \phi} \right)_U (x_D - x_U),$$

$$G_3 = P_3 \left(\frac{\partial d}{\partial \phi} \right)_{U-} (x_d - x_U),$$

and

$$G_4 = \left\{ P_1 \left[d_{U+} - \left(\frac{\partial d}{\partial \phi} \right)_{U+} \phi_{U+} + P_2 d_{U-} - \left(\frac{\partial d}{\partial \phi} \right)_U \phi_U \right] \right. \\ \left. + P_3 \left[d_{U-} - \left(\frac{\partial d}{\partial \phi} \right)_{U-} \phi_{U-} \right] \right\} (x_D - x_U).$$

After substituting Equations (4.2.2), (4.2.11) and (4.2.15) into Equation (4.1.1) and collecting like terms, one obtains the finite difference equations:

$$\phi_D = A \phi_{D+} + B \phi_{D-} + C \quad (4.2.16)$$

where;

$$A = (P_4 + P_5 - P_1 + G_1) / (P_2 - P_6 + P_4 - G_2),$$

$$B = -(P_3 + P_5 + P_6 - G_3) / (P_2 - P_6 + P_4 - G_2),$$

and

$$C = (P_1 \phi_{U+} + P_2 \phi_U + P_3 \phi_{U-} + G_4) / (P_2 - P_6 + P_4 - G_2).$$

It can be shown by using the Gaussian elimination method that the solution of Equation (4.2.16) can be obtained from:

$$\phi_i = A'_i \phi_{i+1} + B'_i \quad (4.2.17)$$

where; A'_i & B'_i are the recursion formulae:

$$A'_2 = A_2$$

$$A'_i = A_i / (1 - B_i A'_{i-1}), \quad i > 2,$$

$$B'_2 = B_2 \phi_1 + C_2,$$

and $B'_i = (B_i B'_{i-1} + C_i) / (1 - B_i A'_{i-1}), \quad i > 2.$

The general form of the solution is thus established by Equation (4.2.17) and the preceding parametric definitions.

4.3 Parameter Evaluation

The conversion from the general Spalding-Patankar symbols to the symbols of the specific problem to be solved are summarized in Table 4.3.1.

The temperature range of applicability of this model will be from 20°C to 50°C, since this range extends beyond the active plant growing temperature extremes for which cooling would be required and/or desirable. The ambient moisture conditions will range from very dry at the high temperatures to nearly saturated at the lower temperatures.

TABLE 4.3.1.--A summary of the general Spalding-Patankar symbols and the specific symbols of the equations to be solved.

General Spalding-Patankar Symbols	Specific Problem Symbols		
	Liquid Water Concentration	Energy	Water Vapor Concentration
ω	ζ	ζ	ζ
$c(\omega)$	$K_C(\zeta)$	$K_H(\zeta)$	$K_\chi(\zeta)$
$\phi(\omega)$	$C(\zeta)$	$T(\zeta)$	$\chi(\zeta)$
d	$\phi_1/u(\zeta)$	$\phi_2/u(\zeta)$	$\phi_3/u(\zeta)$

The variation in several atmospheric parameters of interest within this temperature and moisture range are namely: (1) mixing ratio, (2) compressibility factor i.e. deviation from the ideal gas law, (3) moist air density, (4) moisture concentration, (5) isobaric specific heat, (6) moist air heat capacity, (7) latent heat of vaporization, and (8) evaporative cooling rate. The following is a summary of the definitions and calculation procedures for the above parameters.

$$\text{Mixing ratio, } W = \text{R.H.} \times W_s, \text{ (g/kg),} \quad (4.3.1)$$

where:

R.H. = relative humidity in decimal form,

and W_s = saturated mixing ratio, (g/kg).

The moist air density and compressibility factor, are defined by the gas law, [List (1966, p. 295)],

$$\rho = \frac{P}{C_f R_{da} T_v}, \quad (4.3.2)$$

where;

ρ = ambient density of moist air,

P = ambient atmospheric pressure,

C_f = compressibility factor representing deviation from ideal gas,

R_{da} = dry air gas constant, (2.8704×10^6 erg/g- $^{\circ}$ K),

T_v = virtual temperature, ($^{\circ}$ K),

$$= \frac{1+W/\epsilon}{1+W} T_A$$

ϵ = ratio of the molecular weight of water vapor to the molecular weight of dry air, (0.62197), [List, (1966, p. 332)].

T_A = absolute temperature, ($^{\circ}$ K),

and W = actual mixing ratio, (g/g).

Moisture concentration, χ , is found by:

$$\chi = \frac{W}{1+W} \rho, \quad (4.3.3)$$

where W and ρ are as defined above.

The isobaric specific heat for moist air is, [List (1966, p. 339)]

$$c_p = 0.2399 + 0.4409 + \Delta c_p, \quad (4.3.4)$$

where; Δc_p = isobaric specific heat residual,

and W is as defined above.

The moist air heat capacity and evaporative cooling coefficient are given by (ρc_p) and $(L_v/\rho c_p)$ respectively, where;

L_v = the latent heat of vaporization for water.

The results of these calculations are given in Table 4.3.2 for an atmospheric pressure of 1000 mb.

A close examination of various sections of Table 4.3.2 leads one to the following conclusions:

<u>SECTION EXAMINED</u>	<u>CONCLUSION</u>
1. Compressibility Factor	The deviation of moist air from an ideal gas is negligible.
2. Evaporative Cooling Parameter	The evaporative cooling rate will be on the order of 2°C per gram of water evaporated per cubic meter.
3. Moisture Concentrations and Evaporative Cooling Parameter	The maximum cooling under normal conditions will be less than 20°C.
4. Moist Air Density, Iso-baric Specific Heat, Latent Heat of Vaporization, Heat Capacity, and Evaporative Cooling Rate	All can be assumed constant and evaluated at an intermediate value within the range of conditions applicable to a specific problem. The maximum errors so incurred will be about 3% for the extreme conditions of initially 50°C air cooled to 30°C.

The implied assumption in the development of Equation (3.1.4) that $\rho c_p = \text{constant}$ is completely justified by conclusion (4) above.

For the evaluation of the solution coefficients G1, G2, G3, and G4, not only the values of d are required but

TABLE 4.3.2.--A summary of the variability in the moist air parameters for the temperature and moisture range pertinent to the model being developed and for P=1000 mb.

Temperature T	Mixing Ratio W (g/kg)			Compressibility Factor ³ C _f			
	R.H., %			R.H., %			
	25	50	75	25	50	75	
°C	100 ²	100 ²	100 ²				
°F	25	50	75	25	50	75	
50	122	22.03	44.06	66.09	88.12	.9998	.9996
40	104	12.45	24.90	37.35	49.81	.9997	.9997
30	86	6.92	13.85	20.77	27.69	.9997	.9997
20	68	3.74	7.48	11.22	14.95	.9996	.9996

¹List (1966), Table 4, p. 26.

²List (1966), Table 73, pp. 303, 304.

³List (1966), Table 84, p. 333.

TABLE 4.3.2.--Continued.

T °C	Virtual Temperature Increment ⁴ ΔT , (°C)			Adjusted Virtual Temperature ⁵ $T' = C_f T$, (°C)			Dry Air ⁶ Density ρ_{da} , (kg/m ³) (kg/m ³)
	R.H., %			R.H., %			
	25	50	75	25	50	75	
50	4.24	8.29		54.2	58.3		1.078
40	2.34	4.63	6.85	42.3	44.6	46.9	1.112
30	1.27	2.52	3.76	31.3	32.5	33.8	1.149
20	.66	1.32	1.97	20.7	21.3	22.0	1.188

⁴List (1966), Table 72, pp. 295-301.

⁵The Compressibility was neglected

⁶List (1966), Table 71, p. 293.

TABLE 4.3.2.--Continued.

T	Moist Air Density ⁷ ρ , (kg/m ³)			Moisture Concentration X , (g/m ³)		
	25	50	75	25	50	75
°C	R.H., %			R.H., %		
	25	50	75	100	100	100
50	1.064	1.051		22.9	44.5	
40	1.104	1.096	1.088	13.6	26.6	39.2
30	1.144	1.140	1.135	7.88	15.56	23.0
20	1.186	1.183	1.180	4.41	8.80	13.1
						17.5

⁷List (1966) Table 71, pp. 293, 294.

TABLE 4.3.2.--Continued.

T °C	Isobaric Specific Heat Residual ⁸ , Δc_p			Isobaric Specific Heat c_p , (cal/g - °C)				
	R.H., %			R.H., %				
	25	50	75	100	26	50	75	100
50	.0009	.0013			.250	.261		
40	.0007	.0008	.0012	.0014	.246	.252	.258	.263
30	.0005	.0006	.0007	.0008	.244	.247	.250	.253
20	.0004	.0004	.0005	.0006	.242	.244	.245	.247

⁸List (1966), Table 88, p. 339.

TABLE 4.3.2.--Continued.

T °C	Heat Capacity of Moist Air ρc_p , (cal/m ³ -°C)			Latent Heat of Vapori- zation ⁹ L_v (cal/g)	Evaporative Cooling Parameter $L_v/\rho c_p$, (°C/(g/m ³))		
	R.H., %				R.H., %		
	25	50	75		100	25	50
50	266	274		569.0	2.14	2.08	
40	272	276	281	574.7	2.11	2.08	2.04
30	280	282	284	580.4	2.07	2.06	2.04
20	287	289	290	586.0	2.04	2.03	2.02

⁹List (1966), Table 92, p. 343.

also the values of $\partial d/\partial \phi$. For the liquid water droplet equation this becomes

$$\frac{\partial d_1}{\partial \phi_1} = \frac{\partial}{\partial C} \left[\frac{-c_1 (\chi_s - \chi)}{u(\zeta)} \right]. \quad (4.3.5)$$

Since c_1 and $u(\zeta)$ are assumed constant during the modification process, Equation (4.3.5) becomes:

$$\frac{\partial d_1}{\partial \phi_1} = \frac{-c_1}{u(\zeta)} \frac{\partial}{\partial C} (\chi_s - \chi) = \frac{-c_1}{u(\zeta)} \frac{\partial \chi_s}{\partial T} - \frac{\partial \chi}{\partial T} \left(\frac{\partial T}{\partial C} \right). \quad (4.3.6)$$

If one uses an energy balance, it can be easily seen that the change in T due to the evaporation of liquid water is $L_v/\rho c_p$ and therefore,

$$\frac{\partial d_1}{\partial \phi_1} = \frac{-c_1}{u(\zeta)} \left(\frac{L_v}{\rho c_p} \right) \left[\frac{\partial \chi_s}{\partial T} - \frac{\partial \chi}{\partial T} \right]. \quad (4.3.7)$$

If one uses the moist air relationships, List (1966, p. 347), assumes the water vapor behaves as an ideal gas and uses the Clausius-Clapeyron equation, Hess (1959, p. 48), it can be shown that

$$\frac{\partial \chi_s}{\partial T} = \frac{\chi_s P L_v}{R_v (P - (1-\epsilon) e_s) (T+273.16)^2}, \quad (4.3.8)$$

and
$$\frac{\partial \chi}{\partial T} = \frac{-P}{(1-\epsilon) R_v (T+273.16)^2}, \quad (4.3.9)$$

where:

P = ambient atmospheric pressure, (mb),

R_v = specific gas constant for water vapor,
(0.110226 cal/g-°C) [List, (1966, p. 289)].

and the others are as previously defined. If one substitutes Equations (4.3.8) and (4.3.9) into Equation (4.3.7), converts all units for homogeneity and simplifies the expression, one obtains;

$$\frac{\partial d_1}{\partial \phi_1} = \frac{-c_1 L_v P}{\rho c_p R_v u(\zeta) (T+273.16)^2 (41.8684)} \times \left[\frac{0.0418684 L_v \chi_s}{P - (1-\epsilon) e_s} + \frac{1}{(1-\epsilon)} \right]. \quad (4.3.10)$$

Let:

$$A_1 = -c_1 L_v P / (41.8684 \rho c_p R_v),$$

$$A_2 = 0.0418684 L_v,$$

and $A_3 = (1-\epsilon),$

then;

$$\frac{\partial d_1}{\partial \phi_1} = \frac{A_1}{u(\zeta) (T+273.16)^2} \left[\frac{A_2 \chi_s}{P - A_3 e_s} + \frac{1}{A_3} \right]. \quad (4.3.11)$$

The $\partial d / \partial \phi$ term for the energy equation is:

$$\frac{\partial d_2}{\partial \phi_2} = \frac{\partial}{\partial T} \left[\frac{-L_v}{\rho c_p} \left(\frac{c_1}{u(\zeta)} (\chi_s - \chi) \right) \right]. \quad (4.3.12)$$

The term $(L_v/\rho c_p)$ has been assumed constant, thus Equation (4.3.12) reduces to Equation (4.3.7)

$$\text{and} \quad \frac{\partial d_2}{\partial \phi_2} = \frac{\partial d_1}{\partial \phi_1}. \quad (4.3.13)$$

The $\partial d/\partial \phi$ term for the water vapor equation is

$$\frac{\partial d_3}{\partial \phi_3} = \frac{\partial}{\partial \chi} \left[\frac{c_1}{u(\zeta)} (\chi_s - \chi) \right], \quad (4.3.14)$$

which can be rewritten as:

$$\frac{\partial d_3}{\partial \phi_3} = \frac{c_1}{u(\zeta)} \left[\frac{\partial \chi_s}{\partial \chi} - 1 \right] = \frac{c_1}{u(\zeta)} \left[\frac{\partial \chi_s}{\partial T} \cdot \frac{\partial T}{\partial \chi} - 1 \right]. \quad (4.3.15)$$

Since $\frac{\partial T}{\partial \chi} = 1/(\partial \chi/\partial T)$, if one substitutes Equations (4.3.8) and (4.3.9) into Equation (4.3.15) it yields

$$\frac{\partial d_3}{\partial \phi_3} = \frac{-c_1}{u(\zeta)} (1-\epsilon) \left[\frac{0.0418684 L_v \chi_s}{P - (1-\epsilon) e_s} + \frac{1}{1-\epsilon} \right]. \quad (4.3.16)$$

If one compares Equations (4.3.10), (4.3.11), and (4.3.16), the latter is easily seen to be:

$$\frac{\partial d_3}{\partial \phi_3} = \frac{-c_1 A_3}{u(\zeta)} \left[\frac{A_2 \chi_s}{P - A_3 e_s} + \frac{1}{A_3} \right]. \quad (4.3.17)$$

4.4 Solution Procedure

The solution procedure is to: (1) diffuse the evaporating liquid water droplets from $x = x_U$ to $x = x_D$ and determine the new profile; (2) solve the energy diffusion equation for the same step; (3) solve the water vapor diffusion equation for the same step; (4) check the vapor concentration values for misapportionment with respect to the saturated vapor concentration values at the computed temperatures in step 2; (5) if inconsistent values are found, reapportion the error by a halving iteration in proportion to the concentration at the nodes, adjust the temperature and liquid water profiles accordingly, and print out the adjustments required; (6) sum the integrated liquid and water vapor profiles to verify the continuity of total moisture; and (7) allow this procedure to continue until an arbitrarily small amount of liquid water remains as determined by the integration of the liquid water profile. For this problem, the limiting value will be $0.05 \text{ g/m}_y\text{-sec}$. Beyond this point the diffusion of energy and water vapor will continue with the source terms equated to zero.

A computer program was written in FORTRAN IV language to solve the problem, (see Appendix C). A second program was written utilizing a graphing subroutine,

GRAPHL, [See Breasbois and Nurnberger (1970)] developed for this project to plot field data and model results on the CALCOMP x-y plotter. All programs were executed on the CDC-3600 computer in the Computer Center at Michigan State University, East Lansing, Michigan.

5. EXPERIMENTAL PROCEDURE

5.1 Site Selection

The experimental site requirements for this investigation are: (1) level uniform ground; (2) clear upwind fetch; (3) dry vegetation free strip, and (4) an ample clean water supply. Various values for the ratio of the fetch to measurement height have been suggested for uniform re-establishment of the boundary layer. Some of the investigators and their suggested values are: Inoue, et al. (1958), 100:1; Priestly (1959), 20:1; Brooks (1961), 50 tree heights for an accuracy of 3%; Dyer (1962), a range of 140 to 330 for measurements between .5 and 10m respectively under neutral stability; and Panofsky and Townsend (1964), 10:1.

The site selected for this investigation was a 40 acre (16.2 hectare), square, grass covered field at the Michigan State University Experimental Muck Farm. The minimum fetch to tree height ratio was approximately 20:1. The fetch over the bare strip to the spray line compared to the upwind grass height was maintained at a minimum of 200:1. A strip 300 m long and 120 m wide was established with a NW-SE orientation across the northeast corner of

the field to take maximum advantage of the normal southerly to westerly wind direction. The strip was plowed, tilled, leveled, and sprayed with herbicides to establish a vegetation free surface.

5.2 Water Supply System

The spray line was positioned along the center of the bared strip. The construction of the line consisted of a base feeder pipe of 3 inch irrigation pipe with welded couplings and 3/4 inch galvanized steel pipe risers supplying an elevated 3/4 inch line. The elevated line was positioned at a height of 1 m with Bette fog nozzles pointed downward spaced at intervals of 2/3 m. The nozzle selection and spacing was based upon preliminary laboratory studies by Schissler (1968). The nozzles were calibrated by collecting their discharge in graduated cylinders for one minute time periods.

Water was supplied to the center of the line through a 3 inch feeder line by a high pressure, 125 psi, low volume pump located off of the bared strip on the downwind grass. Two 4 ft high by 18 ft diameter above ground swimming pools were utilized as water reservoirs for a total capacity of approximately 18,000 gallons. The large capacity assured constant water temperature and a slowly changing supply head during any test run. The

water from each pool was filtered by two 100 mesh well point screens on the pump intake. Figure 5.2.1 illustrates the schematic arrangement of the experimental site.

5.3 Instrumentation

5.3.1 Profile Measurements

Profile measurement masts were constructed from 30 foot sections of 3 inch aluminum irrigation pipe mounted on tilt up bases which were staked to the ground. Instrument arms were constructed of 1/2 inch diameter galvanized steel pipe and mounted on the masts with saddle-T risers. The instruments were mounted 2 feet outward from the main mast support. The mast array consisted of five masts aligned normal to the spray line. For convenience in identification, the masts will be referred to by number. Mast number 1 was 10 m upwind from the spray line to monitor initial conditions. Masts 2 through 5 were at 10 m intervals downstream from the spray line starting with mast 2, 10 m downstream.

Wind speed profiles were measured on Masts 1 and 3 with Climet 3-cup anemometers mounted at the 1 m, 2 m, 4 m and 8 m levels.

Temperature and moisture profiles were made on all masts at the 1 m, 2 m, 4 m, 6 m, and 8 m levels with aspirated constant water level radiation shielded psychrometers. The psychrometers were constructed as shown in

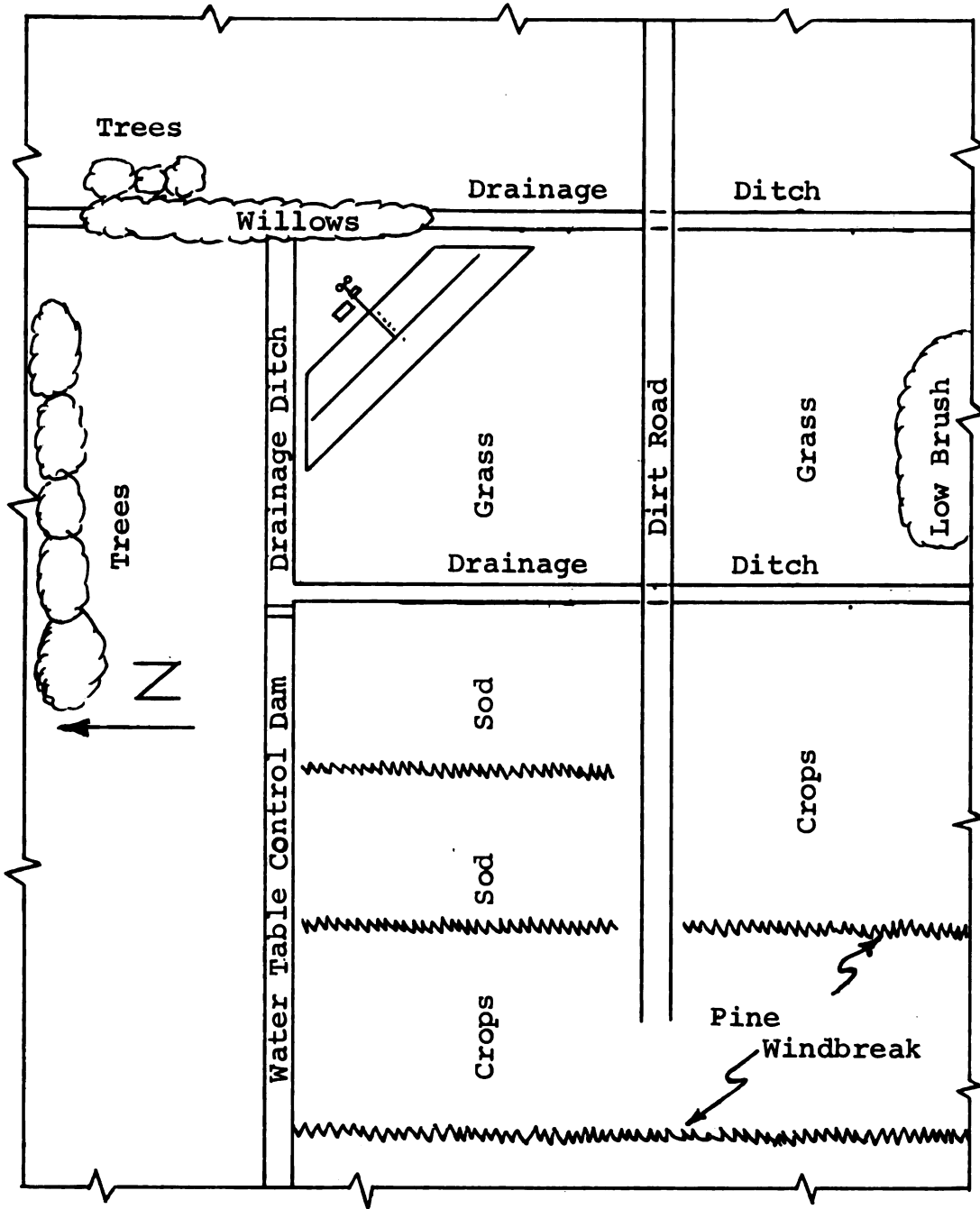


FIGURE 5.2.1.1.--Schematic diagram of the experimental site.

Figures 5.3.1.1, 5.3.1.2 and 5.3.1.3 using dual bakelite tubes for radiation shielding, a squirrel cage fan for aspiration, plexiglass water reservoir and constant water level well, and Yellow Springs Instruments thermo-linear thermistors as the dry and wet bulb sensing elements.

The mast instrumentation is shown in Figures 5.3.1.4 and 5.3.1.5.

The thermistors were calibrated in the lab by testing in a constant temperature water bath at temperatures of 20°C, 30°C, 40°C and 50°C. From an initial supply of 100 thermistors, 60 were selected that were the most closely matched and incorporated into 30 psychrometers, thus providing 5 spare psychrometers.

The digital data signals from the eight light chopper type anemometers and the millivolt analog data from the psychrometers were transmitted via wire to a data acquisition system designed for this project by Information Instruments Inc. of Ann Arbor, Michigan, Figure 5.3.1.6. The anemometer data pulses were counted, the psychrometers scanned sequentially, the analog signals converted to digital data, and all data punched onto paper tape in binary coded decimal at the rate of two cycles per minute. A FORTRAN IV computer program was written to interpret the paper tape, write the data onto magnetic tape, and analyze the data.

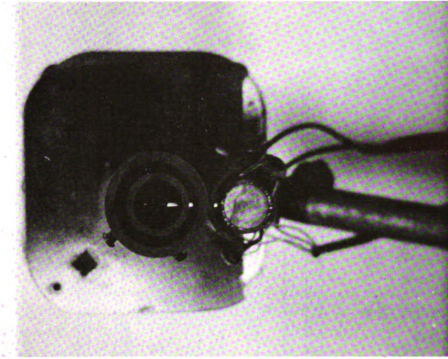


FIGURE 5.3.1.2.--Bottom view of the psychrometer's radiation shielding and sensing unit.

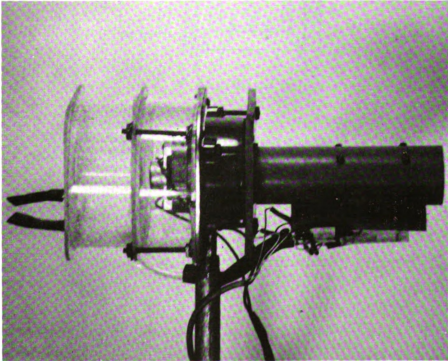


FIGURE 5.3.1.1.--Psychrometer unit. Top section is the water reservoir, middle section is the fan unit, and the bottom section is the radiation shielding and sensing unit.

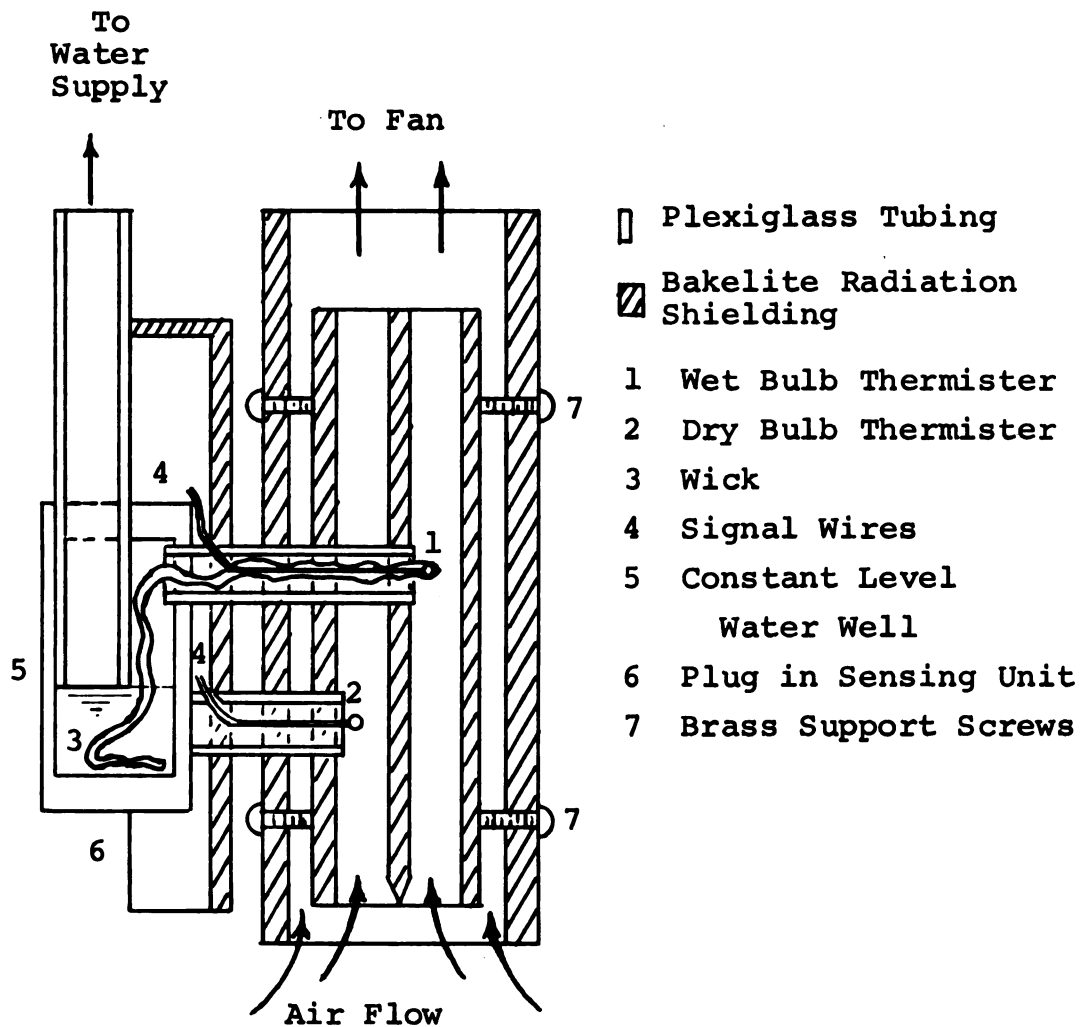


FIGURE 5.3.1.3.--Cross sectional schematic diagram of the psychrometer sensing unit and radiation shielding.

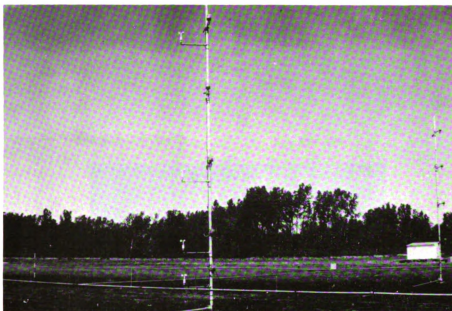


FIGURE 5.3.1.4.--Instrumentation arrangement on Masts 1 and 2 with the elevated spray line in the background.



FIGURE 5.3.1.5.--A close up view of the anemometer and a psychrometer arrangement.

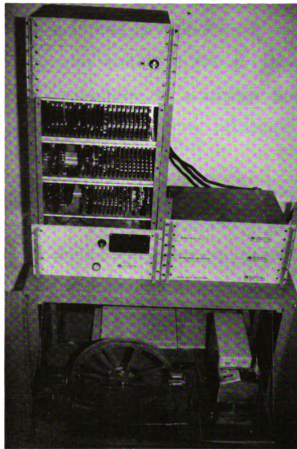


FIGURE 5.3.1.6.--Data acquisition system.

5.3.2 Other Measurements

Wind direction was measured with a Climet anemovane and Esterline-Angus strip chart recorder. The calibration was by distant range pole alignment at 0,15,30, and 45° from the mast array.

Net solar radiation was measured by a Beckman & Whitley net radiometer and recorded on a Brown single pen strip chart recorder modified for millivolt input. Calibration was by comparison to a shaded and unshaded pyroheliometer and evaluated by the calibration factor supplied by the manufacturer.

The soil temperature profile was measured at 2.5 cm intervals to a depth of 60 cm by copper-constantan thermocouples and a Leeds and Northrup 24-point recorder. The top thermocouple was immediately below the soil surface with a thin layer of soil to cover it.

Soil heat flux was measured by a Thornthwaite heat flux plate and a Leeds and Northrup pen recorder. The heat flux plate was placed immediately below the soil surface with a thin layer of soil to cover the sensor. The calibration chart was supplied by the manufacturer.

A schematic diagram of the instrumentation arrangement is shown in Figure 5.3.2.1.

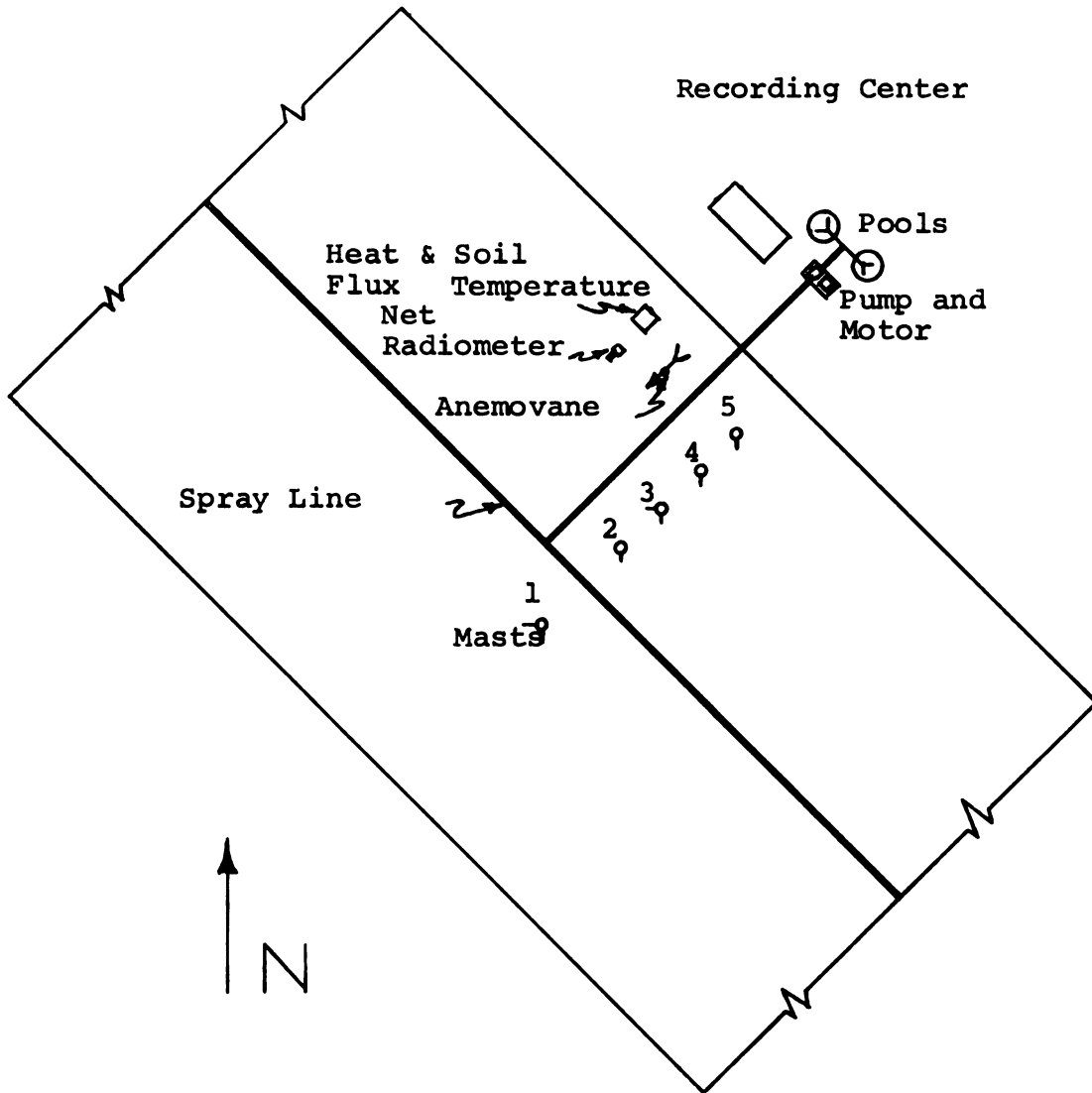


FIGURE 5.3.2.1.--Schematic diagram of the instrumentation and spray line.

6. EXPERIMENTAL RESULTS

6.1 Test Conditions

The data herein reported was collected during an experimental test on 12 September, 1970, under a cloudless sky. The reported data were the results of an average of the data recorded for each sensing element for a 30 minute time period. The test run was terminated when a dense altostratus cloud cover approached. The ambient atmospheric pressure was 984.8 mb. The average spray rate was 8 g/m-sec.

6.2 Wind Speed and Direction

The average wind direction was at an angle of 25 degrees from the normal to the spray line. The deviation from perpendicularity to the spray line resulted in the masts being positioned at different effective distances. The mast positions are summarized in Table 6.2.1. The wind speed data is given in Appendix B, Table B1. The anemometer on mast 3 at the 8 m level was inoperative.

The wind speed profiles are shown in Figure 6.2.1 as the upwind mast, A, and the downwind mast, B. The solid curve is the Swinbank profile for this time period. The values of the profile parameters were found to be:

TABLE 6.2.1.1.--The 30 minute average wind direction and mast positions relative to the spray line.

Wind Direction	Mast Placement (m)								
	No. 1 Upwind & No. 2 Downwind		Mast No. 3		Mast No. 4		Mast No. 5		
Compass Angle From Normal	Normal	Actual	Normal	Actual	Normal	Actual	Normal	Actual	
200°	25°	10	11.0	20	22.0	30	33.0	40	44.1

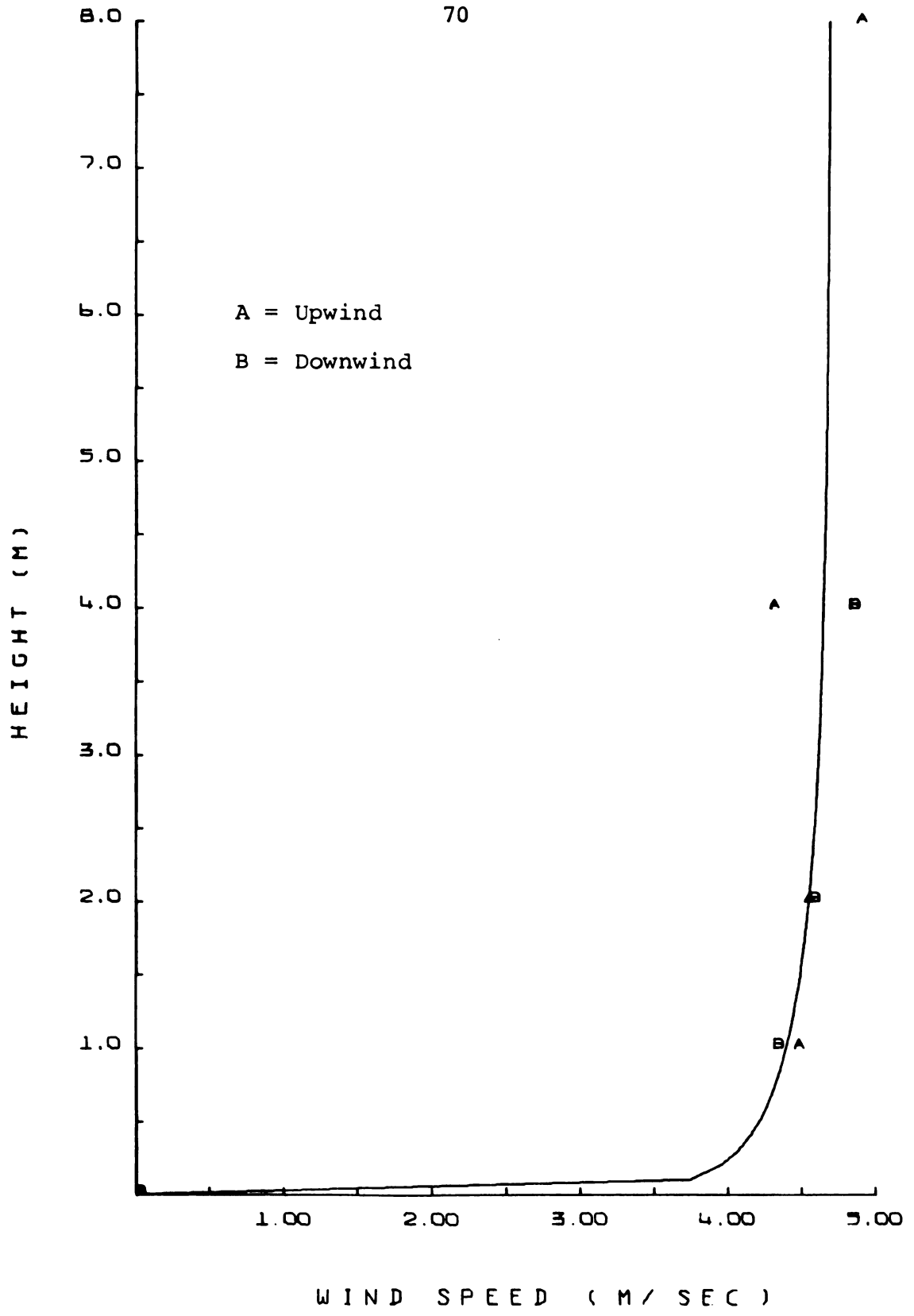


FIGURE 6.2.1.--Wind speed profiles.

$L = -1.66$ m, $u_* = 0.28$ m/sec, and $z_0 = 0.0016$ m.

The very close agreement between the upwind profile and the profile within the active evaporation region justifies the previous constant wind speed profile assumption. The value of z_0 is well within the range of values given by Sutton

(1953, p. 233) which are:	Surface	z_0 , m
	Very smooth mud flats	0.00001
	Lawn grass up to 1 cm	0.001
	Downland, thin grass up to 10 cm	0.007

The value of u_* is also well within the comparable range of values calculated from the values for surface shear stress over 1-5 cm high grass reported by Sutton (1953, p. 259). The values reported by Sutton and the values of u_* computed using a moist air density of 1.15 kg/m^3 are:

Wind Speed at 1m m/sec	τ_0 dynes/cm ²	u_* m/sec
4.03	0.90	0.280
4.78	1.44	0.354

6.3 Net Radiation, Soil Heat Flux and Sensible Heat Flux

The average net radiation for the period was 0.27 ly/min. The soil heat flux as measured by the surface heat flux plate was 0.14 ly/min and thus the sensible heat flux as found by Equation (3.4.1.2) was 0.13 ly/min.

6.4 Temperature and Moisture Measurements

6.4.1 Initial Conditions

The uppermost soil thermocouple recorded an average temperature of 24.5°C (76.1 °F).

The psychrometric data was analyzed by using a field calibration factor. This factor was developed for each dry bulb and wet bulb temperature sensor by initializing in such a manner that the readings for no spray conditions for all psychrometers at a given level were equal. The technique used was to average the temperatures for all psychrometers at a given height for a preliminary time period. The deviation of each sensing element from its corresponding mean value during the initializing period was then used as each element's calibration factor. The resulting dry bulb and wet bulb temperature data for the test run is presented in Appendix B, Table B2.

The comparison of the dry bulb temperature and the Swinbank similarity profile, Equation (2.3.3), is given in Figure 6.4.1.1. The computed value of T_* was

-0.869 °C. The test for goodness of fit to the data was by the method of minimizing the sum of the squared errors. [See Himmelblau (1969).] For the initial conditions, the best agreement occurred with a temperature of 22.5°C at a height of 1 m. The computed value of T_0 was 27.8 °C. The deviation of the measured temperature from the Swinbank profile was consistent for all time periods tested, i.e. measured data was less than the Swinbank profile for z less than or equal to 4 m and greater than the Swinbank profile for z greater than 4 m. This is believed by the author to be the influence of the upwind grass area and its modifying influence on the boundary layer. Measurements seemed to have been made both within and above the reestablishing boundary layer.

It is a commonly accepted fact that wet bulb temperature measurements are much more difficult to make and the accuracy greatly reduced compared to dry bulb temperature measurements. Thus it is expected that the initial moisture concentration data would not agree with Swinbanks similarity profile as well as the dry bulb temperature profile. This is illustrated in Figure 6.4.1.2. The initial moisture conditions at z_0 were assumed to be 80% R.H. at the T_0 temperature and ambient pressure. The minimum sum of squared errors was achieved for a moisture concentration at the 1 m level of 11.5 g/m³.

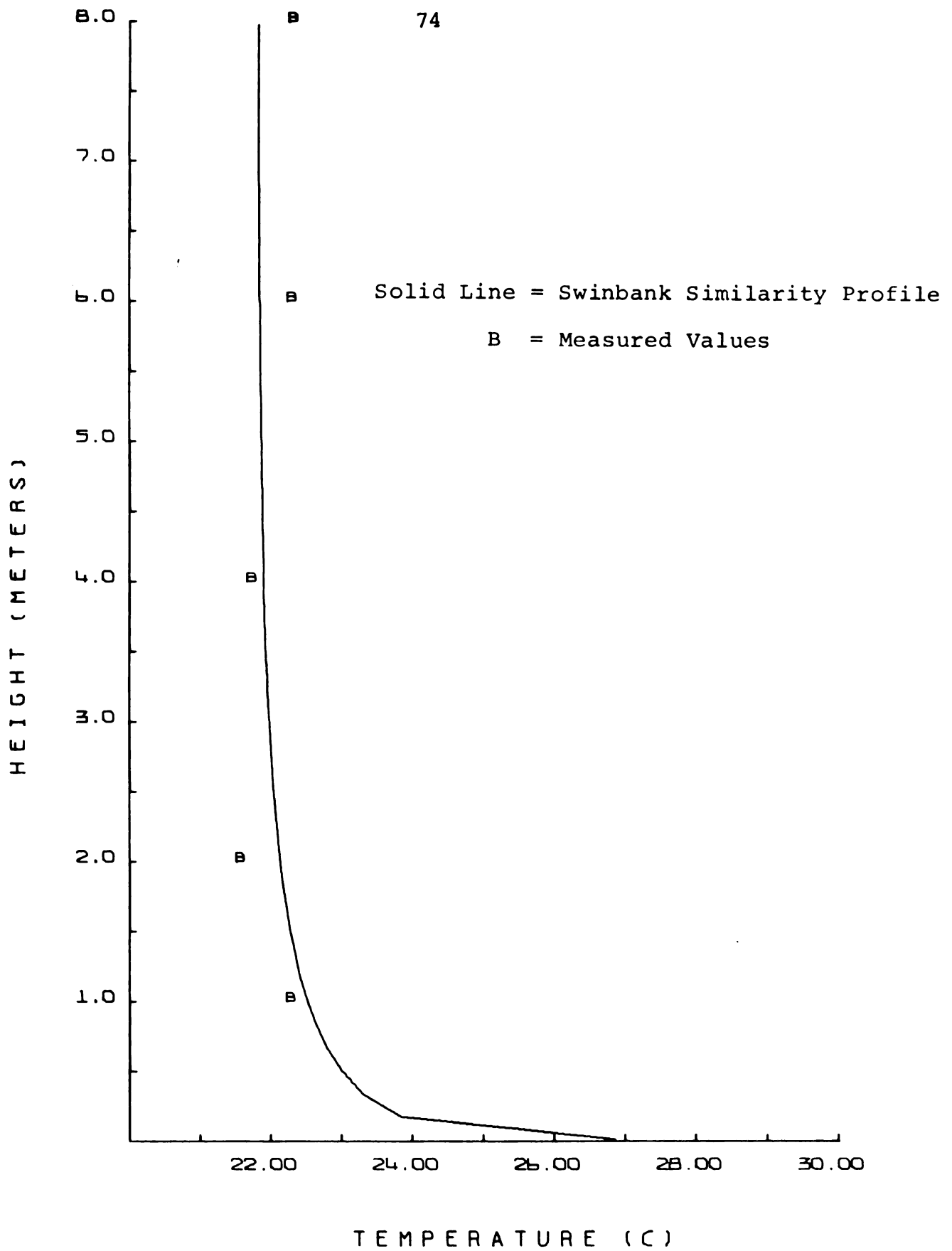
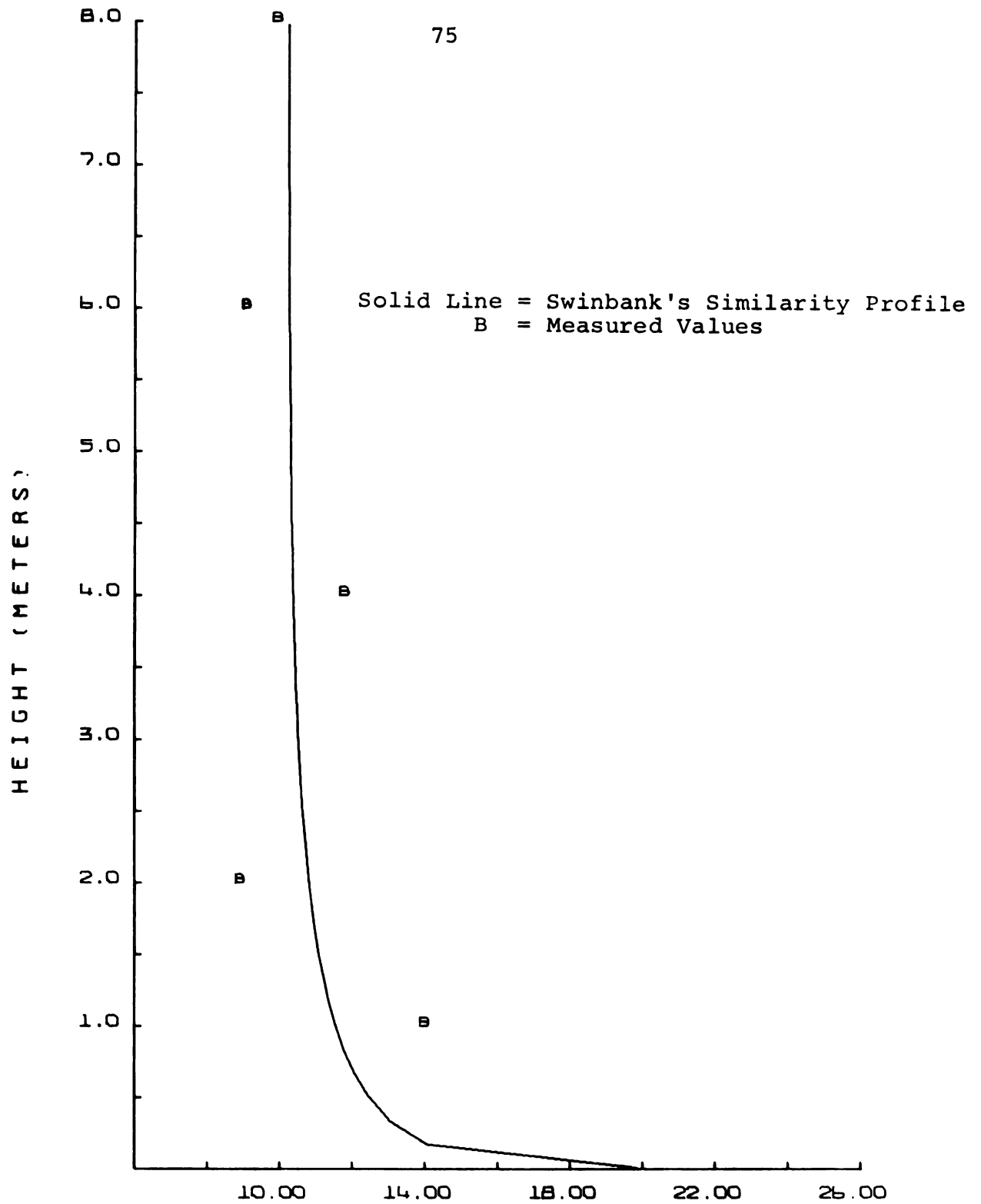


FIGURE 6.4.1.1.--Initial temperature profiles.



MOISTURE CONCENTRATION (G / CU M)

FIGURE 6.4.1.2.--Initial moisture concentration profiles.

The values of χ_0 and χ_* computed for these conditions were 21.7 g/m^3 and -1.66 g/m^3 respectively. The sum of squared errors for the temperature and moisture concentration for the five levels measured were 0.871 and 13.1 respectively. The comparison of these two values further illustrates the reduced accuracy of the moisture profile measurements.

The moisture profile measurements exhibit a peculiar bulge at the 4 m level. This anomaly was consistent for all measurements made and is believed to be the direct result of the evapotranspiration of the upwind grass area mentioned above.

6.4.2 Modified Conditions

The observed dry and wet bulb temperatures are included in Appendix B, Table B3.

Figure 6.4.2.1 illustrates the small water droplet supply at the spray line and Figure 6.4.2.2 the optical disappearance of the mist between the first and second downwind masts, i.e. masts number 2 and 3. The effective evaporation has therefore been assumed to be completed in the neighborhood of mast number 3.

The choice of $\alpha_H = 1$ did not yield satisfactory model results. The active evaporation distance required was between 30 and 40 m if the evaporation source term coefficient, c_1 , was chosen to yield reasonable cooling



FIGURE 6.4.2.1.--Operational spray line for small water droplets.

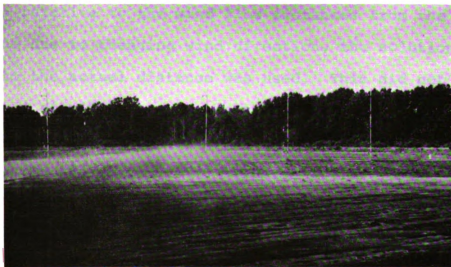
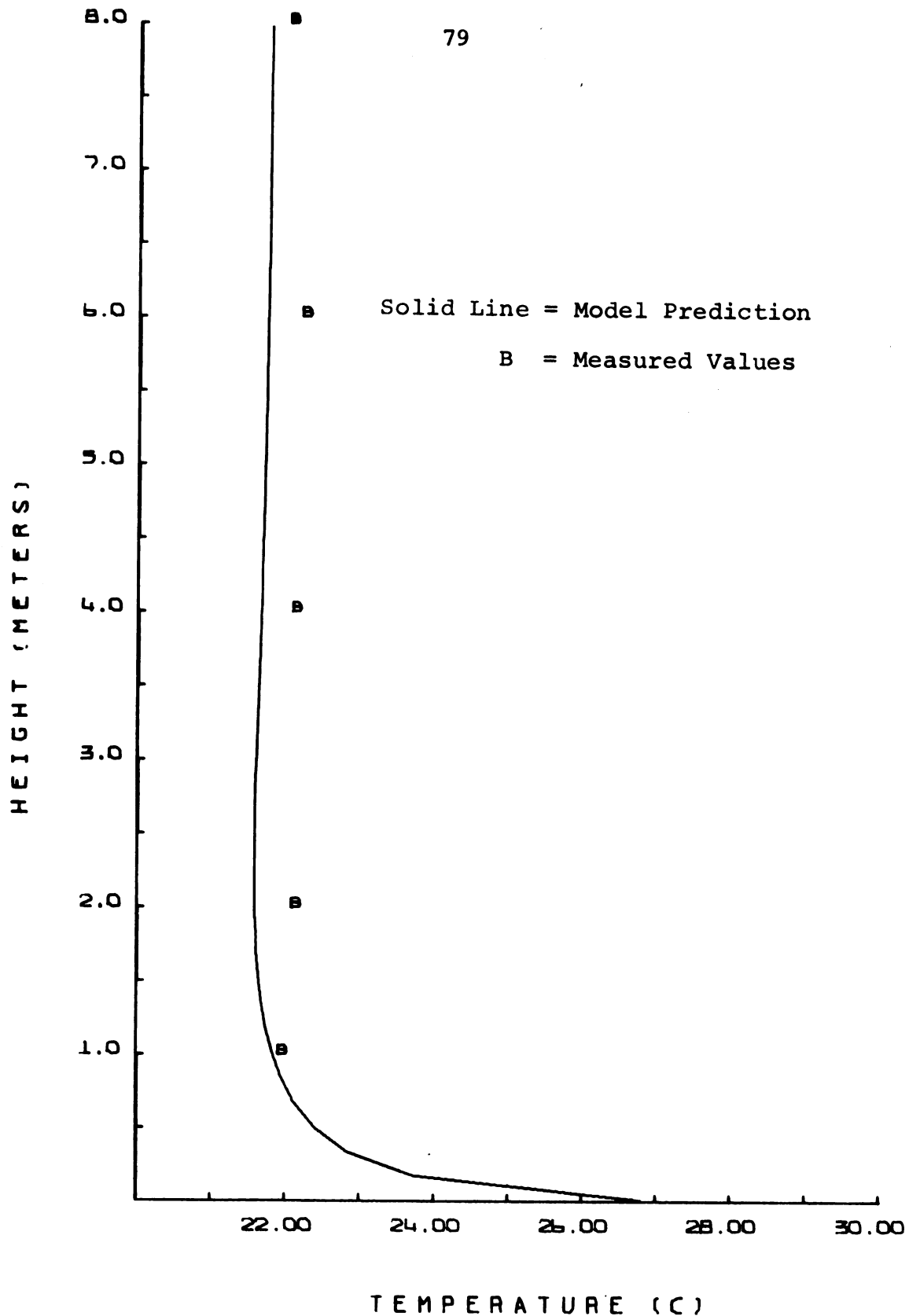


FIGURE 6.4.2.2.--Droplet dispersion and disappearance between masts 2 and 3.

profiles. If larger values of c_1 were used to achieve complete evaporation in the neighborhood of the second mast, then the predicted temperature profiles were much cooler than the observed data.

The choice of α_H to be that of Leichtman and Ponomareva (1969) and a value of $c_1 = 0.02/\text{sec}$ yielded improved results. The active evaporation distance was 21.0 m with the Swinbank similarity profiles used as initial conditions. The values of the constants used in the model are summarized in Appendix B, Table B4.

Figures 6.4.2.3 thru 6.4.2.6 compare the measured dry bulb temperature values and the model profiles for masts 2 thru 5 respectively. Since the model solution step did not always coincide with the exact placement of the masts relative to the wind flow distances from the spray line due to changing wind direction, the solution step closest to the actual distance was used. This did not introduce a significant error because the maximum misalignment distance would be one half of the downwind solution step, i.e. in this case 0.5 m. Figures 6.4.2.7 thru 6.4.2.10 compare the observed and predicted moisture concentration profiles. The sum of squared errors for the five observation levels are given in Table 6.4.2.1. The maximum cooling computed by the model was -1.02°C at 19.0 m downstream and a height of 0.67 m.



TEMPERATURE (C)

FIGURE 6.4.2.3.--Temperature profiles at mast 2 with Swinbank initial conditions.

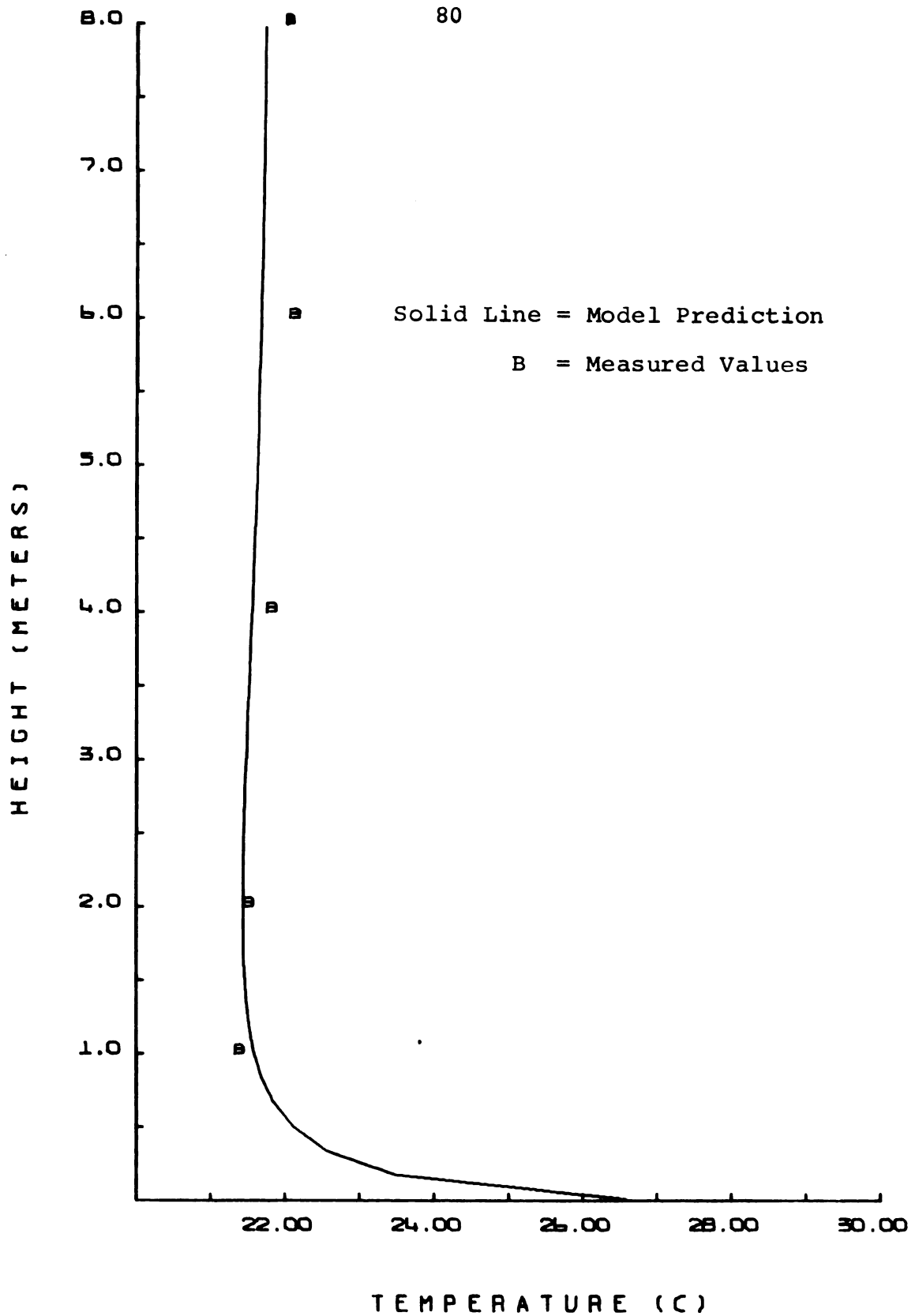
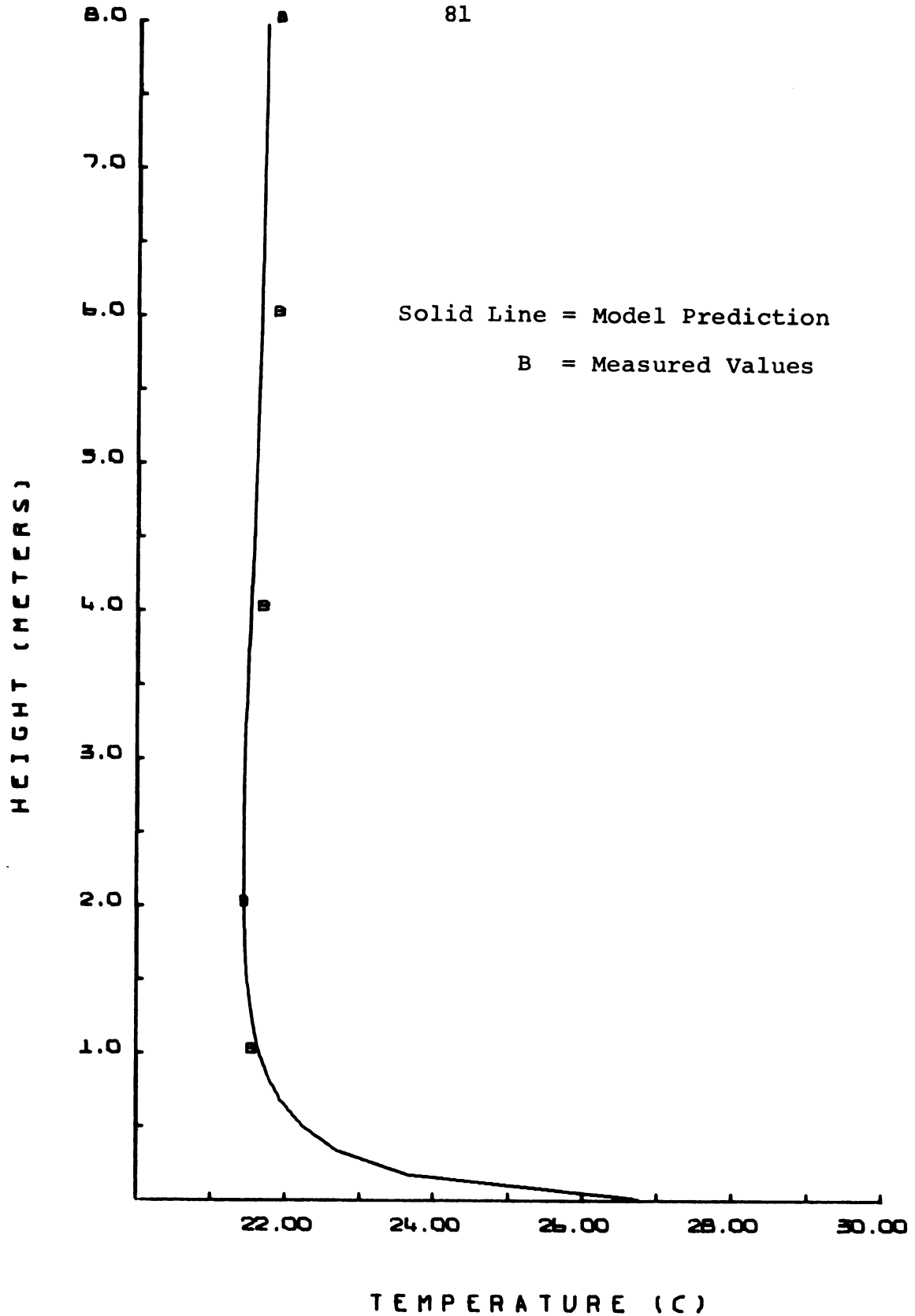


FIGURE 6.4.2.4.--Temperature profiles at mast 3 with Swinbank initial conditions.



TEMPERATURE (C)

FIGURE 6.4.2.5.--Temperature profiles at mast 4 with Swinbank initial conditions.

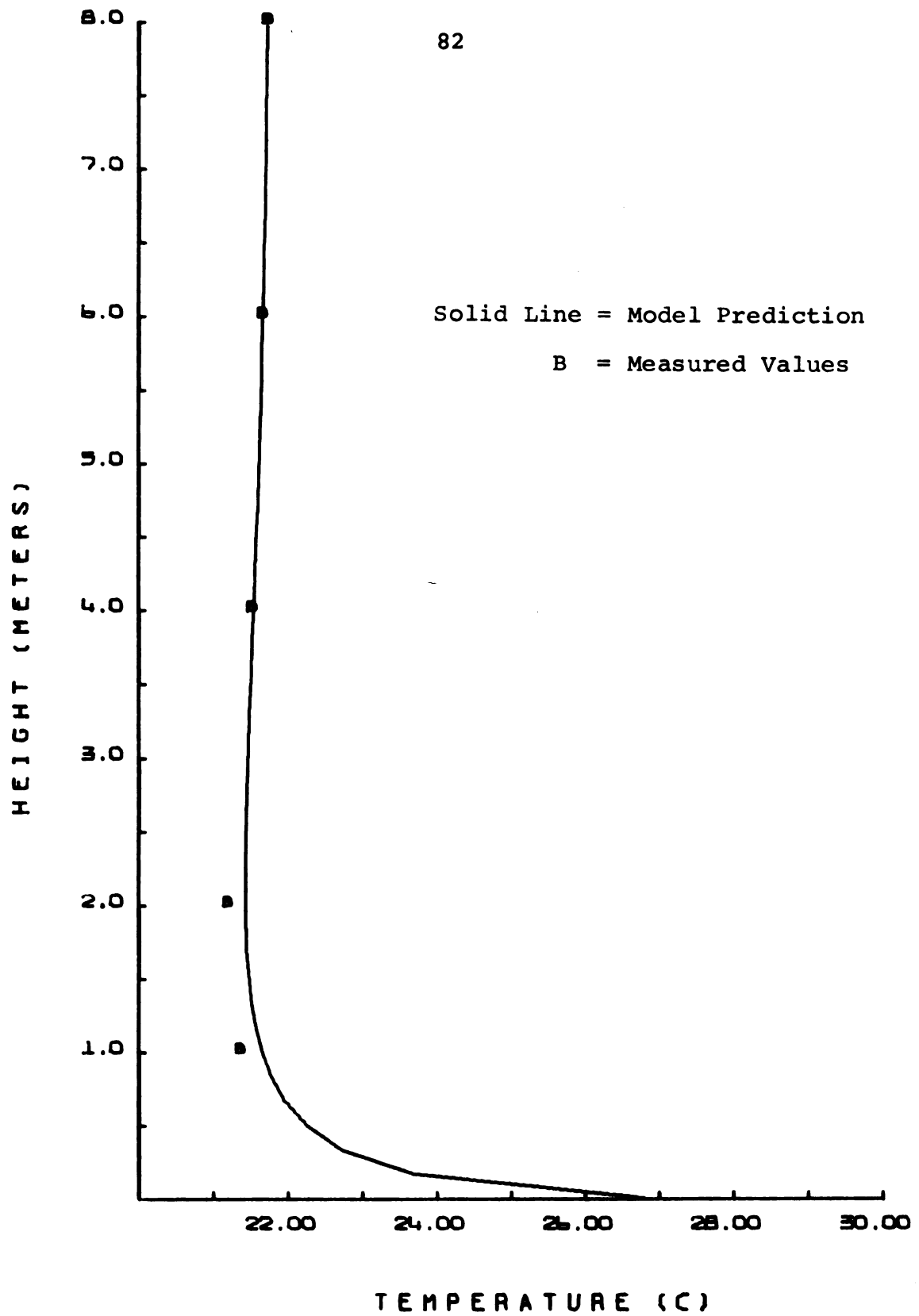
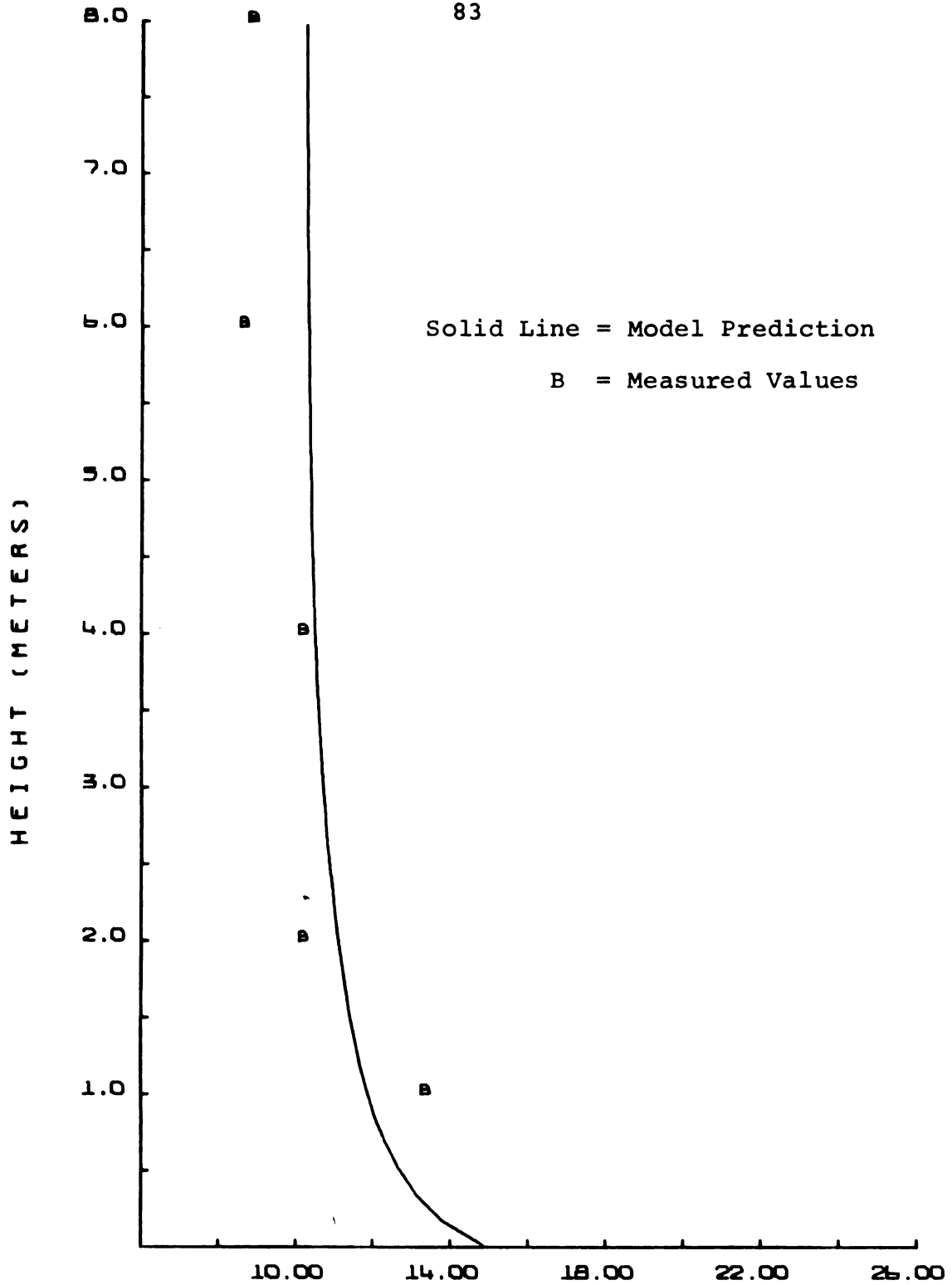
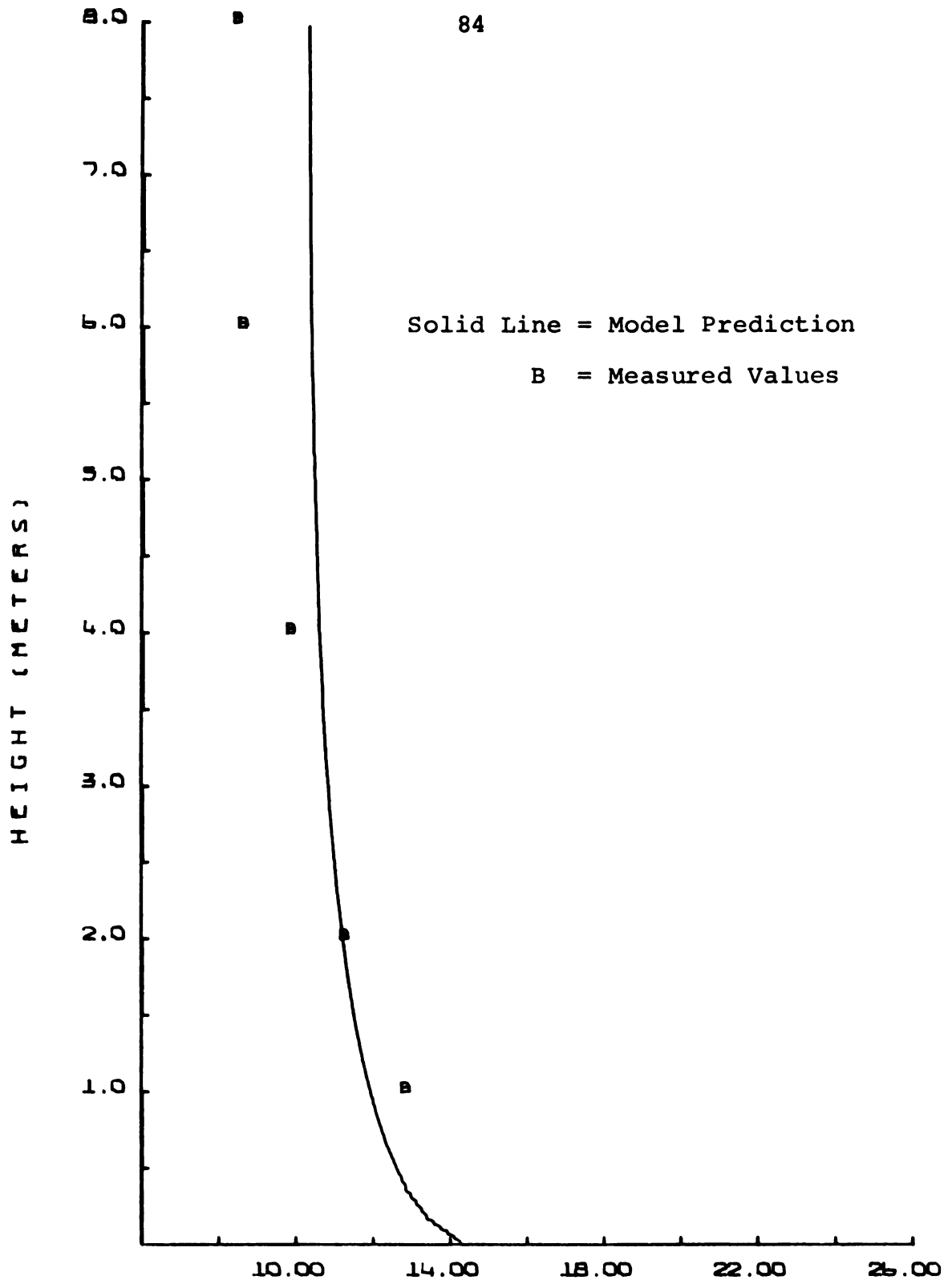


FIGURE 6.4.2.6.--Temperature profiles at mast 5 with Swinbank initial conditions.

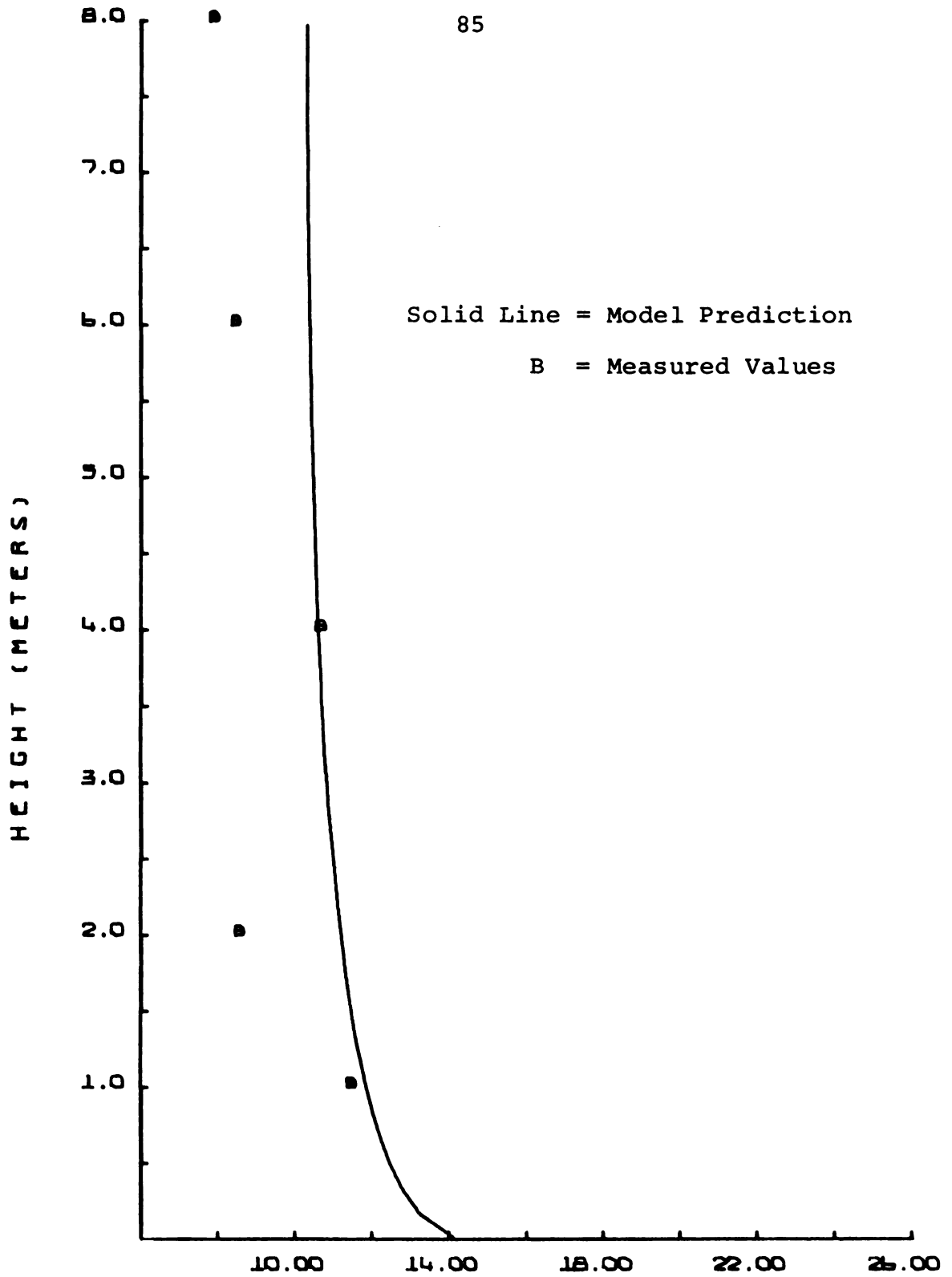


MOISTURE CONCENTRATION (G/ CU M)
FIGURE 6.4.2.7.--Moisture concentration profiles at mast 2
with Swinbank initial conditions.



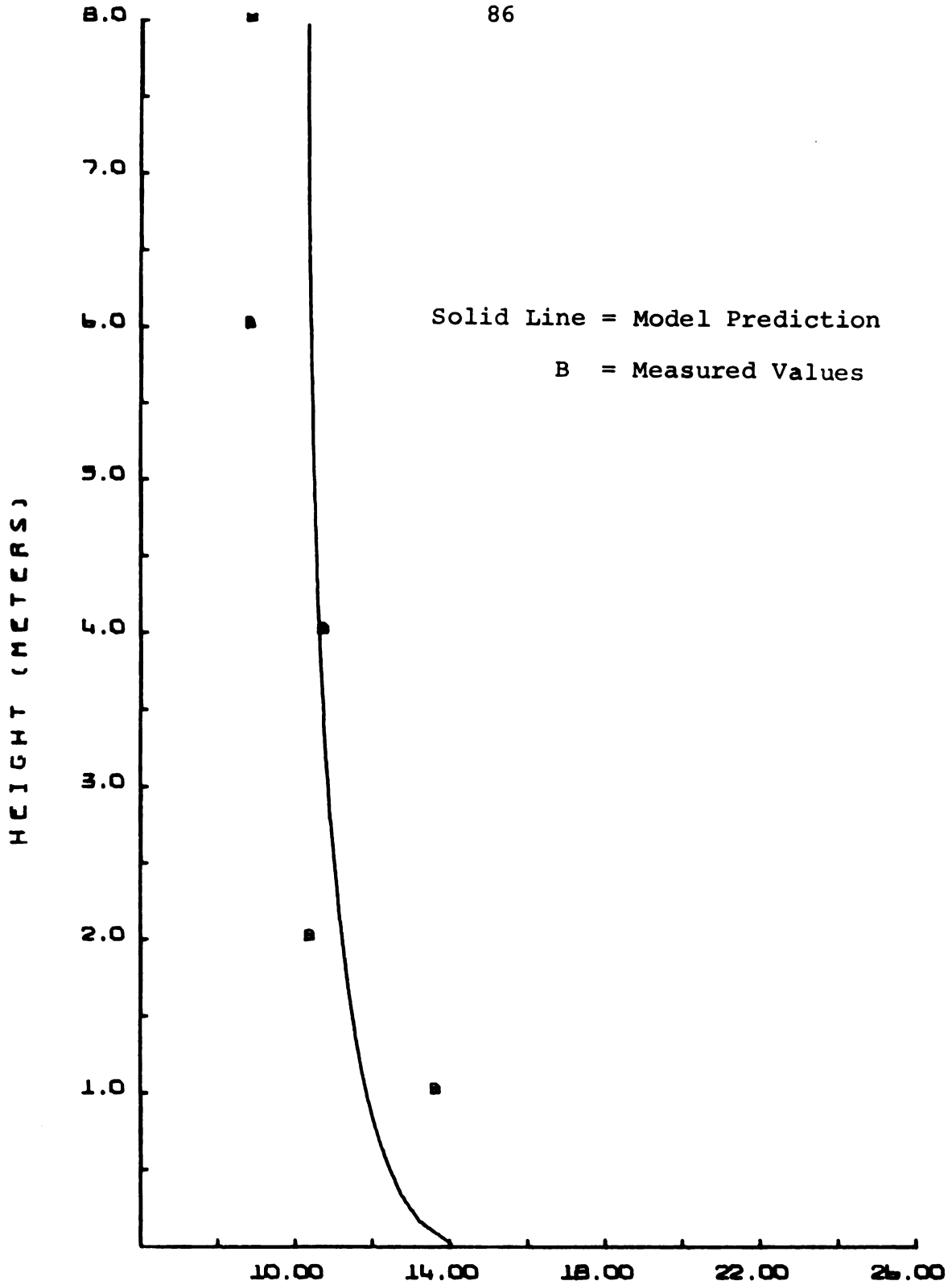
MOISTURE CONCENTRATION (G/ CU M)

FIGURE 6.4.2.8.--Moisture concentration profiles at mast 3 with Swinbank initial conditions.



MOISTURE CONCENTRATION (G/ CU M)

FIGURE 6.4.2.9.--Moisture concentration profiles at mast 4 with Swinbank initial conditions.



MOISTURE CONCENTRATION (G / CU M)
FIGURE 6.4.2.10.--Moisture concentration profiles at mast 5 with Swinbank initial conditions.

TABLE 6.4.2.1.--Sum of the squared errors using Swinbanks similarity profiles as initial conditions.

Profile	Mast Number				
	1	2	3	4	5
Temperature	0.871	.684	.311	.071	.218
Moisture Concentration	13.1	8.51	8.86	17.9	8.82

The moisture concentration profiles are much less in agreement than are the dry bulb temperatures. Mast 4 has the lowest sum of squared errors for temperature but the highest value for moisture concentration.

Since the sum of squared errors is computed for the observation points only, the inexact initial Swinbank profiles could contribute to the downstream errors. To test the influence of the initial profiles, the measured data points were assumed to be connected linearly. The results for the temperature profiles are shown in Figure 6.4.2.11 through Figure 6.4.2.15 and for the moisture concentration profiles in Figure 6.4.2.16 through Figure 6.4.2.20. The solution procedure retained the Swinbank wind speed profile, diffusivities, and lower boundary sensible heat flux relationships. All constants were the same. The sum of squared errors are given in Table 6.4.2.2.

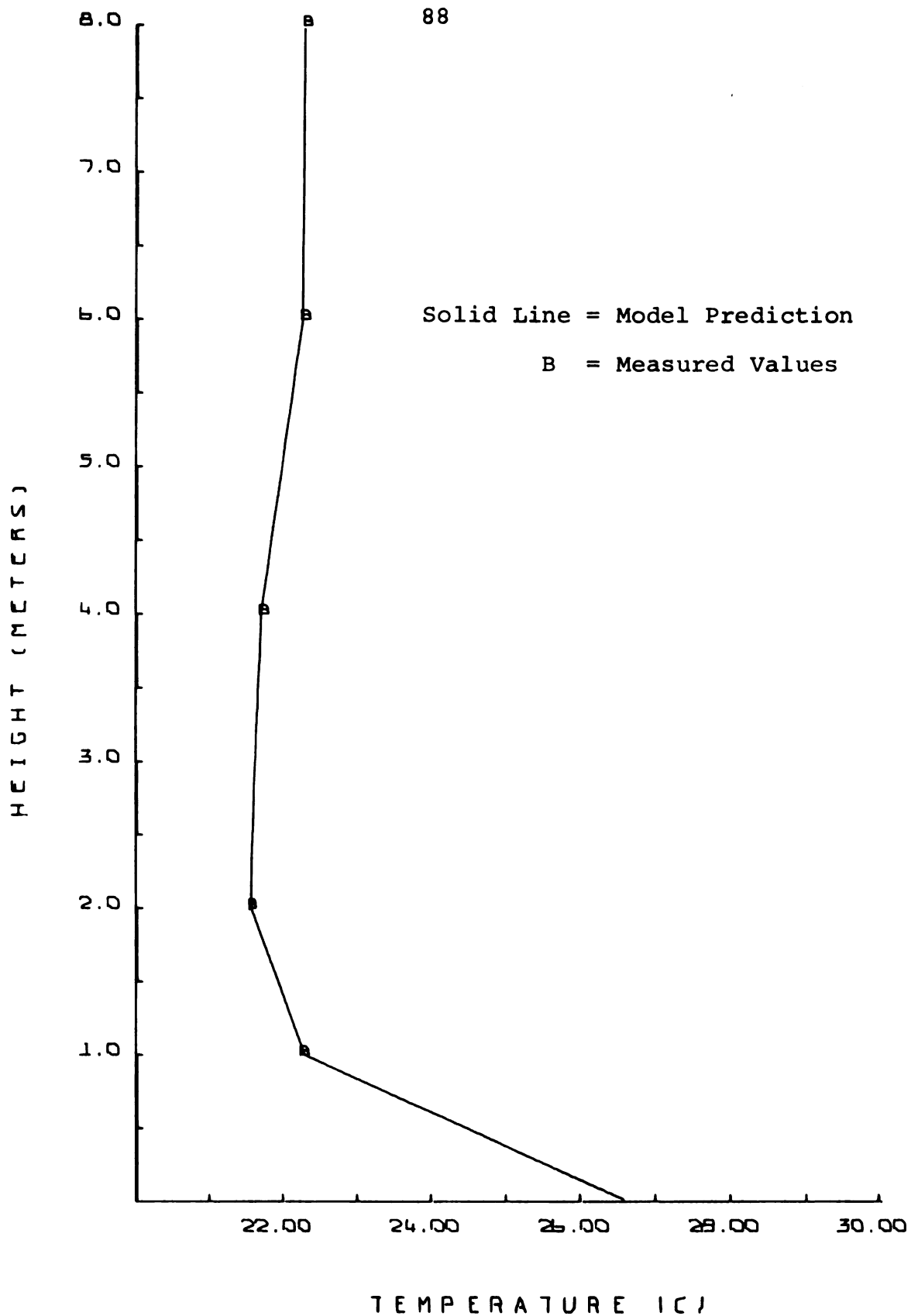
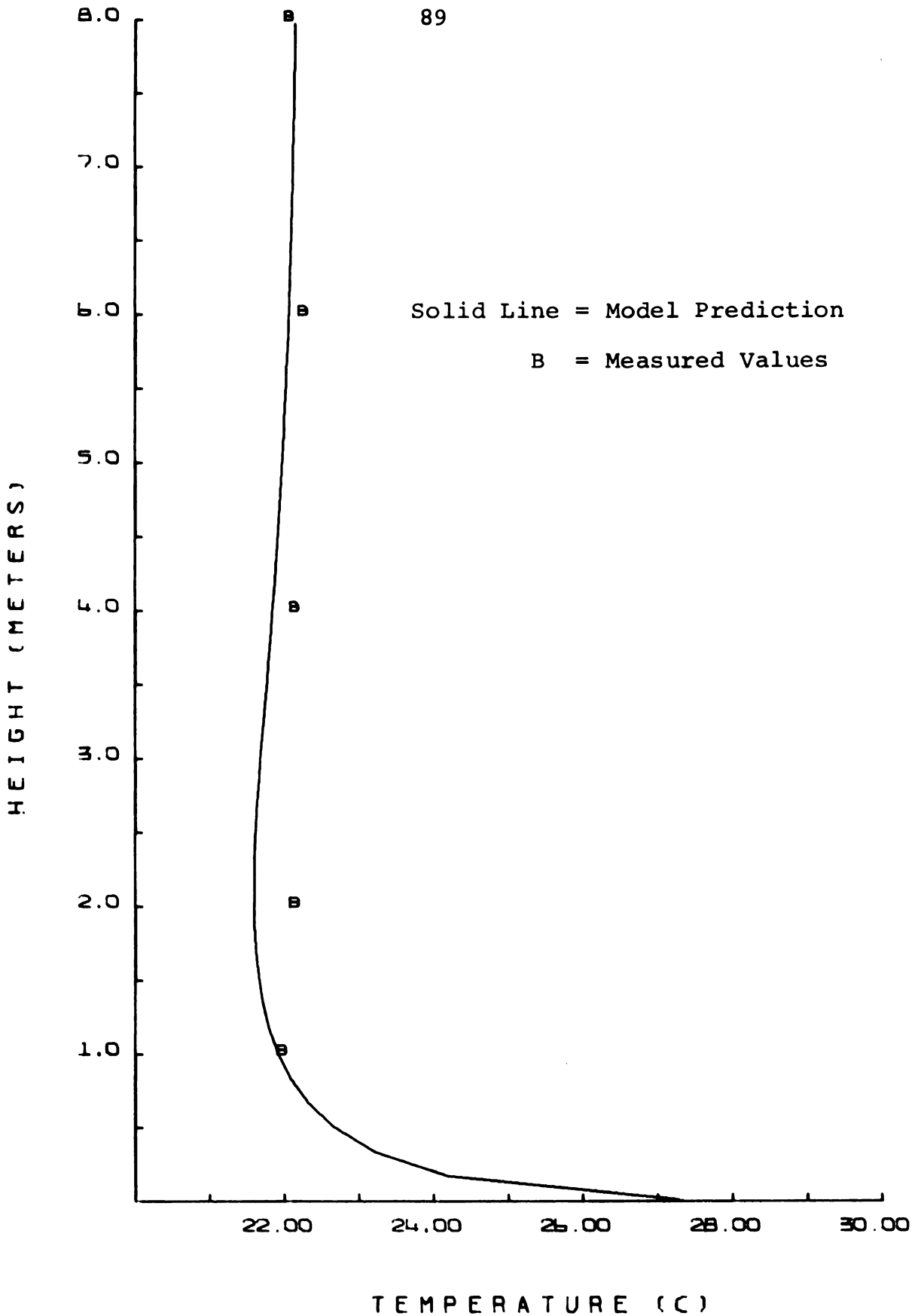


FIGURE 6.4.2.11.--Initial linearized temperature profile.



TEMPERATURE (C)

FIGURE 6.4.2.12.--Temperature profiles at mast 2 with the linearized initial conditions.

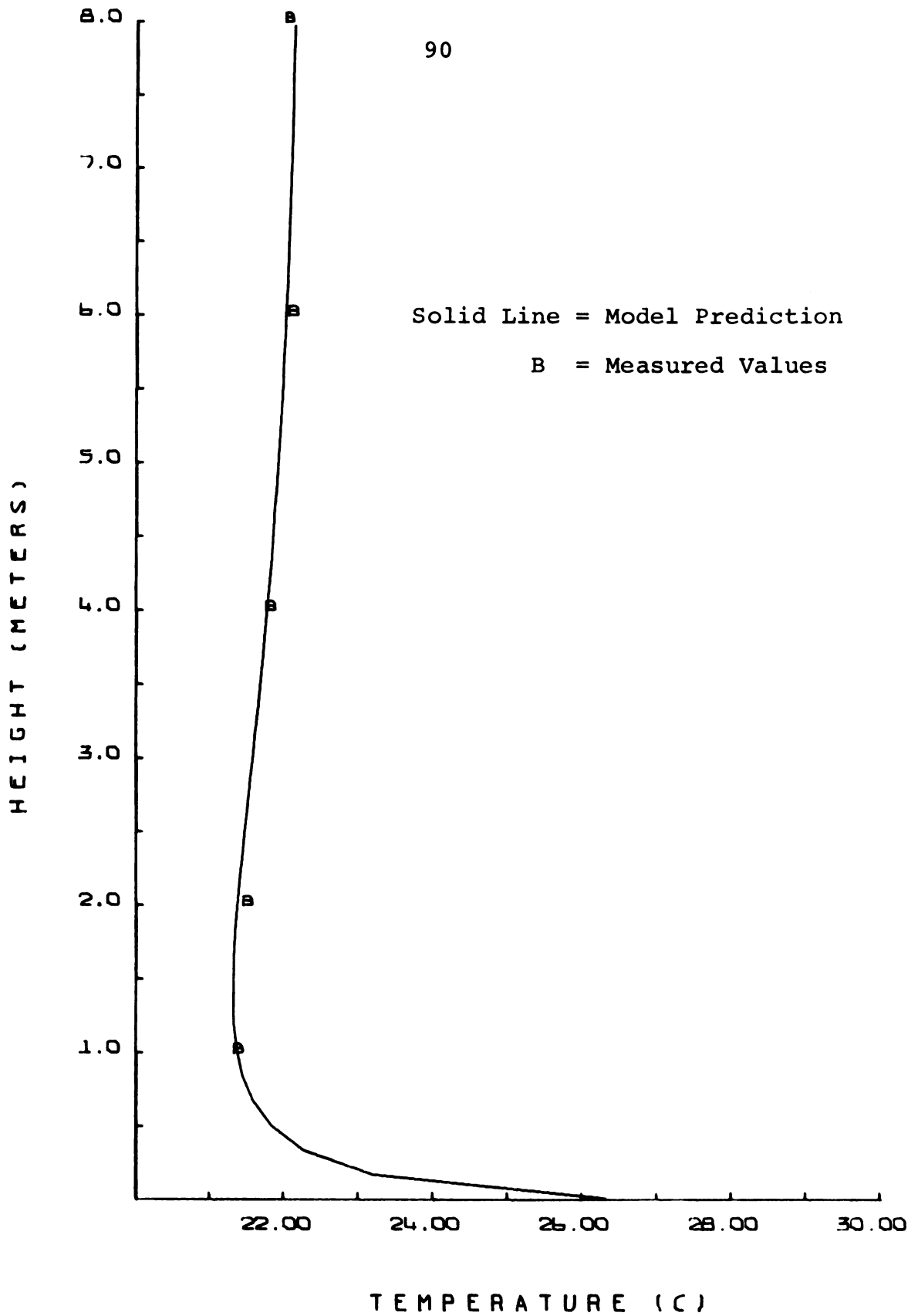
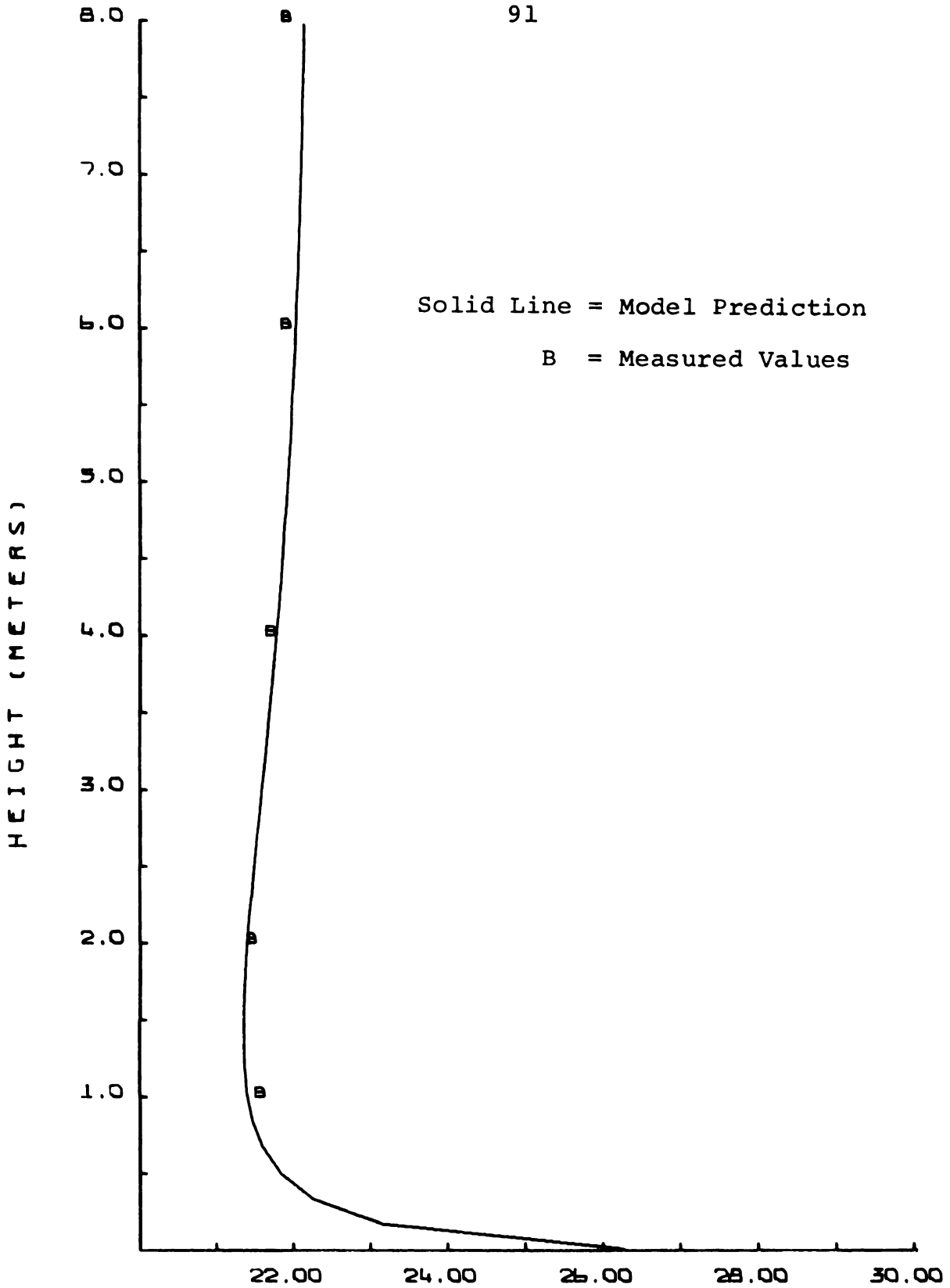


FIGURE 6.4.2.13.--Temperature profiles at mast 3 with the linearized initial conditions.



TEMPERATURE (C)

FIGURE 6.4.2.14.--Temperature profiles at mast 4 with the linearized initial conditions.

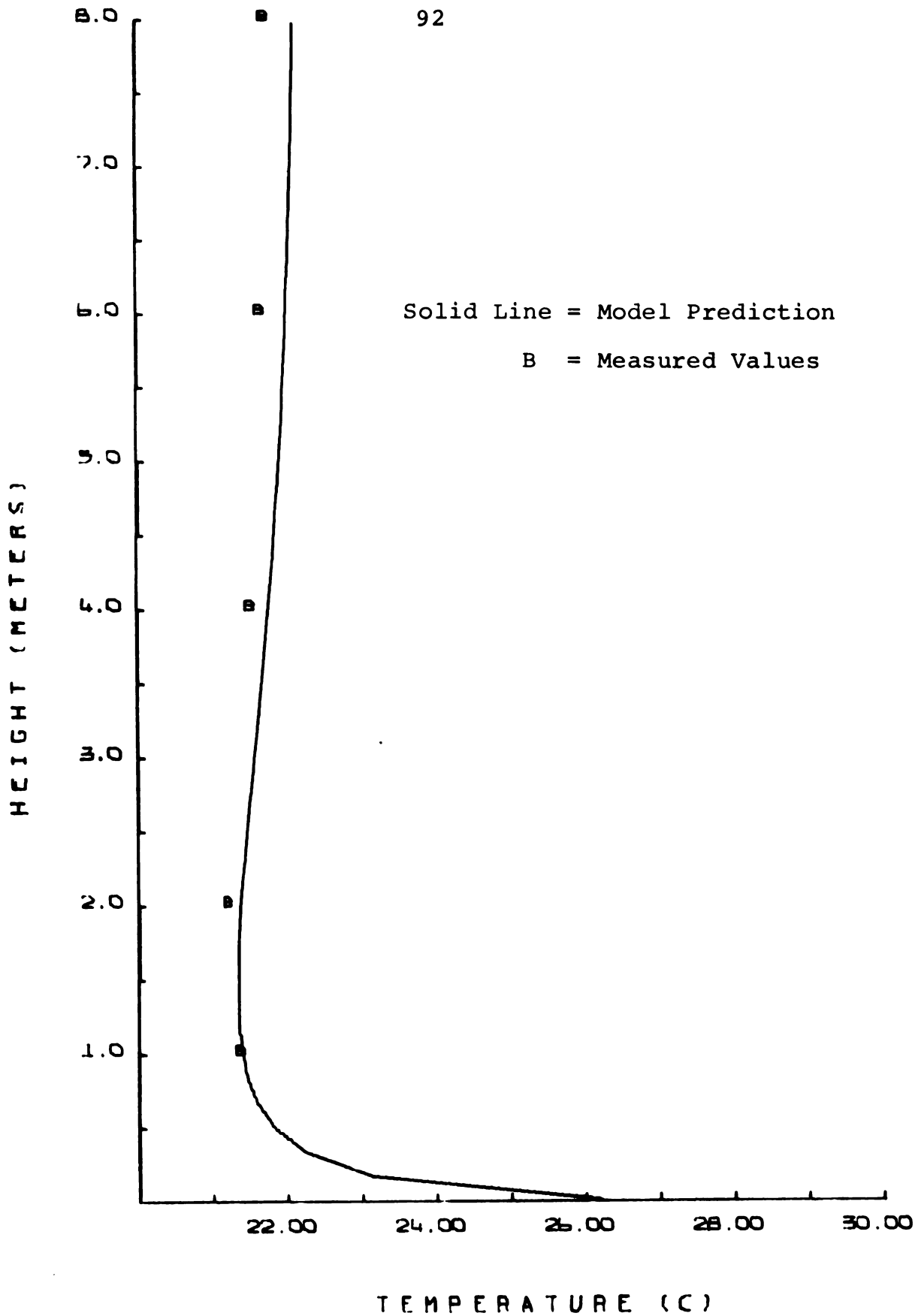
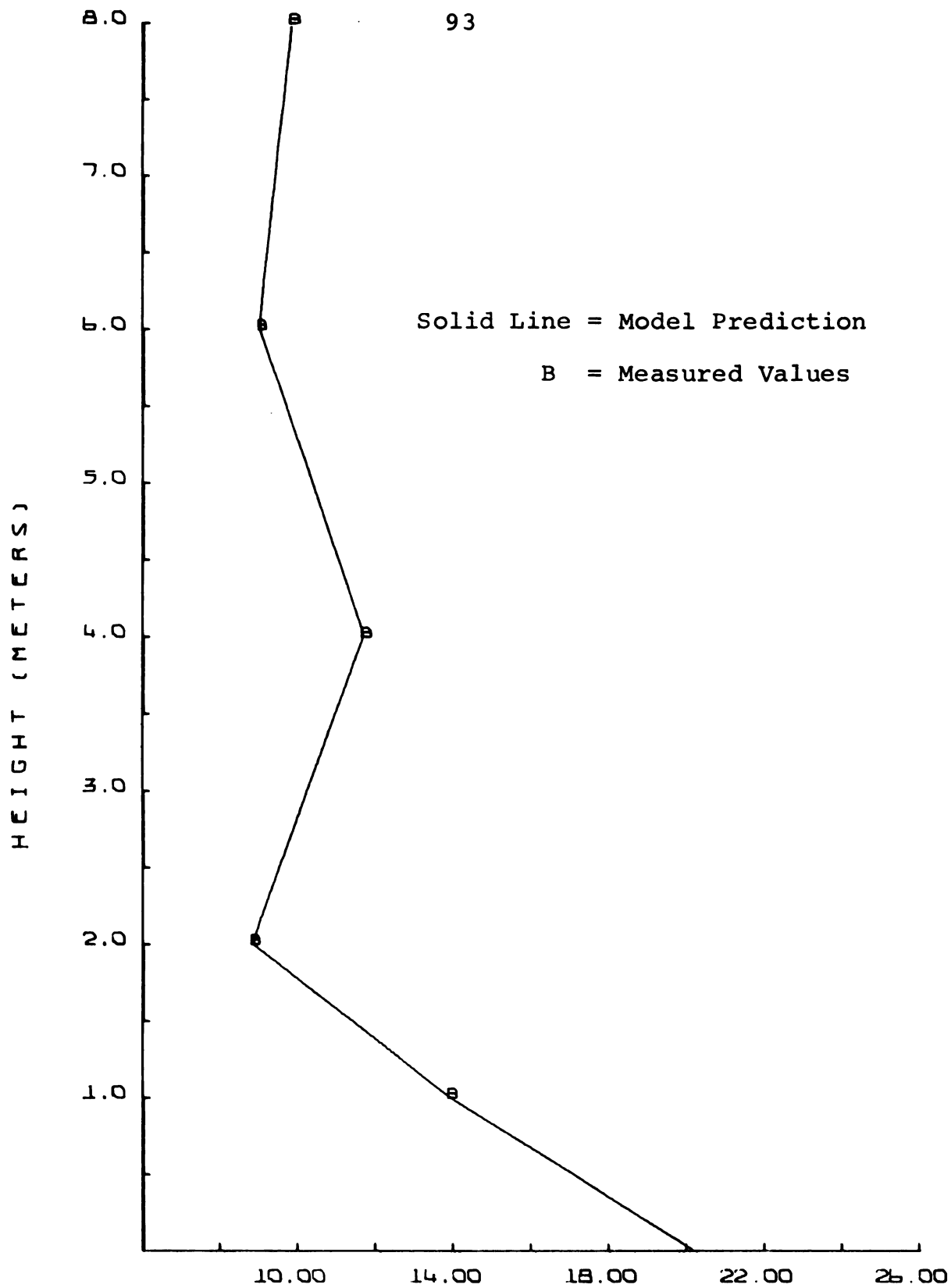
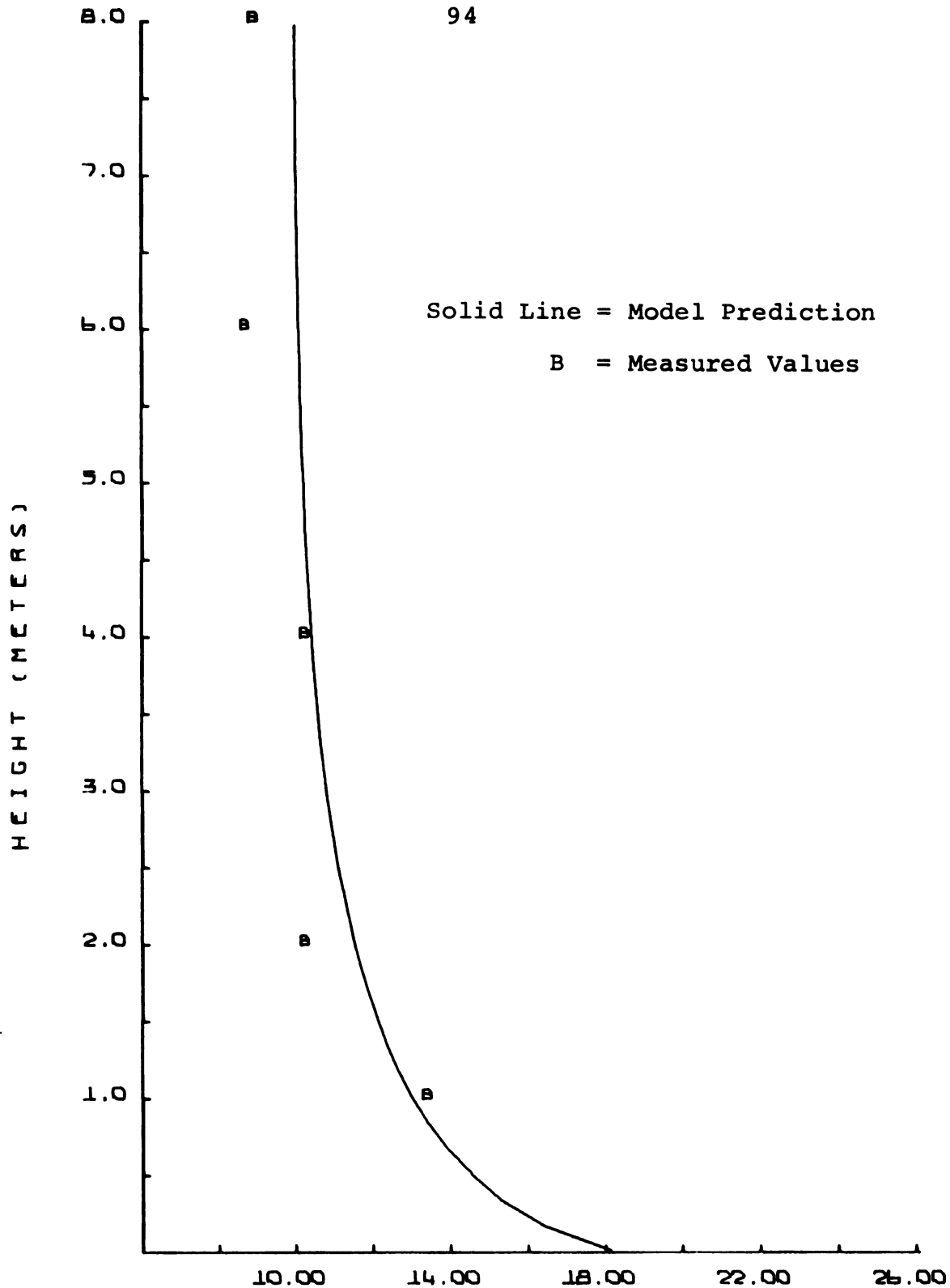


FIGURE 6.4.2.15.--Temperature profiles at mast 5 with the linearized initial conditions.

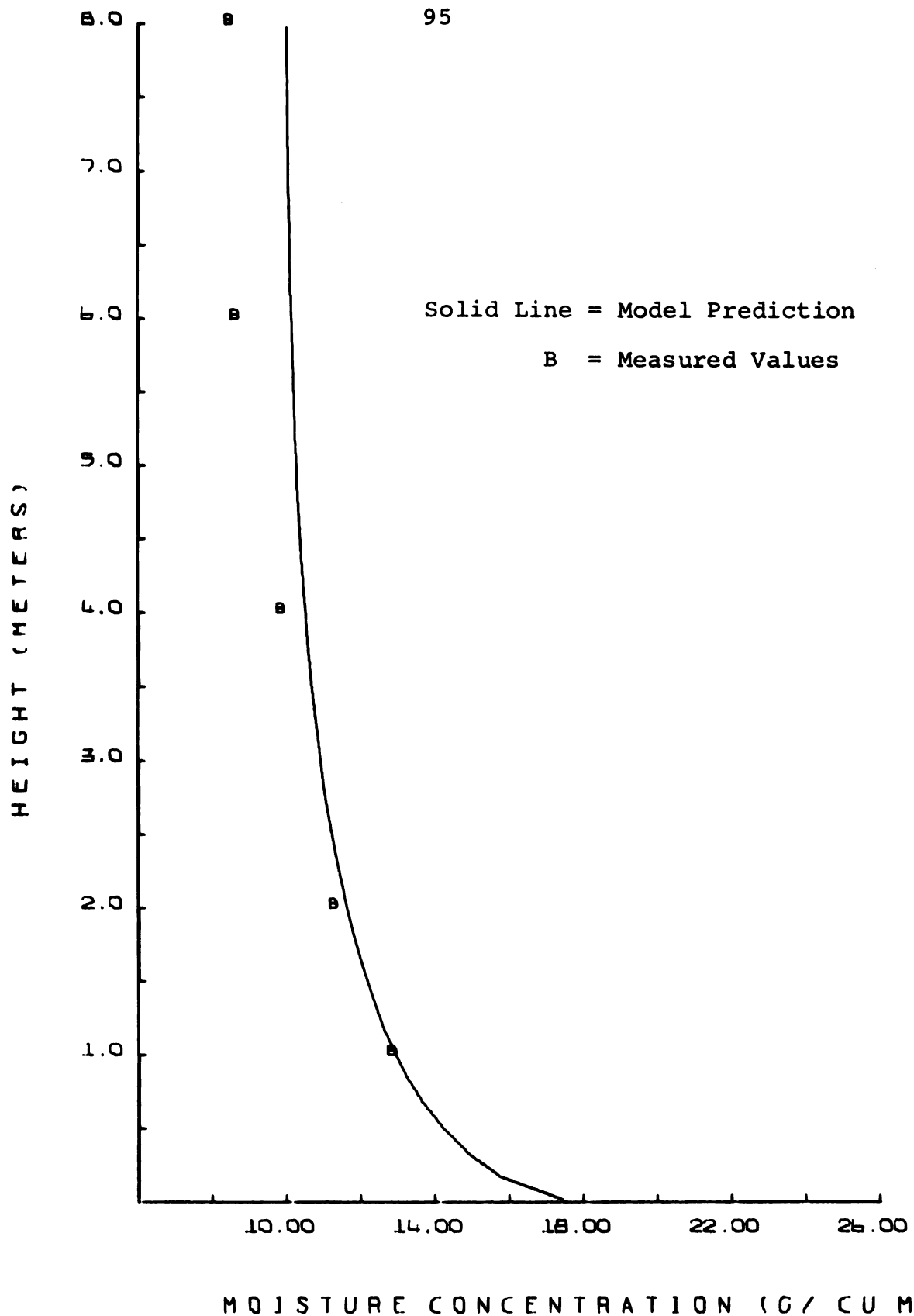


MOISTURE CONCENTRATION (G / CU M)

FIGURE 6.4.2.16.--Initial linearized moisture concentration profile.

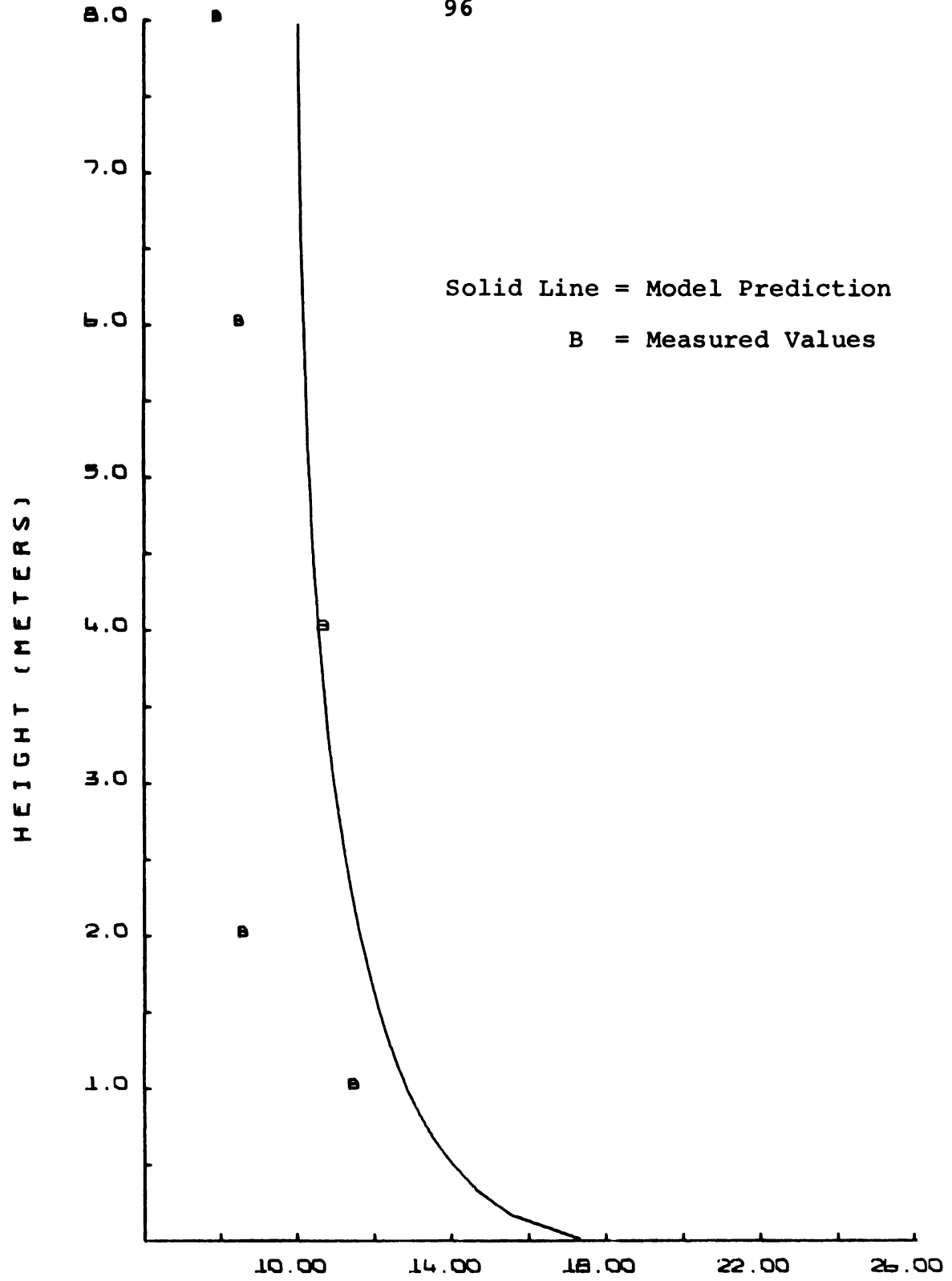


MOISTURE CONCENTRATION (G / CU M)
FIGURE 6.4.2.17.--Moisture concentration profiles at mast 2 with the linearized initial conditions.

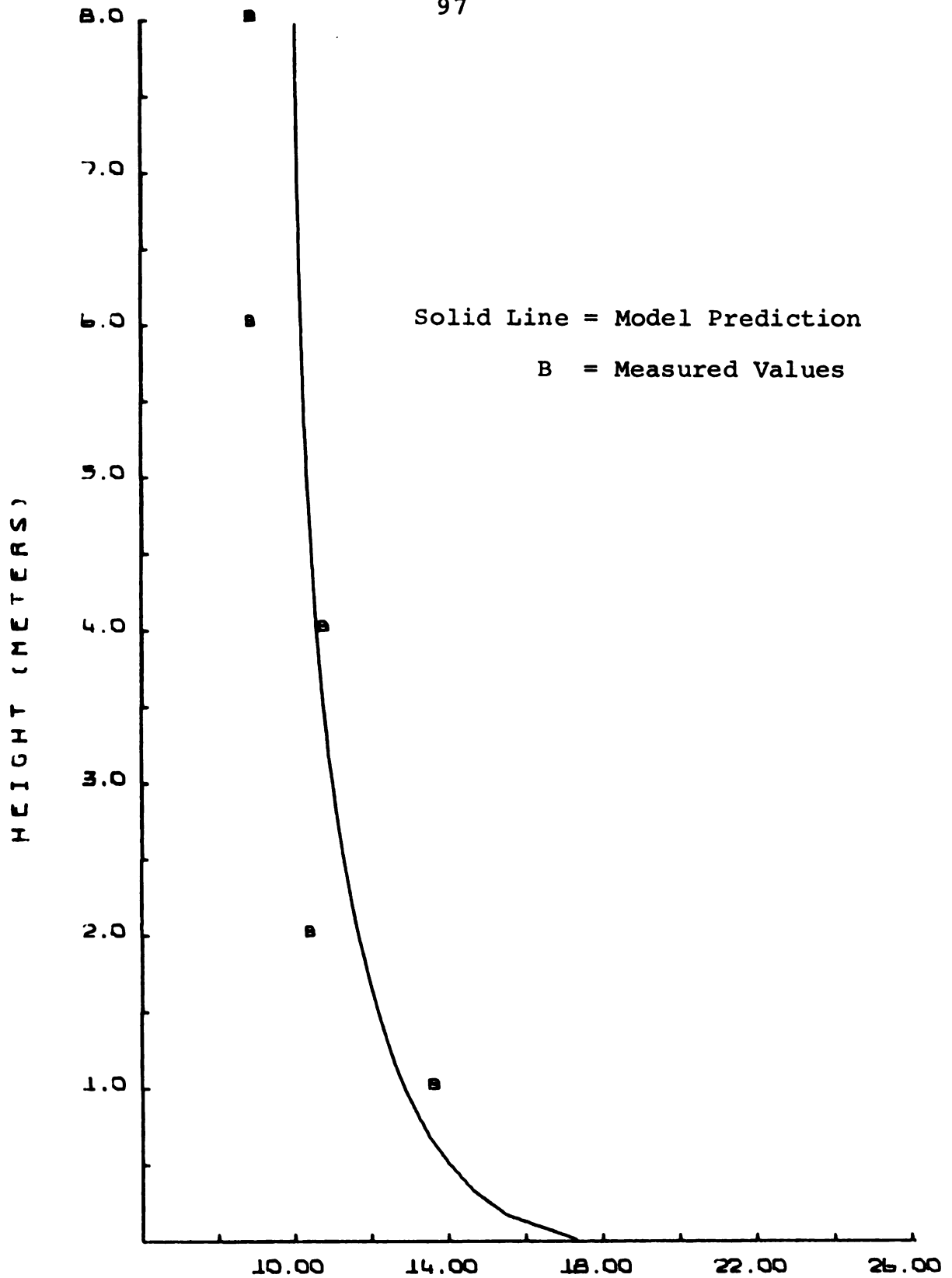


MOISTURE CONCENTRATION (G / CU M)

FIGURE 6.4.2.18.--Moisture concentration profiles at mast 3 with the linearized initial conditions.



MOISTURE CONCENTRATION (G/ CU M)
FIGURE 6.4.2.19.--Moisture concentration profiles at mast 4 with the linearized initial conditions.



MOISTURE CONCENTRATION (G / CU M)

FIGURE 6.4.2.20.--Moisture concentration profiles at mast 5 with the linearized initial conditions.

TABLE 6.4.2.2.--Sum of squared errors using linearized initial conditions.

Profile	Mast Number				
	1	2	3	4	5
Temperature	0.002	0.329	0.029	0.158	0.565
Moisture Concentration	0.008	5.68	6.27	20.0	5.86

The nonzero sum of squared errors for the initial conditions is due to the noncoincidence of the measured heights and the solution heights. The errors thus incurred are negligible.

The linearized initial conditions improved the model results compared to the results obtained with the Swinbank initial conditions, for temperature profiles at masts 1, 2, and 3, but the results were slightly poorer for masts 4 and 5.

The moisture concentration profile results were improved for all masts except number 4. Mast 4 consistently exhibited the highest error throughout the test runs. A change of psychrometers did not significantly affect the anomaly. The cause of the deviation of mast 4 is unknown to the author.

The active evaporation distance for the linearized initial conditions was 23.0 m. This is about 10% farther than with the Swinbank initial conditions. The maximum cooling computed by the model was -2.90°C at 23.0 m downstream and a height of 0.34 m.

Neither of the two forms of the initial conditions caused saturation in the active lower layers.

7. MODEL PREDICTION

The basic model was used to predict the temperature modification under various atmospheric conditions. The parameters that were allowed to vary were: (1) the Monin-Obukhov stability factor, L ; (2) the initial temperature at 1 m; (3) the initial wind speed at 1 m; and (4) the spray rate. The values used for the four selected variables are summarized in Table 7.1. Not all combinations of all variables were utilized.

TABLE 7.1.--A summary of the values of L , T_i , u_i , and the spray rate used in the prediction model.

Variable	Range of Values			
L , m	-0.1	-1.0	-10.0	
T_i (@ $z=1$ m), °C	30.0	35.0	40.0	
u_i (@ $z=1$ m), m/sec	0.5	1.0	2.0	4.0
Spray rate, g/m-sec	10.0	15.0	20.0	

The combinations for $u_i \geq 2.0$ m/sec and $L = -0.1$, for example, produces an impossible requirement for the sensible heat flux. The consistency between L , u_* , T_* , and H for the temperature range of 30 to 40 °C would require H to be nearly three times the solar constant. These combinations were therefore

omitted. The constants used in the prediction model and selected results are tabulated in Appendix B, Table B5 and Table B6 respectively.

The results for two different initial temperatures have been selected for graphical presentation. The two temperatures are 30.0 and 40.0 °C. The parameters used were: $L = -1.0$, $u_1 = 2.0$ m/sec, spray = 20.0 g/m-sec, and all the other constants are as reported above in Table B5.

Figures 7.1 and 7.2 are the temperature and moisture concentration profiles for 30 °C initial temperature and 25% initial relative humidity at the 1 m level. Curve A is the initial condition and curve B is the profile at the point downstream where maximum cooling occurred. The maximum cooling for these conditions was -8.4 °C at 21.0 m downstream and at a height of 0.15 m.

Figures 7.3 and 7.4 are the temperature and moisture concentration profiles for the 40 °C initial temperature and 25% initial relative humidity. The maximum cooling was -9.5 °C at 19.0 m downstream and at a height of 0.15 m.

Figures 7.5 through 7.8 illustrate the maximum temperature change with respect to the initial 1 m temperature for the three spray rates at each selected wind speed. The maximum cooling occurs with the lowest wind speed and highest initial temperature and spray rate.

This is due to the higher wind speeds diffusing and transporting the water much more than the lower wind speeds. Thus the lower wind speeds provide greater localized cooling. The maximum cooling for all conditions tested was -14.6°C at 41.0 m downstream and at a height of 1.25 m for $T_i = 40.0^{\circ}\text{C}$, $u_i = 0.5$ m/sec, spray rate = 20.0 g/m-sec and $L = -10.0$ m. The maximum cooling value is within the expected range of values concluded from Table 4.3.2.

A comparison of Figures 7.5 and 7.8 reveals that the rate of change in the maximum cooling with respect to the initial temperature is reduced with increasing wind speed. The variation between spray rates is also reduced in a similar manner.

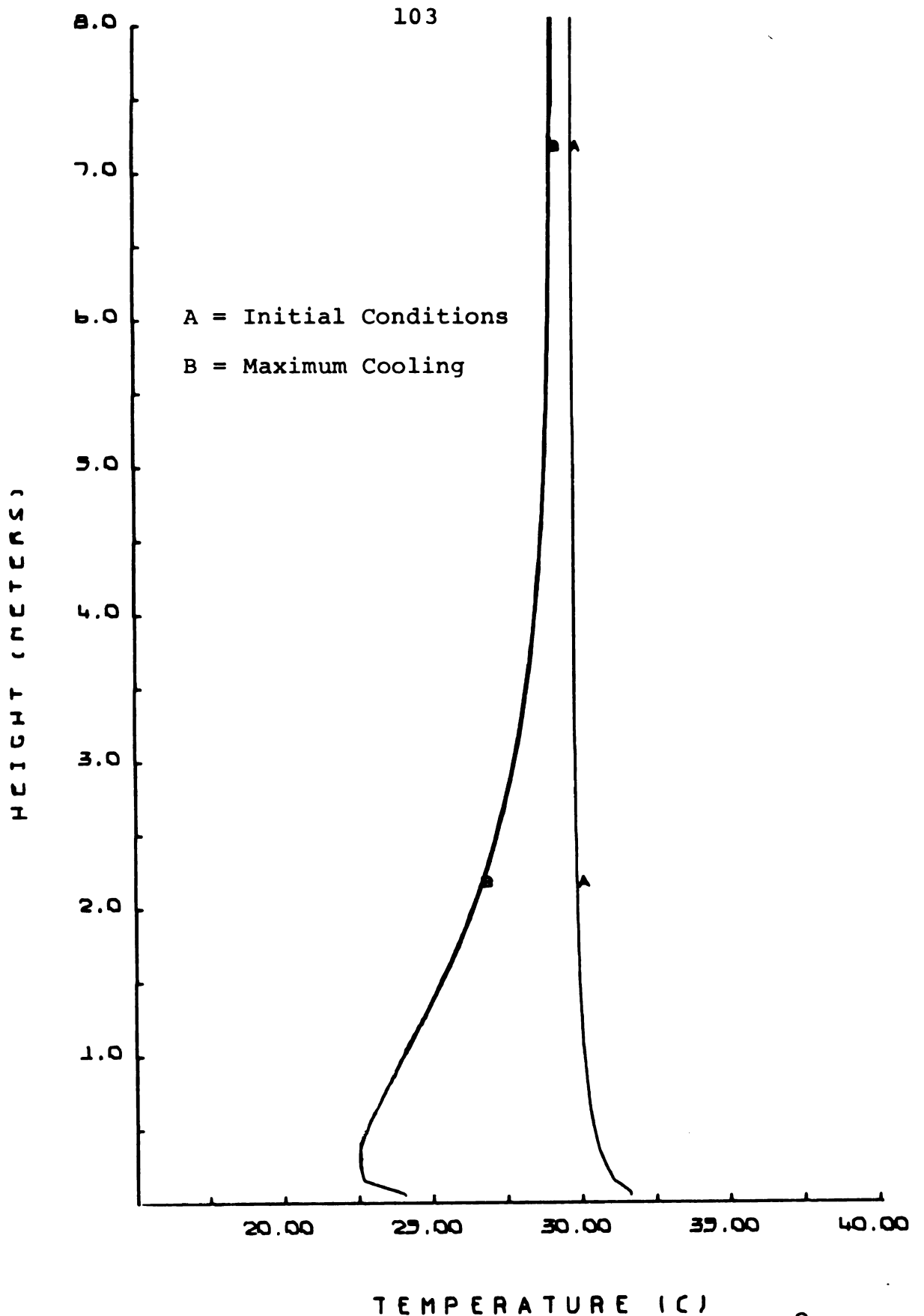
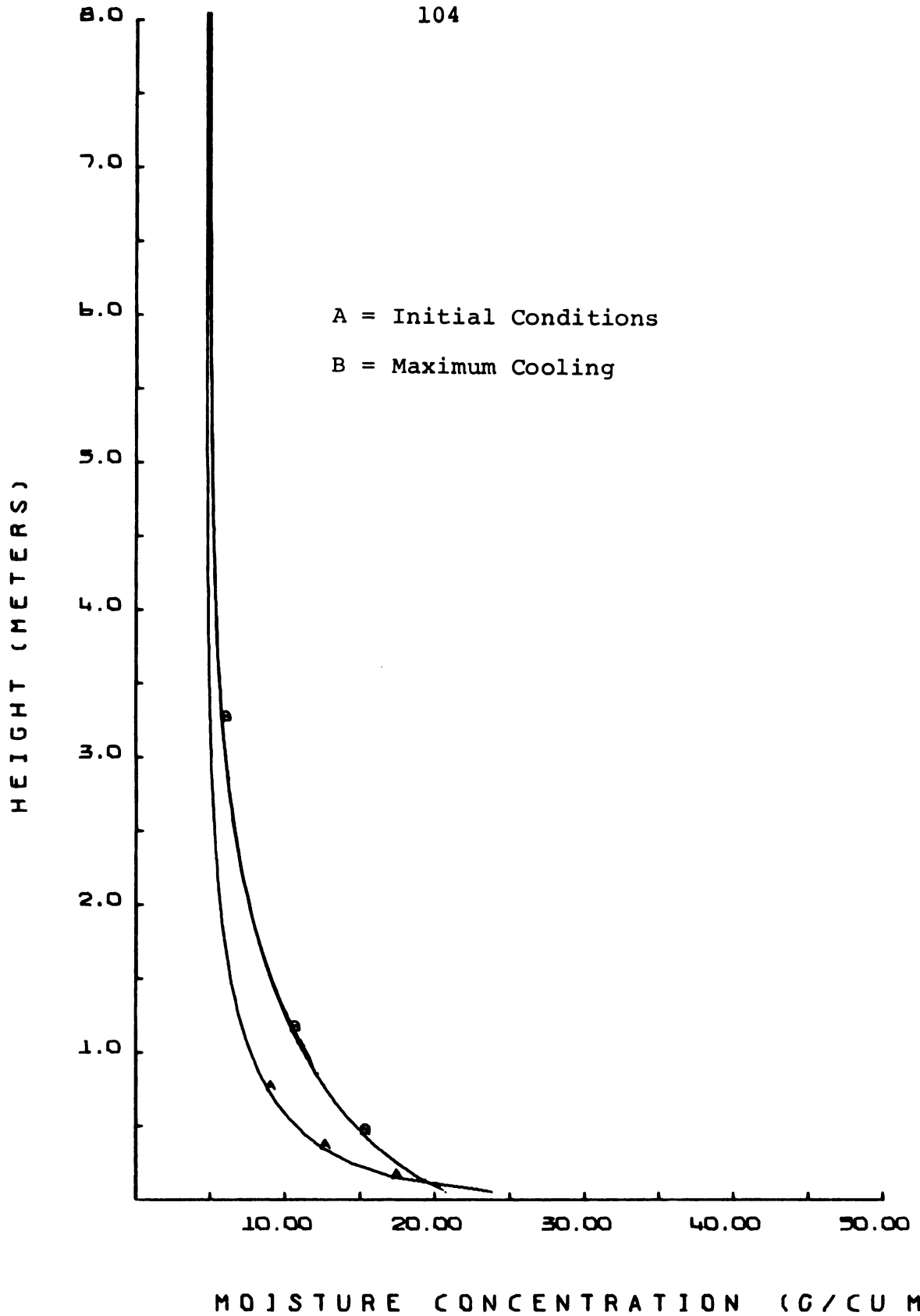


FIGURE 7.1.--Predicted temperature profiles with $T_i=30.0^{\circ}\text{C}$.



MOISTURE CONCENTRATION (G/CU M)

FIGURE 7.2.--Predicted moisture concentration profiles for $T_i=30.0^{\circ}\text{C}$ and $\text{R.H.}_i = 25\%$.

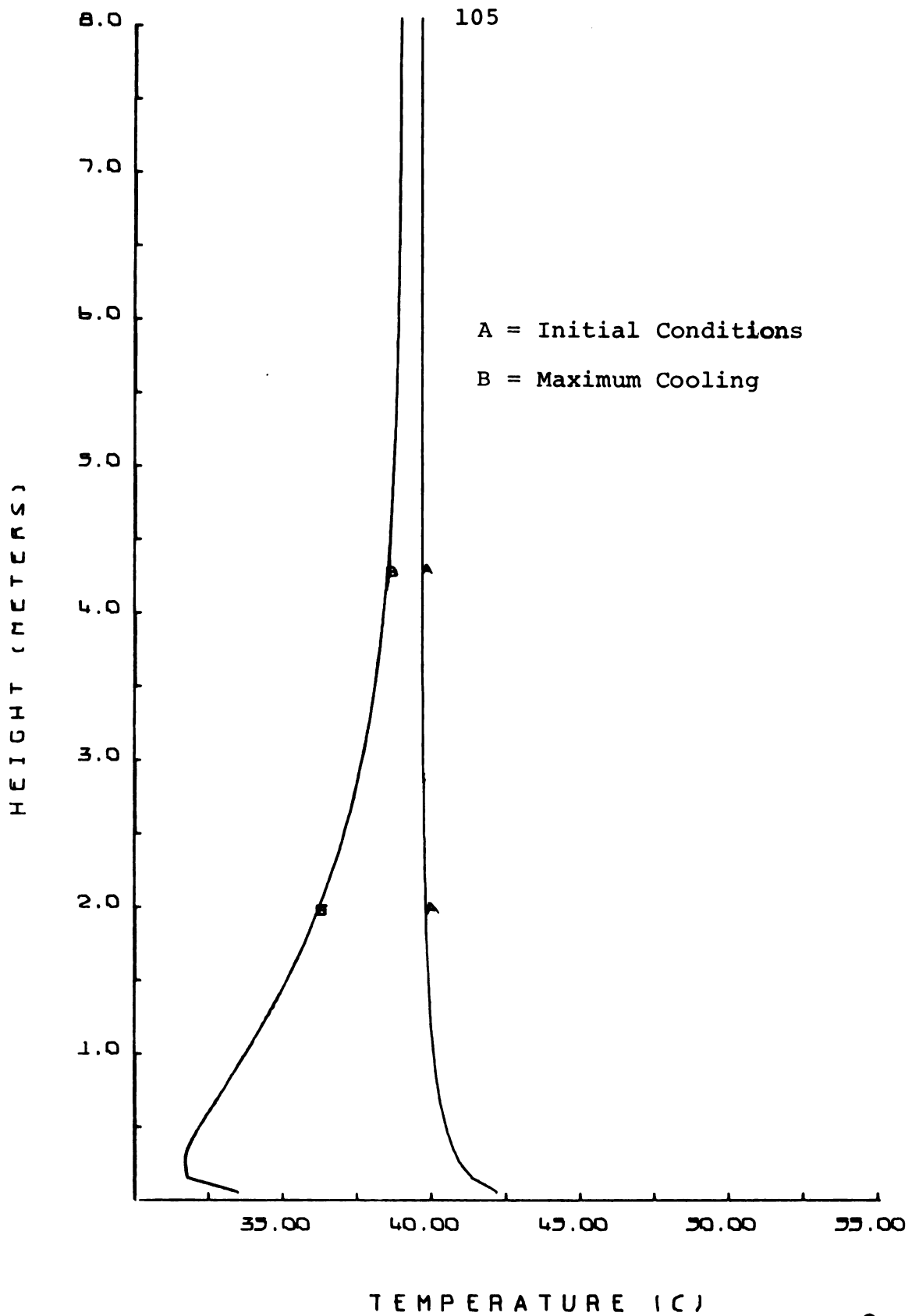
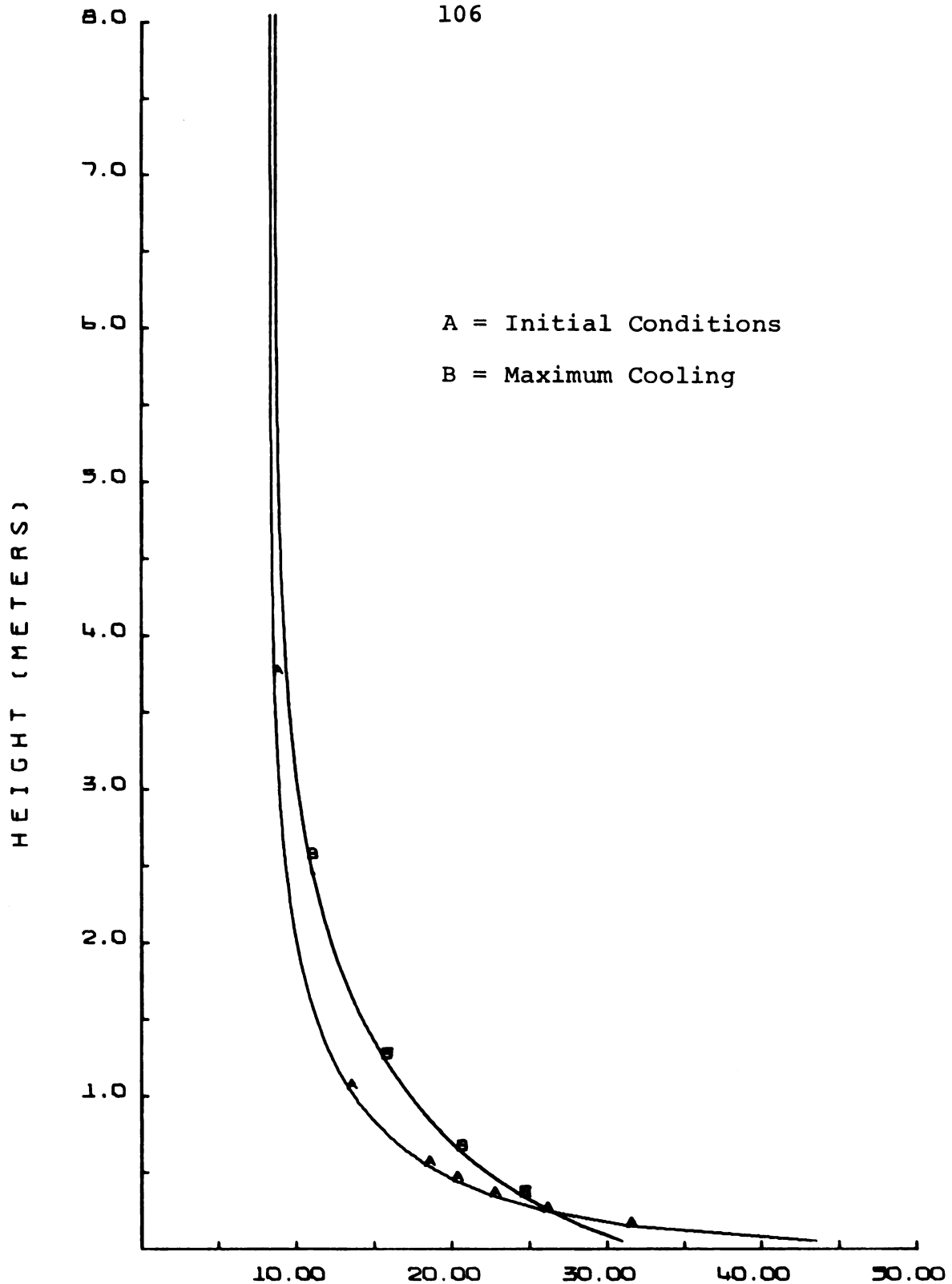


FIGURE 7.3.--Predicted temperature profiles with $T_i=40.0^{\circ}\text{C}$.



MOISTURE CONCENTRATION (G/CU M)
FIGURE 7.4.--Predicted moisture concentration profiles for
 $T_i=40.0^{\circ}\text{C}$ and $\text{R.H.}_i=25\%$.

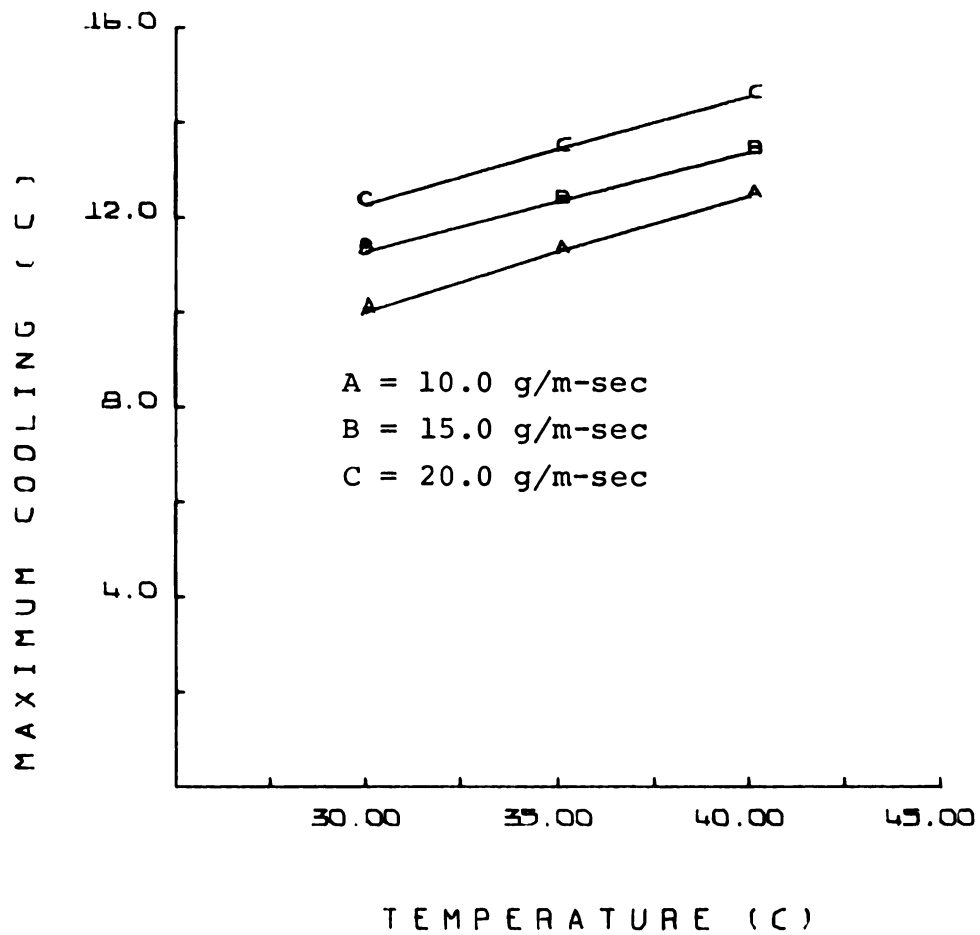


FIGURE 7.5.--Maximum cooling with $u_i=0.5$ m/sec and three spray rates.

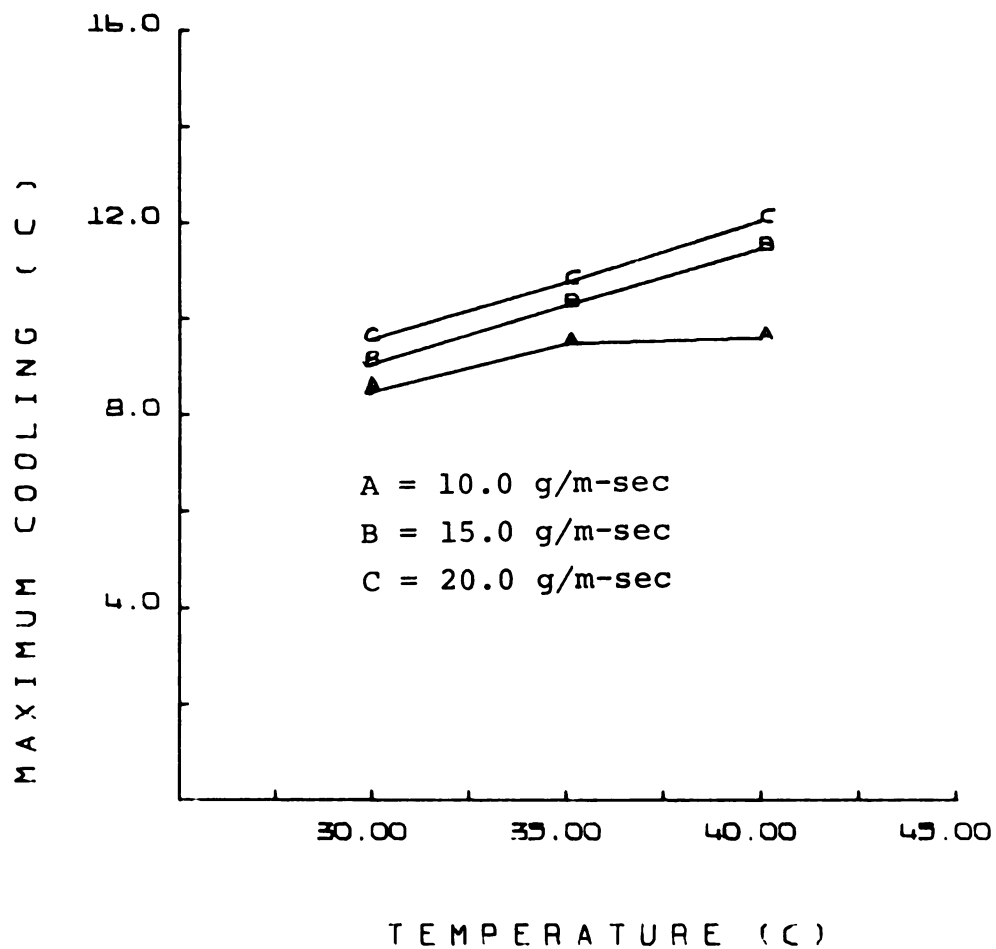


FIGURE 7.6.--Maximum cooling with $u_i=1.0$ m/sec and three spray rates.

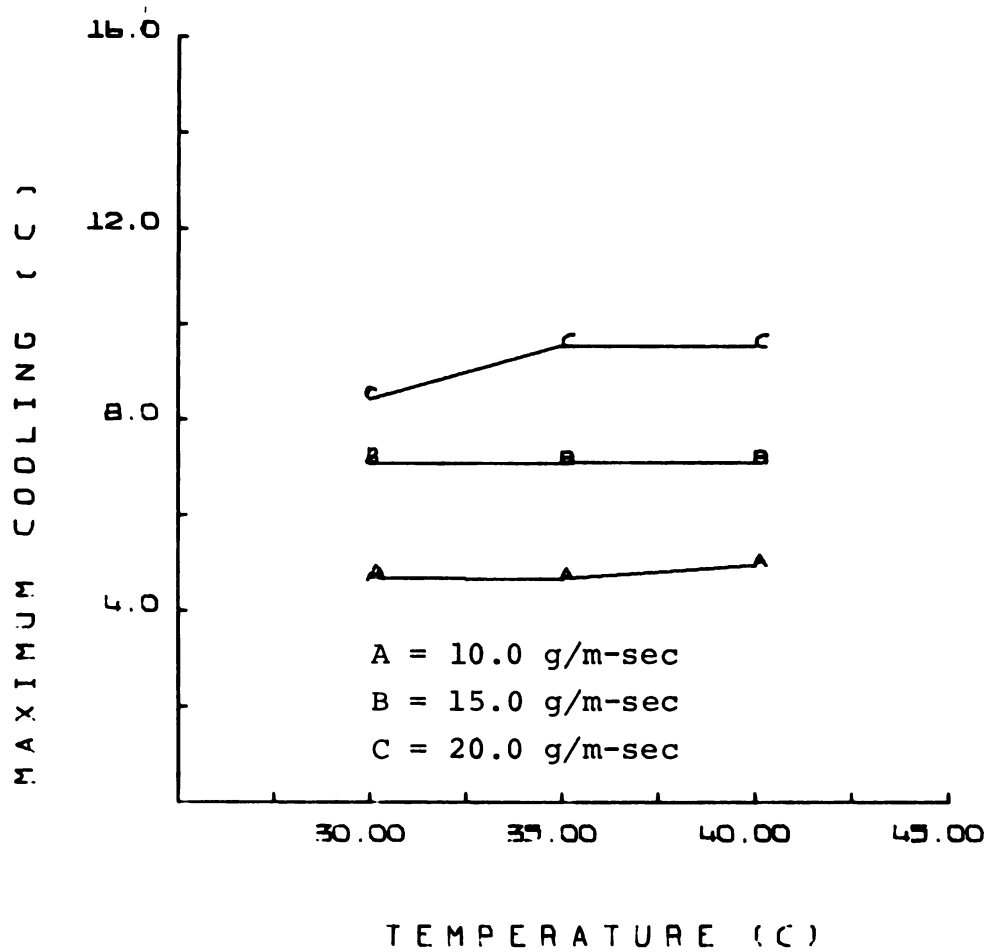


FIGURE 7.7.--Maximum cooling with $u_i=2.0$ m/sec and three spray rates.

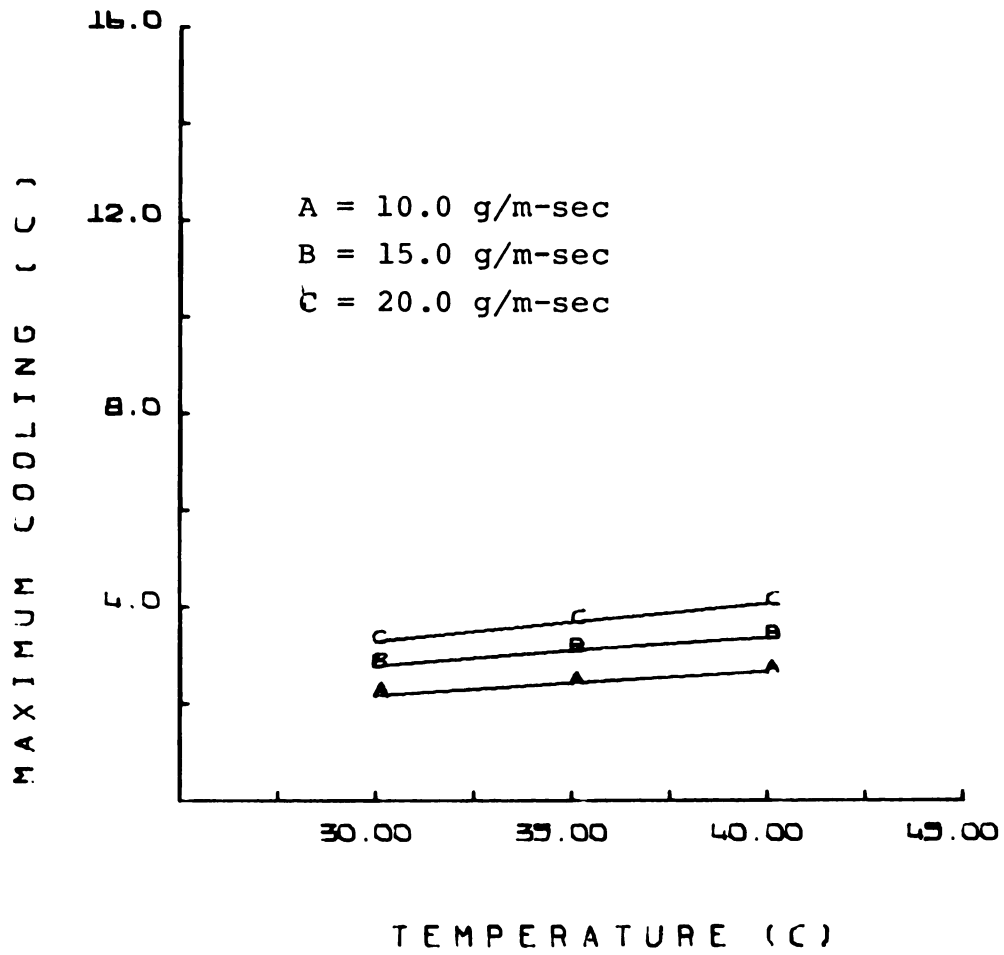


FIGURE 7.8.--Maximum cooling with $u_i=4.0$ m/sec and three spray rates.

8. DISCUSSION

The solution of the differential equations in the form of Equation (4.2.17) was required to be above the roughness height z_0 . By definition, at the height z_0 the wind speed is zero. The solution coefficients have terms involving division by $u(z)$, therefore for the coefficients to remain finite, $u(z)$ must be greater than zero. The lowest solution height chosen was $z_1 = 0.005$ m, which introduces no appreciable error since z_0 was 0.0016 m.

Early preliminary results disclosed that the selection of the vertices of the initial triangular liquid water droplet concentration profile was not critical. The points chosen below the 1 m spray line were: bottom, $z_2 = 0.4$ m; middle, maximum spray concentration, $z_{MS} = 0.6$ m; and the top, $z_3 = 0.8$ m. Turbulent diffusion was sufficient to mask variations about these values.

An implied assumption in the development of the source term for Equation (3.1.2) was that gravitational settling of the drops was negligible. The meteorological definition of a cloud drop is one whose diameter is less than 200 μ , [Huschke (1959), p. 111]. The mean diameter of the spray drops are well within the cloud definition.

Stokes Law, [Huschke (1959), p. 543], can be used to estimate the terminal velocity of the drops in still air, Equation (8.1).

$$v_T = \frac{2}{9} a^2 g (\rho_w - \rho) / \eta \quad (8.1)$$

where: v_T = terminal velocity of spherical drops in still air, (cm/sec),
 a = droplet radius, (cm),
 g = acceleration of gravity, (cm/sec²),
 ρ_w = water droplet density, (g/cm³),
 ρ = density of medium, (g/cm³),
and η = dynamic viscosity, (g/cm-sec).

For this case the air density is much less than the droplet density so it can be neglected. The dynamic viscosity for air at 30°C is 1.866×10^{-4} g/cm-sec, [List (1966), p. 395]. The terminal velocities for 10 and 50 μ radius drops become 0.012 and 0.291 m/sec respectively. Since the droplet radius is constantly decreasing due to evaporation, its terminal velocity will also be decreasing. Thus the fall velocity is much less than the turbulent velocity fluctuations and the assumption is justified.

The use of the method of images for the liquid water and water vapor concentration profiles to establish a zero flux lower boundary condition caused a point of discontinuity in the wind speed profile. The diffusivity profile was

likewise affected at the lowest solution point since it is a function of the wind speed gradient. The value of the wind speed gradient at the lowest node was therefore assumed zero. Zero provided reasonable results in contrast to using either of the gradients from above or below this point.

The choice of zero for the velocity gradient caused the calculation of the intermediate solution coefficient, P_4 , at that node to produce erroneous solutions near the boundary if the downwind solution step was too small. The size of the solution step, DX , was therefore chosen to be greater than $0.125 / P_{4IZ1}$, where P_{4IZ1} is the value of P_4 at the node $IZ1$ closest to the ground surface. In all cases the minimum value set for DX was 1.0 m to reduce computer time. This caused no problem since for the Leichtman-Ponomareva form of α_H , the computed minimum for DX was 0.25 m whereas the use of $\alpha_H=1$ required DX to be 1.25 m.

The continuity check of the three profiles at each solution step revealed an error of less than 0.5% of the total integrated value for each profile, i.e. liquid water concentration, energy, and water vapor concentration, at that solution step. The low value of the error demonstrates the accuracy of the solution procedure used. The small amount of water vapor added to and sensible heat removed from the total system with respect to the water vapor and energy

initially present was severely masked by the compounding of the relatively small percent error at each step. A scheme was therefore developed for reapportioning the error at each solution step to each vertical node in proportion to that nodes contribution to the total sum of profile values for all nodes at that solution step. The change was very minor at each node but the elimination of the compounding error problem was achieved. The exact cause of the error was never determined.

The solution for water vapor concentration at each downstream step was checked for saturation at the lowest active nodes. None of the runs reported in this thesis achieved saturation. If an excessive amount of water was sprayed into the air, e.g. 40 g/m-sec, the combined small evaporation source term and vapor diffusion caused local saturation. These conditions were beyond the applicability of the model, however, since large amounts of water would require higher droplet concentrations and/or larger drops which in turn affects the evaporation coefficient, c_1 , and the assumed negligible settling rate of the drops.

For solutions of the problem using drops larger than 200 μ (0.2 mm diameter), e.g. evaporation in sprinkler irrigation, the source term must be rewritten to include the settling rate. The droplet deposition process could be included at the same time the model is redeveloped for

a plant canopy. With a plant canopy at the lower boundary and droplet deposition at the surface, all three profiles would have flux rates as the lower boundary condition. The method of images could then be replaced thereby reducing the number of solution nodes by a factor of two for the liquid and vapor profiles. Model wise, the redevelopment is not believed particularly difficult. The complexity of the problem would instead lie in the experimental verification of the flux terms at the "surface" of the plant canopy.

9. CONCLUSIONS

The following conclusions have been drawn from this investigation.

- (1) Significant cooling can be achieved by mist evaporation.
- (2) Maximum cooling occurs with light winds when the liquid water is not diffused out of the region.
- (3) Minimum distances required for complete evaporation occur with high winds creating more turbulent diffusion and dispersion of the liquid water drops.
- (4) More precise humidity measurement systems are required.
- (5) The Leichtman-Ponomareva approximate relationship for α_H was adequate for this investigation and much more realistic than $\alpha_H=1$.
- (6) The Swinbank profile for wind speed was very good, but the similarity profiles for temperature and moisture concentration were much poorer for this investigation.

APPENDICES

APPENDIX A
DETAILED REVIEW OF CLOUD DROPLET
EVAPORATION MODELS

The following is a more detailed review of the models developed by Zung (1967,a,b, and 1968) for cloud droplet evaporation.

Zung (1967,a) developed the modified cellular method. In the modified cellular method, the mass balance equation for a cell was used to determine the average concentration of molecules per unit volume:

$$\bar{c}(t) = [\int_a^b c(r,t)4\pi r^2 dr] / \frac{4}{3}\pi (b^3 - a^3). \quad (A1)$$

It was then assumed that $c_0 = c_\infty = 0$, i.e. the initial vapor concentration was zero, to obtain

$$\bar{c}(t) = \rho_w (a_0^3 - a^3) / m_2 (b^3 - a^3). \quad (A2)$$

By equating $\bar{c}(t)$ to c_s , the droplet radius at cellular saturation, a_s , was determined to be

$$a_s^3 = (\rho_w a_0^3 - m_2 c_s b^3) / (\rho_w - m_2 c_s). \quad (A3)$$

The value of a_s^3 was then used to ascertain if the cloud would become saturated internally during its lifetime. If $a_s^3 > 0$ the cloud would become saturated and if $a_s^3 \leq 0$, it would not. Through the use of Equation (2.5.7), the relationship of droplet mass to radius, and Equation (A2), the equation for the steady-state evaporation time was found by integration to be:

$$\frac{-\rho_w}{DW} [b^3 - a_s^3] \int \frac{ada}{(a^3 - a_s^3)} - \frac{1}{2}a^2] = t + \text{const.} \quad (\text{A4})$$

where;

$$W = \rho - c_s m_2.$$

For the unsaturated case, i.e. $a_s < 0$, Equation (A4) was integrated to:

$$\begin{aligned} t_u = & [\rho_w / D(\rho_w - c_s m_2)] \left(-\frac{1}{2}a_o^2 + (b^3 - a_s^3) \left(\frac{1}{3}a_s \right) \{ \ln(a_o - a_s) - \right. \\ & \left. \frac{1}{2} \ln(a_o^2 + a_o a_s + a_s^2) + (3)^{\frac{1}{2}} \tan^{-1} \left[\frac{a_o + \frac{1}{2}a_s}{\frac{1}{2}(3)^{\frac{1}{2}}a_s} \right] \right. \\ & \left. \left. - \frac{1}{6}(3)^{\frac{1}{2}}\pi \right\} \right) \end{aligned} \quad (\text{A5})$$

which is the lifetime of the cloud when its interior remains unsaturated under initially dry ambient conditions.

The time required to reach saturation was found in a similar manner to be:

$$\begin{aligned} t_s = & \frac{\rho}{D(\rho - c_s m_2)} \left\{ \frac{1}{2}(a_s^2 - a_o^2) + \frac{(b^3 - a_s^3)}{3a_s} \left[\frac{1}{2} \ln \left(\frac{3a_s^2}{a_o^2 + a_o a_s + a_s^2} \right) \right. \right. \\ & \left. \left. + \ln(a_o - a_s) + (3)^{\frac{1}{2}} \tan^{-1} \left(\frac{a_o + \frac{1}{2}a_s}{\frac{1}{2}(3)^{\frac{1}{2}}a_s} \right) - (3)^{\frac{1}{2}}\pi \right] \right\}. \quad (\text{A6}) \end{aligned}$$

Equation (A6) would be the final result for an enclosed system of droplets. In the atmosphere, however, the droplets around the periphery of the cloud will continue to evaporate since they will not reach an equilibrium state of saturation.

The cellular model must be modified to account for this. The outer droplets were assumed to evaporate at one half the rate of a free drop, since they were evaporating into a semi-infinite medium. Thus the droplet lifetimes would be twice that of a free droplet. The lifetime of outer droplets before saturation were found to be:

$$t_{\text{outer}} = a_o^2 \rho_w / [m_2 D (c_o - c_\infty)] , \text{ Maxwell,} \quad (\text{A7})$$

$$= \frac{\rho_w}{m_2 D (c_o - c_\infty)} \left[\frac{1}{2} a_o^2 + \frac{Da_o}{v\alpha} \left(\phi_0^{-1} - \frac{z}{a_o} E_i \left(\frac{z}{a_o} \right) \right) \right. \\ \left. - a_o \Delta + \Delta^2 \ln \left(\frac{a_o + \Delta}{\Delta} \right) \right] , \text{ F-O-Z,} \quad (\text{A8})$$

where;

$$z = 3 v \sigma_s / k_B T_A$$

$$\phi_o = \phi(a_o) ,$$

and
$$E_i(x) = \int_{-\infty}^x t^{-1} e^t dt .$$

The lifetimes of the outer droplets after saturation, t_j , has the same form as equations (A7) and (A8) with a_s substituted for a_o . The cloud lifetime after saturation was found to be:

$$t_e = \left\{ [R(1-E)^{\frac{1}{2}}/2a_0] - \left(\frac{t_s}{t_{\text{outer}}} \right) \right\} t_j, \quad (\text{A9})$$

where; E = void fraction, and the other symbols are as previously defined.

The term t_s/t_{outer} is the number of layers evaporated prior to saturation and $R(1-E)^{\frac{1}{2}}/2a_0$ is the total number of layers in the cloud. The total lifetime of the cloud in the saturated case would be:

$$t_{\text{cloud}} = t_s + t_e. \quad (\text{A10})$$

A few of the results reported by Zung using the above equations are given in Tables A1, A2 and A3.

TABLE A1.--A comparison of saturation times and cloud lifetimes for the Maxwell and Fuchs-Okuyama-Zung relationships with cloud radius, $R_0=10\text{m}$, degree of dilution, $b/a=20$, and $T=25^\circ\text{C}$.

$a, (\mu)$	$t_s, (\text{sec})$	$t_{\text{cloud}}, (\text{sec})$	
		Maxwell	FOZ
100	8.40	38,036	41,392
10	.11	3,804	7,162

TABLE A2.--Cloud lifetimes for the Maxwell relationship for various cloud radii and with $a=100\mu$, $b/a=20$, and $T=25^\circ\text{C}$.

Cloud Radius	$t_{\text{cloud}}, (\text{sec})$
1	3.8×10^3
10	3.8×10^4
100	3.8×10^5

TABLE 3A.--A comparison of saturation radii, saturation times, and cloud lifetimes for the Maxwell and Fuchs-Okuyama-Zung relationships for various degrees of dilution, b/a , with $a=10\mu$, $R=1m$, and $T=25^{\circ}C$.

b/a	$a_s, (\mu)$	$t_s, (sec)$	$t_{cloud}, (sec)$	
			Maxwell	FOZ
2	9.9994	1.57×10^{-4}	4356	7951
10	9.9226	1.59×10^{-2}	857	1571
30	7.2292	.41	152	325
40	-7.8016		.165	
50	-12.343		.112	

It is also reported that for fairly high concentrations, $b/a \leq .4(b/a)_{critical}$, a_s is nearly the same as a_o and t_s is much less than t_{cloud} . The critical value of b/a is the degree of dilution where the cloud changes from one that remains unsaturated to one that becomes saturated. From the results for the saturated cloud conditions evaporating into initially dry ambient air, the above results indicate that the cloud lifetimes predicted by the Fuchs-Okuyama-Zung relationship are approximately twice that predicted by Maxwell for $a_o=10\mu$ but about the same for $a_o=100\mu$.

Zung (1967,b) developed an alternate model for the cloud evaporation problem, using the continuum approach developed by Milburn (1957, 1958). The resulting highly non-linear model for a droplet system in a fixed atmosphere,

for a dilute cloud or one in the initial phase of evaporation where $c(r,t) \approx c(r)$, was found to be:

$$\frac{\partial}{\partial t} c(r,t) = D \nabla^2 c(r,t) + n \alpha' [m_0^{2/3} + \frac{2}{3} \beta t]^{1/2} [c_s - c(r,t)], \quad (\text{All})$$

where;

- D = diffusivity of vapor in air, (cm^2/sec),
 ∇^2 = Laplacian operator,
 n = number of droplets/unit volume,
 m_0 = initial mass of a single droplet, (g),
 c = vapor concentration, ($\text{molecules}/\text{cm}^3$),
 $\alpha' \equiv 4\pi D (3/4\pi\rho_w)^{1/3}$
 $\beta \equiv \alpha [c(r,t) - c_s] m_2$.
- and m_2 = mass of a water molecule.

Equation (All) is essentially the same as that proposed by Milburn. To linearize the cloud equation Zung assumed the vapor concentration $c(r,t)$ is approximately linear with the droplet mass. Under steady-state conditions this leads to:

$$Q_{ss} = - \frac{dM}{dt} = 4\pi R m_2 D' (c_s - c_\infty), \quad (\text{A12})$$

where;

- Q_{ss} = rate of evaporation, (g/sec),
 M = total cloud mass, (g),
 D' = new diffusion coefficient,
 $\equiv D/(1-E)$,

E = void fraction = $1 - (a/b)^3$,
i.e. the fraction of the total volume of
the cloud occupied by the gas phase,

c_s = droplet surface saturated concentration,
(molecules/cm³),

and c_∞ = water vapor concentration outside the
sphere of influence, (molecules/cm³).

note: D' = $D/(a/b)^3$.

For nonstationary conditions the rate of evaporation would
be:

$$Q_{NS} = 4\pi R D' m_2 (c_s - c_\infty) [1 + R(\pi D' t)^{-1/2}]. \quad (A13)$$

The resulting cloud lifetime equation for the steady-state
condition is:

$$t_{\text{cloud}} = (1-E)^2 [\rho_w / m_2 D (c_s - c_\infty)] (R_0^2 / 2), \quad (A14)$$

where;

ρ_w = liquid density, (g/cm³),

R_0 = initial cloud radius, (cm),

and the others are as previously noted.

An extraction of the results of calculations using equation
(A14) and those using the cellular model, as reported by
Zung (1967,b, Table I), are given in Table A4. The below
results illustrate the conclusions from Zung (1967,b, p. 3580)
that "The cellular model gives good results for an unsaturated

TABLE 4A.--A comparison of cloud lifetimes for the continuum and cellular models for various degrees of dilution with $a=10\mu^1$, $R_0=1.0m$, and $T=25^\circ C$.

b/a	t_{cloud} , (sec)	
	Continuum Model	Cellular Model
1	8.71×10^8	7.00×10^3
2	1.36×10^7	4.36×10^3
6	1.87×10^4	1.45×10^3
10	8.71×10^2	8.58×10^2
30	1.20	1.52×10^2
40	2.13×10^{-1}	1.65×10^{-1}
50	5.58×10^{-2}	1.12×10^{-1}

¹For a free single 10μ radius droplet, $t=8.714 \times 10^{-2}$ sec.

cloud but fails to converge to the upper limit where $(b/a)=1.0$, where the cloud should evaporate as a giant drop of radius R according to the Maxwell equation. The continuum model . . . yields the desired lifetime for $(b/a)=1.0$ and also shows a small transition from a saturated cloud to an unsaturated one. However, the lifetimes for an unsaturated cloud do not approach exponentially the lower limit as $(b/a) \rightarrow \infty$ as seen in the cellular model." Zung's final conclusion was to combine the two models and use the cellular method to compute cloud lifetimes for an unsaturated cloud and for calculating the time required to achieve saturation.

For saturated clouds and for the elapsed time, t_e , after saturation, Equation (A14) should be used with some modifications, namely:

$$(1) \quad R_0 \text{ should be replaced by } R_s = R_0 - (t_s/t_{\text{outer}})2b$$

where t_{outer} is computed from Equation (A7),

$$(2) \quad E = 1 - (a_s/b)^3,$$

and $(3) \quad t_{\text{cloud}} = t_s + t_e.$

Some of the results of this more general model are reported in Table A5.

TABLE A5.--A comparison of saturation radii, saturation times, and cloud lifetimes for various degrees of dilution for Zung's generalized model with $a=10\mu$, $R_0=1 \text{ m}$, and $T=25^\circ\text{C}$.

b/a	a_s , (μ)	t_s , (sec)	t_{cloud} , (sec)
1	saturated 10.0000	0	8.71×10^8
2	9.9994	1.57×10^{-4}	1.36×10^7
10	9.92	1.59×10^{-2}	8.32×10^2
30	7.23	.41	.581
40	unsaturated -7.80		.165
50	-12.3		.112

All of the models discussed to this point have been for evaporation into still air. Zung (1968) extended his model to include the effects of turbulent diffusion and cloud

expansion. He also investigated the effects of Brownian Motion and Electric Charge and found that they were much less significant than the turbulence. The current review will, therefore, be limited to the turbulent portion of the paper. The basic assumptions employed in this model were: (1) a monodisperse droplet system; (2) uniform spreading throughout the cloud; and (3) Maxwellian single droplet evaporation. The cellular and continuum models were included for comparison. The semi-empirical formula for $\bar{b}(t)$ for small values of t , i.e. lifetimes of small droplets in dilute clouds, given by Batchelor and Townsend was used:

$$\bar{b}(t) = (b_0 + 0.25 \bar{v}_t^2 t^2)^{\frac{1}{2}}, \quad (\text{A15})$$

where; \bar{v}_t = average turbulent relative velocity,
and b_0 = initial cell radius.

For the cloud radius, Zung obtained:

$$R(t) = R_0 \left[1 + \left(\frac{\bar{v}_t t}{2b_0} \right)^2 \right]^{\frac{1}{2}}. \quad (\text{A16})$$

The cellular model yields the equation;

$$\frac{da}{dt} = -\frac{Dm_2}{\rho_w} \left(\frac{c_s}{a(t)} - \frac{\rho_w}{m_2} \frac{(a_0^3 - a^3(t))}{(a(t)b^3(t) - a^4(t))} \right), \quad (\text{A17})$$

which Zung solved numerically using a combination of the second-order Runge-Kutta and the Predictor-Corrector methods.

A portion of the reported results computed from the above equation is given in Table A6.

TABLE A6.--A comparison of cloud lifetimes for the cellular model for fixed and turbulent clouds for various degrees of dilution with $a = 10 \mu$, $R = 1 \text{ m}$, $T = 25^\circ\text{C}$, $v_t = 1 \text{ cm/sec}$, and Maxwellian evaporation assumed.

Degree of Dilution b/a	Cellular Model t_{cloud} , (sec)		F/T
	Fixed ¹	Turbulent ²	
18	440	.140	3.14×10^3
30	152	.130	1.18×10^3
40	.165	.115	1.43
50	.112	.110	1.02

¹from Zung (1956, a), p. 2069, Table III.

²from Zung (1968), p. 5185, Table V.

The column labeled F/T contains the ratio of cloud lifetimes for the fixed and the turbulent clouds. The less dilute clouds differ by an order of 10^3 . The more dilute cloud ratios approach unity since the turbulence has a minimal dilution effect on an already diluted system.

The continuum model now contains a diffusion equation that is a function of time, (see the note following Equation (A12).)

$$D'(t) = D b^3(t)/a_o^3 \quad (A18)$$

Solution of the equation

$$\frac{\partial c}{\partial t} = D'(t) \nabla^2 c$$

gave for steady-state conditions,

$$Q_C = 4\pi R(t) D'(t) m_2 (c_s - c_\infty), (g/sec), \quad (A19)$$

and for non steady-state conditions,

$$Q_{NS} = Q_C [1 + R(t)/(\pi T_C)^{1/2}], (g/sec), \quad (A20)$$

where;

$$\begin{aligned} T_C = & (D/a_o^3) \{0.25t(b_o^2 + 0.25v_t^2 t^2)\}^{3/2} \\ & + \frac{3}{8} b_o^2 t (b_o^2 + 0.25v_t^2 t^2)^{1/2} \\ & + (3 b_o^4 / 4v_t) \ln[0.5v_t t + (b_o^2 + 0.25v_t^2 t^2)^{1/2}]. \end{aligned}$$

A portion of the results reported for the stationary continuum model using the same conditions as the cellular model above are given in Table A7. The below results cannot be compared directly with those given for the cellular model in Table A6 since the latter is for cloud lifetimes, not evaporation rates. To convert the below results to cloud lifetimes, Zung (1968, p. 5186) suggests using the results for the fixed cloud lifetimes reported in Zung (1967,b) and the ratio

TABLE A7.--A comparison of evaporation rates for the continuum model for fixed and turbulent clouds for various degrees of dilution with $a_0 = 10 \mu$, $R_0 = 1 \text{ m}$, $T = 25^\circ\text{C}$, $v_t = 1 \text{ cm/sec}$, and Maxwellian evaporation assumed.

Degree of dilution b/a	Continuum Model	
	Evaporation rates, (g/sec)	
	Fixed	Turbulent
18	4.20×10^1	6.33×10^{10}
30	1.94×10^2	3.80×10^{10}
40	4.61×10^2	2.85×10^{10}
50	9.01×10^2	2.28×10^{10}

of the above evaporation rates. This does not give a comparable result, however. The values above would indicate a cloud lifetime of the order of 10^{-9} less for the turbulent case versus the fixed case which is inconsistent with the cellular model's results of $O(10^3)$. The values reported above were "averages over the entire lifetimes of the cloud--". No indication of the actual times used was reported.

To check this, Equations (A15) and (A16) were rewritten to be:

$$\bar{b}(t) = [b_0^2 + (\frac{v_t t}{2})^2]^{\frac{1}{2}} \text{ and } R(t) = R_0 \frac{b(t)}{b_0} \quad (\text{A21})$$

By substituting equations (A18) and (A21) into equation (A19) one obtains:

$$Q_C = \frac{4\pi DR_0 m_2}{b_0 a_0^3} b^4(t) (c_s - c_\infty). \quad (\text{A22})$$

If one solves Equation (A22) for $b(t)$ and utilizes the results with the expression for $\bar{b}(t)$, a value of t can be found. For the following conditions:

$$a_0 = 10\mu = 10^{-3} \text{ cm}, \quad T=25^\circ\text{C},$$

$$R_0 = 100 \text{ cm}, \quad v_t = 1 \text{ cm/sec},$$

$$c_\infty = 0 \text{ (the most severe condition, i.e. maximum evaporation),}$$

$$m_2 c_s = 2.33 \times 10^{-5} \text{ g/cm}^3 \text{ @ } T=25^\circ\text{C}, \text{ (List(1966))},$$

$$D = 0.249 \text{ cm}^2/\text{sec}, \text{ (Zung(1967,a))},$$

$$b/a = 18,$$

and $Q_C = 6.333 \times 10^{10} \text{ g/sec}, \text{ (Table A7)},$

t was found to be 7.06 sec, clearly outside the lifetime of the cloud as indicated by the cellular model.

The variation of Q_C with t for the above conditions is given in Table A8.

TABLE A8.--A comparison of the evaporation rates for various average cloud lifetimes using Equation (A22) with $a_0=10 \mu$, $R_0=1 \text{ m}$, $T=25^\circ\text{C}$, $v_t=1 \text{ cm/sec}$, $c_\infty=0$, $m_2 c_s=2.33 \times 10^{-5} \text{ g/cm}^3$, $D=0.249 \text{ cm}^2/\text{sec}$ and $b/a=18$.

t , (sec)	Q_C , (g/sec)
0	42.7
.01	49.1
.1	3.23×10^3
1.0	2.55×10^7
10.0	2.55×10^{11}

For a cloud lifetime of the order of 0.1 sec as indicated by the cellular model the average evaporation rate during its lifetime would be of the order of 10^3 g/sec not 10^{10} g/sec as reported.

The mass of the cloud can be found by:

$$\text{cloud mass} = \left(\frac{\text{volume/cloud}}{\text{volume/cell}} \right) \left(\frac{1 \text{ drop}}{\text{cell}} \right) \left(\frac{\text{mass}}{\text{drop}} \right). \quad (\text{A23})$$

By substitution of the formulae for the respective spherical volumes, the cloud mass becomes:

$$\text{cloud mass} = \frac{4\pi}{3} R_o^3 \left(\frac{a_o}{b_o} \right)^3 \rho_w \quad (\text{A24})$$

where;

$$\rho_w = \text{water density, (g/cm}^3\text{)}.$$

For the above conditions the cloud mass becomes 7.23×10^2 g/cloud. Thus the "average" evaporation rate of $O(10^3)$ would yield a cloud lifetime of $O(10^{-1})$ as in the purely cellular model. Clearly the evaporation rates reported for the continuum model with turbulent diffusion are inconsistent with the cellular model and the conclusions derived therefrom suspect. The evaporation rates in the expanding cloud are greater than those in a fixed cloud by a factor more nearly 10^3 rather than the reported value of 10^7 or 10^8 .

None of the above models have been experimentally verified and can be therefore used only as a guide to the evaporation process. The use of the Maxwell formulation in the diffusing cloud would not be expected to be accurate since Zung (1967,b) pointed out that it was valid only for droplets with $a_0 > 100\mu$. The models do serve the purpose of demonstrating the complexity and incomplete solution of the problem.

APPENDIX B
FIELD DATA AND PREDICTION MODEL RESULTS

TABLE B1.--30 min mean wind speed data, m/sec.

Height m	Mast 1		Mast 3	
	Mean	Standard Deviation	Mean	Standard Deviation
8	4.88	1.34		
4	4.28	1.24	4.83	1.19
2	4.53	1.20	4.56	1.08
1	4.45	1.08	4.32	1.03

TABLE B2.--30 min mean initial conditions (mast 1).

Height m	Dry Bulb °C	Wet Bulb °C	Moisture Concentration g/m ³	Mixing Ratio g/kg	Relative Humidity %
8	22.3	15.7	9.81	8.56	50.7
6	22.2	15.0	8.94	7.79	46.2
4	21.7	16.9	11.66	10.18	62.3
2	21.5	14.6	8.78	7.63	47.4
1	22.2	18.7	13.86	12.17	71.8

TABLE B3.--30 min mean temperature and moisture values.

Mast No.	Height m	Dry Bulb OC	Wet Bulb OC	Moisture Concentration g/m ³	Mixing Ratio g/kg	Relative Humidity %
2	8	22.0	14.8	8.76	7.63	46.0
	6	22.2	14.7	8.53	7.43	44.2
	4	22.1	15.8	10.06	8.78	52.6
	2	22.1	15.8	10.05	8.77	52.5
	1	21.9	18.1	13.24	11.60	69.8
3	8	22.0	14.4	8.30	7.22	43.5
	6	22.1	14.6	8.46	7.37	44.2
	4	21.8	15.4	9.69	8.44	51.5
	2	21.5	16.4	11.11	9.69	60.1
	1	21.3	17.5	12.72	11.11	69.3
4	8	21.8	13.9	7.77	6.75	41.1
	6	21.8	14.4	8.34	7.26	44.1
	4	21.6	16.0	10.56	9.21	56.5
	2	21.4	14.3	8.43	7.32	45.8
	1	21.5	16.6	11.33	9.89	61.2
5	8	21.7	14.6	8.74	7.60	46.7
	6	21.6	14.6	8.70	7.57	46.7
	4	21.5	16.0	10.61	9.25	57.4
	2	21.1	15.6	10.24	8.91	56.5
	1	21.3	18.1	13.48	11.79	73.6

TABLE B4.--A summary of the assigned constants used in the theoretical model.

L	$= -1.66 \text{ m}$
u_*	$= 0.28 \text{ m/sec}$
z_0	$= 0.0016 \text{ m}$
H	$= 0.13 \text{ ly/min}$
T_*	$= -0.869 \text{ }^\circ\text{C}$
T_0	$= 27.8 \text{ }^\circ\text{C}$
χ_*	$= -1.66 \text{ g/m}^3$
χ_0	$= 21.7 \text{ g/m}^3$
ρ	$= 1.15 \text{ kg/m}^3$
L_v	$= 585.0 \text{ cal/g}$
c_p	$= 0.242 \text{ cal/g-}^\circ\text{C}$
Δx	$= 1.0 \text{ m}$
$\Delta \omega$	$= 0.1$
SPRAY	$= 8 \text{ g/m-sec}$
c_1	$= 0.02 \text{ sec}^{-1}$
z_2	$= 0.4 \text{ m}$
z_{MS}	$= 0.6 \text{ m}$
z_3	$= 0.8 \text{ m}$

TABLE B5.--Values of the constants used in the Prediction model.

$R.H._i$	=	0.25
ρ	=	1.12 kg/m ³
L_v	=	580.0 cal/g
c_p	=	0.250 cal/g-°C
c_l	=	0.02 /sec
P	=	1000 mb
z_0	=	0.01 m
z_2	=	0.4 m
z_{MS}	=	0.6 m
z_3	=	0.8 m
$\Delta\omega$	=	0.1
Δx	=	1.0 m

TABLE B6.--Prediction model results.

Spray g/m-sec	T _i °C	L m	ΔT_{OC}^{max}	X _{max} m	Z _{max} m	H ly/min	u* m/sec	T _O °C	T* °C	X _O g/m ³	X* g/m ³
For u _i = 0.5 m/sec											
10	30	- 1.0	-10.0	16.0	0.75	<0.00	0.05	30.16	-0.04	29.37	-5.25
	35	- 1.0	-11.3	15.0	0.15	<0.00	0.05	35.19	-0.05	39.17	-6.99
	40	- 1.0	-12.4	13.0	0.55	<0.00	0.05	40.22	-0.05	51.85	-9.23
15	30	-10.0	-11.3	43.0	1.05	<0.00	0.04	30.02	>-0.00	29.12	-4.72
	35	-10.0	-12.3	38.0	0.95	<0.00	0.04	35.02	-0.01	38.80	-6.27
	40	- 1.0	-13.36	16.0	0.85	<0.00	0.05	40.22	-0.05	51.85	-9.23
20	30	-10.0	-12.27	53.0	1.55	<0.00	0.04	30.02	<-0.00	29.12	-4.72
	35	-10.0	-13.43	46.0	1.35	<0.00	0.04	35.02	-0.01	38.80	-6.27
	40	-10.0	-14.55	41.0	1.25	<0.00	0.04	40.03	-0.01	51.31	-8.27
For u _i = 1.0 m/sec											
10	30	- 1.0	- 8.47	17.0	0.25	0.01	0.10	30.66	-0.16	30.22	-5.46
	35	- 1.0	- 9.47	15.0	0.15	0.01	0.10	35.77	-0.18	40.46	-7.30
	40	- 1.0	- 9.57	13.0	0.15	0.02	0.10	40.88	-0.21	53.76	-9.69
15	30	- 1.0	- 9.04	20.0	0.55	0.01	0.10	30.66	-0.16	30.22	-5.46
	35	- 1.0	-10.27	19.0	0.45	0.01	0.10	35.77	-0.18	40.46	-7.30
	40	- 1.0	-11.44	17.0	0.35	0.02	0.10	40.88	-0.21	53.76	-9.69
20	30	-10.0	- 9.56	42.0	0.35	<0.00	0.09	30.08	-0.02	29.23	-4.74
	35	- 1.0	-10.74	21.0	0.65	0.01	0.10	35.77	-0.18	40.46	-7.30
	40	- 1.0	-12.03	19.0	0.55	0.02	0.10	40.88	-0.21	53.76	-9.69

TABLE B6.--Continued.

Spray g/m-sec	T _i °C	L m	ΔT _{max} °C	X _{max} m	Z _{max} m	H ly/min	u* m/sec	T _O °C	T* °C	X _O g.m ³	X* g/m ³
For u _i = 2.0 m/sec											
10	30	- 1.0	-4.69	15.0	0.15	0.09	0.19	32.63	-0.63	33.86	- 6.33
	35	- 1.0	-4.65	13.0	0.15	0.11	0.19	38.07	-0.74	46.03	- 8.64
	40	-10.0	-4.95	13.0	0.35	0.01	0.18	40.45	-0.10	52.51	- 8.53
15	30	- 1.0	-7.08	20.0	0.15	0.09	0.19	32.63	-0.63	33.86	- 6.33
	35	- 1.0	-7.08	17.0	0.15	0.11	0.19	38.07	-0.74	46.03	- 8.64
	40	- 1.0	-7.10	15.0	0.15	0.12	0.19	43.51	-0.84	62.06	-11.68
20	30	- 1.0	-8.42	21.0	0.15	0.09	0.19	32.63	-0.63	33.86	- 6.33
	35	- 1.0	-9.54	23.0	0.15	0.11	0.19	38.07	-0.74	46.03	- 8.64
	40	- 1.0	-9.54	19.0	0.15	0.12	0.19	43.51	-0.84	62.06	-11.68
For u _i = 4.0 m/sec											
10	30	-10.0	-2.15	15.0	0.45	0.06	0.35	31.34	-0.29	31.44	- 5.22
	35	-10.0	-2.42	13.0	0.45	0.06	0.35	36.57	-0.34	42.33	- 7.04
	40	-10.0	-2.66	11.0	0.45	0.07	0.35	41.79	-0.39	56.52	- 9.40
15	30	-10.0	-2.78	20.0	0.45	0.06	0.35	31.34	-0.29	31.44	- 5.22
	35	-10.0	-3.09	17.0	0.45	0.06	0.35	36.57	-0.34	42.33	- 7.04
	40	-10.0	-3.36	15.0	0.45	0.07	0.35	41.79	-0.39	56.52	- 9.40
20	30	-10.0	-3.28	25.0	0.35	0.06	0.35	31.34	-0.29	31.44	- 5.22
	35	-10.0	-3.68	21.0	0.35	0.06	0.35	36.57	-0.34	42.33	- 7.04
	40	-10.0	-4.07	18.0	0.35	0.07	0.35	41.79	-0.39	56.52	- 9.40

APPENDIX C

FORTRAN IV PROGRAM FOR THEORETICAL MODEL

The following FORTRAN IV program is for the theoretical solution of the environmental modification problem with Swinbank initial conditions. The total program is composed of the main program DIFSN, subroutines CONST, BEGIN, TOTAPE, I C, B C, SATURAT, CORRECT, ODDEVEN, OTPT, SOURCE, COEFF, SOLVE and INTGRL, and functions ALPHA, FRCTN, and FSUM.

Subroutine CONST initializes all the constants that must be set to start the solution. The integer node numbers are calculated for several points of interest, eg. IZ1 for z_1 , IZ2 for z_2 , IZ for z_{\max} , etc.

Subroutine BEGIN computes the nodal and bi-nodal midpoint values for: wind speed, U (J) and UM (J), wind speed gradient, DUDZ (J) and DUDZM (J), diffusivities, AK (J) and AKM (J), and diffusivities divided by wind speed, AKBU (J) and AKBUM (J).

Subroutine TOTAPE writes the array O (J) onto magnetic tape for later access for graphing purposes. The array O (J) acts as a buffer for intermediate handling of other arrays or portions of arrays. The first call to TOTAPE also writes the vertical node heights. All subsequent calls write only O (J) plus identification information.

Subroutine I C calculates the initial profiles for liquid water concentration, temperature, and water vapor concentration. Subroutine B C is an entry within I C and establishes the fixed boundary conditions.

Subroutine SATURAT computes the saturated vapor pressure, saturated mixing ratio, and saturated water vapor concentration.

Subroutine CORRECT provides the continuity error reapportionment.

Subroutine ODDEVEN determines if the number of intervals between two specified nodes is odd or even because the Simpson's integration procedure has been modified to include an odd number of spaces.

Subroutine OTPT is used to write model profiles. Any single dimension array can be written with the appropriate call to OTPT.

Subroutine SOURCE calculates the modification source term for all three solutions. Some of the intermediate parameters are also computed.

Subroutine COEFF calculates the remaining intermediate parameters and the solution coefficients.

Subroutine SOLVE physically solves the diffusion equations.

Subroutine INTGRL uses Simpson's approximation to integrate any array between specified nodal limits. If the limits are out of sequence an error diagnostic is printed.

Function FRCTN calculates the weight function for the initial liquid water concentration profile.

Function SUM computes the sum of the elements in any one dimensional array. The value from SUM is used in CORRECT.

```

PROGRAM DIFSN
DIMENSION TOTAL(3),TOTALI(3),CTOTAL(3),YD(3),FYD(3),PEVA(3),TAW(3)
1,CORERR(3),FCRRER(3)
COMMON XU,XD,XL,IX,INTG,ZMX,ZMN,ZZ,Z1,H,ROC,IZ,IZ1,IZ2,IZ3,NEQ,TI,
IZ2,Z3,AL,USTAR,VK,AC ,IZM1,DOM,DDP,DX,DZ,TSTAR,USBK,DTLB,K,X1,ZTI,
2U( 201),UM( 201),IX1,RLH,OM( 201),Z( 201),AK( 201),AKM( 201),ZMS,
3DUDZ( 201),DUDZM( 201),AKBU( 201),AKBUM( 201),O( 201),ZUB( 201),
4EVEN,TSF,SPRAY,WATER,AXZ,TZ,UBL,F(3, 201),PI(3, 201),DELF(3, 201)
COMMON/SATBLK/ P,ORDA,RV,CP,CPV,EPS,CHISAT(201),CHISTAR,CHIZ,ITI
COMMON/SOBLK/ZB(201),M,ALRC,ALEV,EVAP,ES(201),Q(201),RHOMA,C1,J
COMMON/COEBLK/ A(201),B(201),C(201),QBU(201),PDPF(201),ALPHAH
READ 200,IUNIT1,IUNIT2
200 FORMAT (2A4)
C-----TO DELETE TAPE OUTPUT, SET IOTAPE = 0, REMOVE THE EQUIP CARD, AND REMOV
C      E THE TAPE CONDITION CARD IN THE SOLUTION SECTION
IOTAPE = 5
K = 0
CALL CONST
CALL BEGIN
P4IZ1 = AC*AKBUM(IZ1)*(1.0+DOM*DUDZM(IZ1)/(6.0*UM(IZ1)))/(DOM*DOM)
DX = 0.125/P4IZ1
IF (DX .LE. 1.0) 1,2
1 DX = 1.0
GO TO 14
2 IDX = DX
DEL = DX-IDX
IF (DEL.LE.0.25) 6,7
6 DX = IDX + 0.25
GO TO 14
7 IF (DEL.LE.0.50) 8,9
8 DX = IDX + 0.50
GO TO 14
9 IF (DEL.LE.0.75) 12,13
12 DX = IDX + 0.75
GO TO 14
13 DX = IDX + 1.00

```

```

PROGRAM DIFSN (CONT'D)

14 CONTINUE
  IX = XL/DX + 1.
  AXZ = DX * DZ
  CALL I C
  HLANG = H*0.006
  HSFC = H*DX
  PRINT 128,DX,DOM,DZ,IZ1,Z(IZ1),IZ2,Z(IZ2),IZ3,Z(IZ3),IZ,Z(IZ),IX1,
  1IX,TSF,ZMS,AXZ
128 FORMAT(*1*,4X*DX*3X*DOM*3X*DZ*3X*IZ1*2X*Z(IZ1)*2X*IZ2*2X*Z(IZ2)*2X
  1*IZ3*2X*Z(IZ3)*3X*IZ*3X*Z(IZ)*2X*IX1*3X*IX*4X*TSF*5X*ZMS*5X*AXZ*/
  26X*M*2(10X*M*),2(12X*M*),13X*M*17X*C*7X*M*6X*SQ M*//
  3 1X,2F6.2,F6.3,4(15,F8.4),2I5,3F8.4)
  PRINT 100,H,ROC,TSTAR,DTLB,TZ,AL,USTAR,HSFC,WATER,RLH,ALPHAH,CHIST
  1AR,CHIZ
100 FORMAT(*--*,7X,**,6X,**RHO X CP**,4X,*TSTAR*,3X,*DT/ DZETA**,3X,*TZER
  10*,7X,*L*,8X,*USTAR**,6X,**HSFC**,5X,**WATER**,6X,**RLH**,4X,**ALPHAH**,3X,
  2*CHISTAR CHI ZERO*/,1X, *CAL/SQ M/SEC CAL/CU M/C**,5X,3(*C**,9X).
  3M*,8X,*M/SEC CAL/M(Y) SEC *,*G/SQ M**,3X,*CAL/M SEC**, 8X,2(2X,*G/C
  4U/ M*)// 3X,9F10.4,F12.4, F 8.4,F9.4,F10.4)
  PRINT 129 , ALEV,ALRC,HLANG
129 FORMAT (*--* 3X*ALEV*5X*ALEV/ROC*6X*H*/
  14X*CAL/G*4X*CU M C/G*3X*LY/ MIN*///3F10.4)
  M = 1
  IOT = 1
  DO 30 K = 1,NEG
  DO 21 I=1,IZ
C-----LOADING OF THE INITIAL PROFILE ARRAY, PI(K,I)
  21 O(I) = PI(K,I) = F(K,I)
  CALL OTPT (O,IZI,IZ,K)
  IF (IOTAPE .EQ. 5) CALL TOTAPE (IOT,K)
  IOT = IOT+1
  DO 22 J=IZ1,IZ
  22 O(J) = F(K,J)*U(J)
  CALL INTGRL (IZ1,IZ,O,DZ,WAT)

```

```

PROGRAM DIFSN (CONT'D)

      IF (K.EQ.2) 31,32
31  TOTAL(K) = TOTALI(K) = WAT * ROC
      IUNIT = IUNIT2
      GO TO 30
32  IUNIT = IUNIT1
      TOTAL(K) = TOTALI(K) = WAT
30  WRITE(61,136) K,TOTAL(K),IUNIT
136  FORMAT ('*0*.*THE INTEGRATED VALUE OF F(*I1*.*J) X U(J) =*F12.4,A4*/
      1 M(Y) SEC*')
      TOTALW = TOTAL(1)+TOTAL(3)
      WRITE(61,112) TOTALW
112  FORMAT ('*0*.*THE TOTAL WATER PRESENT =*F12.4,* G/ M(Y) SEC*')
      XDELFMX = 0.0
      SUMEV = 0.0
      SUMFR = SUMFN = 0.0
      ZUB(1) = Z(123)
      AK(1) = I23
      KK = 1
      SUMS1 = 0.0
      WATLOS = 0.0
C-----DELFI(K,J) AND PI(K,J) ARE SUBSEQUENTLY USED AS FOLLOWS
C      PI(K,J) = INITIAL F(K,J)-----DELFI(K,J) = CHANGE IN F(K,J)
C-----AFTER (COEFF) HAS BEEN CALLED THE FIRST TIME ,AK, AKM, DUDZ, DUDZM,
C-----AKBU, AND AKBUM ARE NO LONGER USED WITH THEIR ORIGINAL MEANING
C      AK(M) = NODAL POSITION OF THE UPPER BOUNDARY LIMITS
C      AKM(I) = ADJUSTED ENERGY OUTPUT ARRAY FOR INTERGRATION
C      AKBU(J) = SATURATION DEFICIT
C      AKBUM(M) = ENERGY EXCHANGE FROM THE SOURCE
C      ZB(M) = MOISTURE EXCHANGE FROM THE SOURCE
C      DUDZ(J) = WATER VAPOR ADJUSTMENT IF SUPERSATURATION OCCURED
C      DUDZM(J) = TEMPERATURE ADJUSTMENT IF SUPERSATURATION OCCURED
      DO 4 K = 1,NEG
      DO 4 J = 1, IZ
      4 DELFI(K,J) = 0.0

```

PROGRAM DIFSN (CONT'D)

```

C-----BEGINNING OF THE SOLUTION SECTION
DO 10 M=2,IX
XD = XU+DX
IOTAPE = 0
IF (DX .EQ. 1.0) 15,16
15 GO TO (153,150,153,153,151,152,152,153,158),ITI
150 IF (XD.EQ.12.00.OR.XD.EQ.23.00.OR.XD.EQ.35.00.OR.XD.EQ.46.00)18,19
151 IF (XD.EQ.10.00.OR.XD.EQ.21.00.OR.XD.EQ.31.00.OR.XD.EQ.41.00)18,19
152 IF (XD.EQ.11.00.OR.XD.EQ.22.00.OR.XD.EQ.33.00.OR.XD.EQ.44.00)18,19
153 IF (XD.EQ.12.00.OR.XD.EQ.24.00.OR.XD.EQ.37.00.OR.XD.EQ.49.00)18,19
158 IF (XD.EQ.11.00.OR.XD.EQ.21.00.OR.XD.EQ.32.00.OR.XD.EQ.43.00)18,19
16 IF (DX .EQ. 1.25) 17,19
17 GO TO (156,157,156,156,154,155,155,156,159),ITI
154 IF (XD.EQ.10.00.OR.XD.EQ.20.00.OR.XD.EQ.31.25.OR.XD.EQ.41.25)18,19
155 IF (XD.EQ.11.25.OR.XD.EQ.22.50.OR.XD.EQ.32.50.OR.XD.EQ.43.75)18,19
156 IF (XD.EQ.12.50.OR.XD.EQ.25.00.OR.XD.EQ.36.25.OR.XD.EQ.48.75)18,19
157 IF (XD.EQ.11.25.OR.XD.EQ.22.50.OR.XD.EQ.35.00.OR.XD.EQ.46.25)18,19
159 IF (XD.EQ.11.25.OR.XD.EQ.21.25.OR.XD.EQ.32.50.OR.XD.EQ.42.50)18,19
C-----TAPE OUTPUT CONDITION CARD FOLLOWS. IOTAPE = 0 = NO OUTPUT
18 IOTAPE = 5
19 CONTINUE
IOTPT = 0
IF (IOTAPE .EQ. 5) IOTPT = 5
IF (M .EQ. IX1 + 1) IOTPT = 5
IF (XD.EQ.5.0.OR.XD.EQ.10.0.OR.XD.EQ.15.0.OR.XD.EQ.20.0.OR.XD.EQ.
130.0.OR.XD.EQ.40.0.OR.XD.EQ.50.0) IOTPT = 5
CALL B C
IF (IX1 .GT. 0) KK = 2
DO 5 K=KK,NEG
IF (X1 .EQ. 0.0 .OR. M .EQ. IX1 .OR. M .EQ. IX1+1) CALL SOURCE
CALL COEFF
CALL SOLVE
C-----CONTINUITY CORRECTION SECTION
DO 98 J=IZ1,IZ

```

```

PROGRAM DIFSN (CONT'D)

  98 O(J) = F(K,J)*U(J)
  CALL INTGRL (IZ1,IZ,O,DZ,WAT)
  TAW(K) = WAT
  IF (IX1 .GT. 0 .AND. M .GT. IX1) GO TO 97
  GO TO (37,34,39), K
  37 ZB(M) = EVAP
  GO TO 35
  34 AKBUM(M) = EVAP
  GO TO 35
  39 EVAP = -ZB(M)
  35 TOTAL(K) = TOTAL(K) + EVAP
  IF (IX1 .GT. 0) GO TO 42
  C-----LOWER LIMIT OF THE INTEGRATED WATER DROPLET CONCENTRATION PROFILE
  WDCLL = 0.05
  IF (K .EQ. 1 .AND. TOTAL(1) .LE. WDCLL) 43,42
  43 X1 = XD
  IX1 = M
  IOTPT = 5
  42 CONTINUE
  97 CONTINUE
  IS=1
  IF (IX1 .GT. 0 .AND. M .GT. IX1) EVAP = SPRAY
  IF (K.EQ.2) 70,71
  70 CONTINUE
  IS = IZ1
  WAT = WAT*ROC
  IF (IX1 .GT. 0 .AND. M .GT. IX1) EVAP = RLH
  71 DY = TOTAL(K) - WAT
  FDY = DY / TOTALI(K)
  YD(K) = DY
  FYD(K) = FDY
  PEVA(K) = EVAP
  GO TO 73

```

PROGRAM DIFSN (CONT'D)

```

72 DY = CORERR(K)
73 DEL = DY/DZ
  IF (K.EQ.2) DEL = DEL/ROC
  CALL CORRECT(15,DEL,CTOTAL(K),K)
  IF (K.EQ.2)CTOTAL(K) =CTOTAL(K) * ROC
  CORERR(K) = TOTAL(K) - CTOTAL(K)
  IF ( ABSF(CORERR(K)) .GT. 0.0001) GO TO 72
  FCRER(K) = CORERR(K)/ ABS(EVAP)
C-----SUPERSATURATION EVALUATION SECTION
  IF (IX1 .GT. 0 .AND. M .GT. IX1 .OR. K .NE. 3) GO TO 88
  DO 49 J=IZ1,IZ
  DUDZ(J) = DUDZM(J) = 0.0
  CALL SATURAT(F( 2,J),CHISAT(J))
  49 AKBU(J) = F(3,J) - CHISAT(J)
  L = 0
  LL = 0
  DO 85 J=IZ1,IZ
  SADJ = SADJT = 0.0
  IF (AKBU(J) .GT. 0.0) 80,85
  R0 ADJ = AKBU(J) / 2.0
  SADJ = SADJ + ADJ
  ADJT = ADJ * ALRC
  SADJT = SADJT + ADJT
  IF (J.NE. IZ1) F(1,J) = F(1,J) + ADJ
  F(3,J) = F(3,J) - ADJ
  F(2,J) = F(2,J) + ADJT
  CALL SATURAT (F(2,J),CHISAT(J))
  AKBU(J) = F(3,J) - CHISAT(J)
  L = L+1
  IF (L.EQ.1) IJ =J
  IF (ABS(AKBU(J)) .LT. 0.0001) 82,81
  R1 IF (AKBU(J) .GT. 0.0) 80,82
  R2 DUDZ(J) = SADJ
  DUDZM(J) = SADJT

```

PROGRAM DIFSN (CONT'D)

```

JJ = J
R5 CONTINUE
DO 20 I=IZ1,IZ
  O(I) = DUDZ(I)*U(I)
20 AKM(I) = DUDZM(I)*U(I)
  CALL INTGRL (IZ1,IZ,0,DZ,VAPADJ)
  CALL INTGRL (IZ1,IZ,AKM,DZ,ENG)
  ENGADJ = ENG * ROC
  IF (DUDZ(IZ1) * NE * 0.0) 23,24
23 O(IZ1) = 0.0
  CALL INTGRL (IZ1,IZ,0,DZ,ADJLIQ)
  GO TO 28
24 ADJLIQ = VAPADJ
28 TOTAL(1) = TOTAL(1) + ADJLIQ
  TOTAL(2) = TOTAL(2) + ENGADJ
  TOTAL(3) = TOTAL(3) - VAPADJ
  ZB(M) = ZB(M) + VAPADJ
  AKBUM(M) = AKBUM(M) + ENGADJ
  LL = L
  IF (IOTPT *EQ. 5) 86,99
R6 DO 26 L=1,3
  DO 90 J =IZ1,IZ
  IF (L*EQ.2) 87,89
R7 O(J) = F(2,J)
  GO TO 90
R9 N = IZ-J+1
  O(J) = O(N) = F(L,N) = F(L,J)
90 CONTINUE
  CALL OTPT (O,IZ1,IZ,L)
  IF (IOTAPE *EQ. 5) CALL TOTAPE (IOT,L)
  IUNIT = IUNIT1
  IF (L*EQ.2) IUNIT = IUNIT2
  WRITE (61,132) XD
  WRITE (61,138) L,TAW(L),IUNIT

```

```

PROGRAM DIFSN (CONT'D)

WRITE(61,133) PEVA(L),YD(L),FYD(L)
133 FORMAT (*,*,70X,*EVAP =*F12.4,5X*DY =*F12.4,5X*FDY =*F8.4)
WRITE(61,134)CTOTAL(L),IUNIT,CORERR(L),IUNIT,FCRER(L)
134 FORMAT (* *,*THE CORRECTED VALUE =*F12.4,A4*/M(Y) SEC*5X*THE ERROR
1 =*F12.4,A4*/M(Y) SEC*5X*THE FRACT ERROR WRT EVAP =*F8.4)
IF ( LL.EQ. 0 ) GO TO 26
DO 25 J=IZ1,IZ
25 O(J) = F(L,J)*U(J)
CALL INTGRL (IZ1,IZ,0,DZ,TOT)
IF (L.EQ.2) TOT = TOT * ROC
ERROR = TOT - TOTAL(L)
WRITE(61,140) TOT,IUNIT,ERROR,IUNIT
140 FORMAT(* *,*THE FINAL INTEGRATED VALUE =* .F12.4,A4* / M(Y) SEC*5X
1*THE ERROR =*F12.4,A4* / M(Y) SEC*)
26 CONTINUE
99 IF (LL.EQ. 0) GO TO 88
SUMS1 = SUMS1 + ADJLIG
WATLOS = WATLOS + DUDZ(IZ1)*U(IZ1)*DZ
88 CONTINUE
IF (IX1.GT. 0 .AND. M.GT. IX1) 92,93
92 IF (IOTPT.EQ.5 .OR. IOTAPE.EQ. 5) 83,91
83 DO 84 J=IS,IZ
84 O(J) = F(K,J)
CALL OTPT (O,IZ1,IZ,K)
IF (IOTAPE.EQ. 5) CALL TOTAPE (IOT,K)
91 CONTINUE
WRITE(61,132) XD
132 FORMAT (*0*,*AT X =*F8.4* M*)
IUNIT = IUNIT1
IF (K.EQ.2) IUNIT = IUNIT2
WRITE (61,138) K,WAT,IUNIT
138 FORMAT (* *,*THE INTEGRATED VALUE OF F(*I1*,J) X U(J) =*F12.4,A4*/
1 M(Y) SEC*)
PRINT 137,YD(K),FYD(K)

```

```

PROGRAM DIFSN (CONT'D)
177 FORMAT (*,*,70X,          *DY =*F12.4,5X*FDY =*F8.4)
    WRITE(61,134)CTOTAL(K),IUNIT,CORERR(K),IUNIT,FCRER(K)
93 CONTINUE
    GO TO (41,45,44),K
41 CONTINUE
    ML = 0
    DO 60 J=IZ1,IZ
    IF (F(1,J),GE,UBL) 59,60
59 ZUB(M) = Z(J)
    ML = J
60 CONTINUE
    IF (ML.EQ. 0) 57,58
57 ML = IZ1
    ZUB(M) = Z(IZ1)
58 AK(M) = ML
    GO TO 5
45 CONTINUE
C-----TEMPERATURE MODIFICATION OUTPUT
DELFMX = 0.0
    DO 95 J=IZ1,IZ
    O(J) = DELF(K,J) = F(K,J) - PI(K,J)
    IF (DELFMX.GT. DELF(K,J))96,95
96 DELFMX = DELF(K,J) $ ZTMX = Z(J) $ IZNODE = J
95 CONTINUE
    IF (XDELFMX.GT. DELFMX) 3,33
    3 XDELFMX = DELFMX $ XDMX = XD $ XZMX = ZTMX $ IXZNODE = IZNODE
33 CONTINUE
    IF (IOTPT.EQ. 0) GO TO 94
    PRINT 160,XD
160 FORMAT (*0TEMPERATURE MODIFICATION FROM THE INITIAL PROFILE AT THE
    1 INDICATED GRID POINTS FOR X =*F8.4* M*)
    CALL OTPT (O,IZ1,IZ,4)
94 PRINT 161,XD ,DELFMX,ZTMX, IZNODE
161 FORMAT (*0AT X =*F8.2,* M, THE MAXIMUM COOLING IS*,F6.2,* C AT Z

```

```

PROGRAM DIFSN (CONT'D)
      1=*F6.2,* M 1.E. NODE*14)
      GO TO 5
44 CONTINUE
      IF (IX1.EQ.0 .OR. M.EQ. IX1) 62.63
62 TOTALW = TOTAL(1) + TOTAL(3)
      GO TO 64
63 TOTALW = TOTAL(3)
64 IF(IOTPT.EQ.5) PRINT 112. TOTALW
      IF (IX1.GT.0 .AND. M.GT. IX1) GO TO 5
      IF(LL.EQ.0) 36.38
36 WRITE(61,139)
139 FORMAT (*0*.* NO SUPERSATURATION ADJUSTMENTS WERE REQUIRED*)
      GO TO 5
38 WRITE(61,122)
122 FORMAT (*0*.*TEMPERATURE ADJUSTMENT. C*)
      CALL OTPT (DUDZM,I,J,J,4)
      WRITE(61,124) ENGADJ,TOTAL(2)
124 FORMAT (*0*.*THE ENERGY ADJUSTMENT =*F12.4** CAL/ M(Y) SEC*5X*THE
      1 NEW TOTAL =*F12.4* CAL/ M(Y) SEC*)
      WRITE (61,123)
123 FORMAT (*0*.*WATER VAPOR ADJUSTMENT. G/ CU M*)
      CALL OTPT (DUDZ,I,J,J,4)
      WRITE(61,125) VAPADJ,TOTAL(3),TOTAL(1)
125 FORMAT (*0*.*THE VAPOR ADJUSTMENT. G/ M(Y) SEC*/ *THE VAPADJ TOT
      IAL =*F12.4,5X*THE NEW VAPOR TOTAL =*F12.4,5X*THE NEW LIQUID TOTAL
      2=*F12.4)
5 CONTINUE
      XU = XD
      IF (IX1.GT.0 .AND. M.GT. IX1+1) GO TO 10
      SUMEV = SUMEV + ZB(M)
      SUMFR = SUMFR + AKBUM(M)
      IF (M.EQ. IX1) 11.10
11 NJ = 0
      DO 27 J=1Z1,1ZM1

```

PROGRAM DIFSN (CONT'D)

```

F(3,J) = F(3,J) + F(1,J)
F(2,J) = F(2,J) - F(1,J)*ALRC
F(1,J) = 0.0
F(3,IZ1-NJ) = F(3,IZ1+NJ)
NJ = NJ+1
27 CONTINUE
  ZB(IX1+1) = -CTOTAL(1)
  AKBUM(IX1+1) = ZB(IX1+1)*ALFV
  TOTAL(2) = TOTAL(2) + AKBUM(IX1+1)
  TOTAL(3) = TOTAL(3) +CTOTAL(1)
10 CONTINUE
69 CONTINUE
  PRINT 101, X1
101 FORMAT (*1)THE ACTIVE EVAPORATION DISTANCE, X1, IS*F8.2* M*)
  PRINT 111, XD, XDMX, XZMX, IXZNODE
111 FORMAT (*0)THE MAXIMUM TEMPERATURE MODIFICATION WAS*F6.2* C AT X =*
  1F8.2* M AND AT Z =*F6.2* M I.E. NODE*14)
  WRITE(61,103) UBL
103 FORMAT(*0**UPPER BOUNDARY LIMITS FOR CONCENTRATIONS 0*,F6.3,* G/C
  1U M*)
  CALL OTPT (ZUR,1,IX1, 4)
  CALL INTGRL (1,IX1,ZUR,DX,VOL)
  VOL = VOL - Z(IZ1)*X1
  PRINT 114, VOL
114 FORMAT (*0)THE TOTAL VOLUME INVOLVED IN ACTIVE EVAPORATION =*F12.4*
  1 CU M/ M(Y)*
  AK(1) = IZ3
  WRITE (61,113)
113 FORMAT (*0** NODAL POSITIONS OF THE UPPER BOUNDARY LIMIT*)
  CALL OTPT (AK,1,IX1, 5)
  ZB(1) = 0.0
  AKBUM(1) = 0.0
  WRITE(61,116)
116 FORMAT (*0**EVAPORATION VALUES IN G/ M(Y) SEC*)

```

PROGRAM DIFSN (CONT'D)

```
NJ = IX1+1
CALL OTPT ( ZB ,1, NJ, 4)
WRITE(61,117) SUMEV
117 FORMAT(*0*,*THE TOTAL AMOUNT EVAPORATED =*F12.4,* G/ M(Y) SEC*)
WRITE (61,131)
131 FORMAT (*0*,*LATENT HEAT VALUES IN CAL/ M(Y) SEC*)
CALL OTPT (AKBUM,1, NJ, 4)
WRITE(61,130) SUMFR
130 FORMAT(*0*,*THE TOTAL LATENT HEAT USED =*F12.4,* CAL/ M(Y) SEC*)
FSUMS1 = SUMS1/TOTALI(1)
PRINT 102, SUMS1,FSUMS1
102 FORMAT (*0*THE WATER READJUSTED TO F(1,J) =*F12.4* G/M(Y) SEC*5X*TH
1E FRACTIONAL VALUE =*F12.4)
PCWAT = WATLOS /TOTALI(1)
PRINT 126, WATLOS,PCWAT
126 FORMAT (*0*THE AMOUNT OF WATER LOST =*F12.4* G/M(Y) SEC*5X*THE FRAC
TIONAL LOSS =*F12.4)
50 CONTINUE
END
```

```

SUBROUTINE CONST
COMMON XU,XD,XL,IX,INTG,ZMX,ZMN,ZZ,Z1,H,ROC,IZ,IZ1,IZ2,IZ3,NEQ,TI,
1Z2,Z3,AL,USTAR,VK,AC ,IZM1,DOM,DDP,DX,DZ,DTSTAR,USBK,DTLB,K,X1,ZT1,
2U( 201),UM( 201),IX1,RLH,OM( 201),Z( 201),AK( 201),AKM( 201),ZMS,
3DUDZ( 201),DUDZM( 201),AKBU( 201),AKBUM( 201),O( 201),ZUB( 201),
4EVEN,TSF,SPRAY,WATER,AXZ,TZ,UBL,F(3, 201),PI(3, 201),DELF(3, 201)
COMMON/SATBLK/ P,RDA,RV,CP,CPV,EPS,CHISAT(201),CHISTAR,CHIZ,ITI
COMMON/SOBLK/ZB(201),M,ALRC,ALEV,EVAP,ES(201),Q(201),RHOMA,C1,J
NEQ = 3
C1 = 0.02
AL = -1.66
USTAR = 0.28
DOM = .10
OMMX = 10.00
C------(H) = CAL/ (SQ CM * MIN)
H = 0.13
RHOMA = 1.15
C------(RHOMA) = KG/ CU M
ZZ = 0.0016
Z1 = 0.0005
Z2 = .4
ZMS = 0.6
Z3 = 0.80
ZT1 = 1.0
XD = XU = 0.0
X1 = 0.0
IX1 = 0
XL = 50.0
C------(ALEV) = CAL/ G
ALEV = 585.0
C------(SPRAY) = G/M SEC
SPRAY = 8.0
WATER = 0.0
C-----UBL = THE UPPER LIMIT OF THE MOISTURE CONCENTRATION PROFILE
UBL = 0.005
VK = 0.4

```

```

SUBROUTINE CONST (CONT'D)

C-----SATRLK CONSTANTS
C-----P) = PRESSURE IN MB
      P = 984.76
C-----CP) = CAL/(G * C)
      CP = 0.242
      CPV = 0.441
C-----RDA) = (RV) = CAL/( G * C)
      RDA = 0.068557
      RV = 0.110226
      EPS = 0.62197
C CALCULATIONS SECTION
C-----H) = CAL/ (SQ M * SEC)
      H = (H*10.**3)/6.
C-----ROC) = CAL/(CU M * C)
      ROC = RHOMA*CP*1000.
      ALRC = ALEV / ROC
      RLH = -SPRAY*ALEV
      AC = 1./(AL*AL)
C      DETERMINATION OF GRID POINTS
      DZ = -AL * DOM
      ZMX = -OMMX * AL
      ZMN = - ZMX
      IZ1 = (ABS(ZMN+Z1)/DZ+0.501)
      ZMN = -(Z1+IZ1*DZ)
      IZ1 = IZ1 + 1
      IZ = IZ1 + INT((ZMX - Z1)/DZ + .501)
      IZM1 = IZ - 1
      IZ2 = IZ1 + INT((Z2 - Z1)/DZ + .501)
      IZ3 = IZ1 + INT((Z3 - Z1)/DZ + .501)
      CALL ODDEVEN (IZ2, IZ3, EVEN)
      RETURN
      END

```

```

SUBROUTINE BEGIN
COMMON XU,XD,XL,IX,INTG,ZMX,ZMN,ZZ,Z1,H,ROC,IZ,IZ1,IZ2,IZ3,NEQ,TI,
IZ2,Z3,AL,USTAR,VK,AC,IZM1,DOM,DDP,DX,DZ,TSTAR,USBK,DTLB,K,X1,ZTI,
2U( 201),UM( 201),IX1,RLH,OM( 201),Z( 201),AK( 201),AKM( 201),ZMS,
3DUDZ( 201),DUDZM( 201),AKBU( 201),AKBUM( 201),O( 201),ZUB( 201),
4EVEN,TSF,SPRAY,WATER,AXZ,TZ,UBL,F(3, 201),PI(3, 201),DELF(3, 201)
C-----/SOBLK/ CANNOT BE USED IN THIS SUBROUTINE BECAUSE M IS USED DIFFERENTLY
C      IN THIS ROUTINE
      OM(1) = ZMN/AL
      Z(1) = ZMN
      USBK = USTAR/VK
      USKL = USTAR*VK*AL
      DOM2 = DOM/2.0
      DNOM = EXP(ZZ/AL)-1.0
      DO 10 J = 1,IZ1
      M = IZ -J + 1
      PT = 1.0 - EXP(OM(J))
      U(M)=U(J)=USBK*ALOG( (EXP(-OM(J))-1.0)/DNOM)
      AK(M) = AK(J) = USKL*PT * ALPHA(OM(J))
      AKBU(M) = AKBU(J) = AK(J)/U(J)
      DUDZ(M) = USBK/PT
      DUDZ(J)=- DUDZ(M)
      Z(M) = -Z(J)
      OM(M) = OM(J)
      IF(J.EG,IZ1) GO TO 11
      OM(J+1) = OM(J) - DOM
      Z(J+1) = Z(J) + DZ
      DDP = OM(J) - DOM2
      PT = 1.0 - EXP(DDP)
      N = M - 1
      UM(N)=UM(J)=USBK*ALOG((EXP(-DDP)-1.0)/DNOM)
      AKM(N) = AKM(J) = USKL* PT * ALPHA(DDP)
      AKBUM(N) = AKBUM(J) = AKM(J)/UM(J)
      DUDZM(N) = USRK/PT
      DUDZM(J) =-DUDZM(N)
      O(N) = O(J) = DDP

```

```
SUBROUTINE BEGIN (CONT'D)
```

```

10 CONTINUE
11 CONTINUE
   DUDZ(IZ1) = 0.0
   Z(IZ1) = Z1
   Z2 = Z(IZ2)
   Z3 = Z(IZ3)
   IZMS = IZ2+(ZMS-Z2)/DZ
   ZMS = Z(IZMS)
RETURN
END
```

```

SUBROUTINE TOTAPE (IOT,IK)
COMMON XU,XD,XL,IX,INTG,ZMX,ZMN,ZZ,Z1,H,ROC,IZ,IZ1,IZ2,IZ3,NEQ,TI,
IZ2,Z3,AL,USTAR,VK,AC ,IZM1,DOM,DDP,DX,DZ,TSTAR,USBK,DTLB,K,X1,ZTI,
ZU( 201),UM( 201),IX1,RLH,OM( 201),Z( 201),AK( 201),AKM( 201),ZMS,
3DUDZ( 201),DUDZM( 201),AKBU( 201),AKBUM( 201),O( 201),ZUB( 201),
4EVEN,TSF,SPRAY,WATER,AXZ,TZ,UBL,F(3, 201),PI(3, 201),DELF(3, 201)
   N = IZ - IZ1 + 1
   IF (IOT.EQ.1) 31,32
31 WRITE(20) N, (Z(J),J=IZ1,IZ)
   ENDFILE 20
32 WRITE(20) X1,XD,IK,(O(J),J=IZ1,IZ)
   ENDFILE 20
RETURN
END
```

```

SUBROUTINE I C
DIMENSION TPC(6),CMP(6)
COMMON XU,XD,XL,IX,INTG,ZMX,ZMN,ZZ,Z1,H,ROC,IZ,IZ1,IZ2,IZ3,NEG,TI,
I2,Z3,AL,USTAR,VK,AC ,IZM1,DOM,DDP,DX,DZ,TSTAR,USBK,DTLB,K,X1,ZTI,
2U( 201),UM( 201),IX1,RLH,OM( 201),Z( 201),AK( 201),AKM( 201),ZMS,
3DUDZ( 201),DUDZM( 201),AKBU( 201),AKBUM( 201),O( 201),ZUB( 201),
4EVEN,TSF,SPRAY,WATER,AXZ,TZ,UBL,F(3, 201),PI(3, 201),DELF(3, 201)
COMMON/SATBLK/ P,RDA,RV,CP,CPV,EPS,CHISAT(201),CHISTAR,CHIZ,ITI
COMMON/COEBLK/ A(201),B(201),C(201),QBU(201),PDPF(201),ALPHAH
C THIS SECTION IS FOR THE PROFILE OF MOISTURE
1 DO 10 J= IZ1,IZ
5 IF(J,LT,I22,OR,J,GE,I23) 5*6
5 F(1,J) = 0.0
GO TO 10
6 FW = FRCTN(Z(J)+DZ/2.0,Z2,ZMS,Z3,DZ)*SPRAY/U(J)
WATER = WATER + FW
F(1,J) = FW/DZ
10 CONTINUE
IT = IZ1-1
DO 40 J = 1,IT
40 F(1,IZ1-J) = F(1,IZ1+J)
WLB = F(1,1)
WUB = F(1,IZ)
IF (NEG.EQ.1) RETURN
C THIS SECTION IS FOR THE PROFILE OF TEMPERATURE
2 DTLB= -AL*H/(ROC*AK(IZ1))
ALPHAH = ALPHA(OM(IZ1))
TSTAR = -H/(USTAR*VK*ROC*ALPHAH)
TI = 22.5
TZ = TI - TSTAR*ALOG((EXP(ZTI/AL)-1.)/(EXP(ZZ/AL)-1.))
DO 20 J=1,IZ
IF(J,LT,IZ1)12,13
12 F(2,J) = 0.0
GO TO 20
13 IF (Z(J) .GT. 8.0) 14,15
14 F(2,J) = F(2,J-1)
GO TO 20

```

```

SURROUTINE I C (CONT'D)

15 F(2,J) = TZ+TSTAR*U(J)/USBK
20 CONTINUE
   TUB = F(2,IZ)
   IF (NEG.EQ.2) RETURN
C THIS SECTION IS FOR THE PROFILE OF WATER VAPOR CONCENTRATION
   CHII = 11.5
   ZB = Z(IZ + 1)
   IZTI = IZ1 + INT((ZTI - Z1)/DZ + 0.501)
   CALL SATURAT (TZ,CHIZ)
   CHIZ = CHIZ*0.8
   CHISTAR = (CHII - CHIZ) * USBK/ U(IZTI)
   DO 30 J=IZ1,IZ
   IF (Z(J) .GT. 8.0) 60,61
60 F(3,J) = F(3,J-1)
   GO TO 30
61 F(3,J) = CHIZ + CHISTAR*U(J) / USBK
   IF (Z(J) .LT. ZB) 31,30
71 CALL SATURAT(F(2,J),CHISAT(J))
   IF (F(3,J) .LE. CHISAT(J)) 30,32
72 F(3,J) = CHISAT(J)
   ZB = Z(J+1)
70 CONTINUE
   DO 41 J = 1,IT
41 F(3,IZ1-J) = F(3,IZ1+J)
   VLB = F(3,1)
   VUB = F(3,IZ)
   RETURN
C THIS IS THE BEGINNING OF B C
   ENTRY B C
   F(1,1) = WLB
   F(1,IZ) = WUB
   F(2,IZ) = TUR
   F(3,1) = VLB
   F(3,IZ) = VUB
   RETURN
   END

```

```

FUNCTION ALPHA(Y)
C-----ALPHA FROM LEICHTMANN AND PONOMAREVA
  IF(Y.LT.0.03) 1.2
    1 ALPHA = 0.8
    RETURN
    2 IF(Y.LT.0.8) 3.4
    3 ALPHA = 3.2* Y**0.35
    RETURN
    4 ALPHA = 3.0
    RETURN
  END

```

```

FUNCTION FRCTN (S,SB,SM,SE,DS)
  IF (SM .EQ. SE) GO TO 1
  IF (SM .EQ. SR) GO TO 2
  IF (S.LE.SM) 1.2
    1 FRCTN = 2.0*DS*(S-SB)/((SM-SB)*(SE-SB))
    RETURN
    2 FRCTN = 2.0*DS*(SE-S)/((SE-SB)*(SE-SM))
    RETURN
  END

```

```

SUBROUTINE SATURAT(T,CHIS)
COMMON/SOBLK/ZB(20),M,ALRC,ALEV,EVAP,ES(20),Q(20),RHOMA,C1,J
COMMON/SATBLK/ P,RDA,RV,CP,CPV,EPS,CHISAT(20),CHISTAR,CHIZ,ITI
ES(J) = EXP(ALEV*(1.0/273.16-1.0/( T +273.16)))/RV)* 6.11
WP = EPS* ES(J) / (P - ES(J))
WPP1 = 1.0/(1.0 + WP)
CHIS = RHOMA * WP * WPP1 * 1000.0
RETURN
END

```

```

SUBROUTINE CORRECT (IB,DEL,CTOTAL,L)
COMMON XU,XD,XL,IX,INTG,ZMX,ZMN,ZZ,Z1,H,ROC,IZ,IZ1,IZ2,IZ3,NEQ,TI,
IZ2,Z3,AL,USTAR,VK,AC ,IZM1,DOM,DDP,DX,DZ,TSTAR,USBK,DTLB,K,X1,ZTI,
ZU( 201),UM( 201),IX1,RLH,OM( 201),Z( 201),AK( 201),AKM( 201),ZMS,
3DUDZ( 201),DUDZM( 201),AKBU( 201),AKBUM( 201),O( 201),ZUB( 201),
4EVEN,TSF,SPRAY,WATER,AXZ,TZ,UBL,F(3, 201),PI(3, 201),DELF(3, 201)
SUM = 0.0
IF (K.EQ.2) 5,6
5 ISS = IZ1+1
O(IZ1) = F(K,IZ1) * U(IZ1)
GO TO 10
6 ISS = IZ1
10 IS = IS + 1
DO 200 I = ISS,IZM1
SUM = SUM + F(L,I)
200 CONTINUE
W = DEL/SUM
DO 205 I=IS,IZM1
F(K,I) = F(K,I) + F(L,I) * W/U(I)
O(I) = F(K,I) * U(I)
205 CONTINUE
O(IZ) = F(K,IZ) * U(IZ)
CALL INTGRL (IZ1,IZ,O,DZ,CTOTAL)
RETURN
END

SUBROUTINE ODDEVEN(N1,N2,E0)
IF(FLOAT((N2-N1)/2) .EQ. (FLOAT(N2)-FLOAT(N1))/2.0) 10,15
10 E0 = 2.0
RETURN
15 E0 = 1.0
RETURN
END

```

```

SUBROUTINE OTPT (Y,IB,IE,L)
DIMENSION Y(IE)
COMMON XU,XD,XL,IX,INTG,ZMX,ZMN,ZZ,Z1,H,ROC,IZ,IZ1,IZ2,IZ3,NEG,TI,
1Z2,Z3,AL,USTAR,VK,AC ,IZM1,DOM,DDP,DX,DZ,TSTAR,USBK,DTLB,K,X1,ZTI,
2U( 201),UM( 201),IX1,RLH,OM( 201),Z( 201),AK( 201),AKM( 201),ZMS,
3DUDZ( 201),DUDZM( 201),AKBU( 201),AKBUM( 201),O( 201),ZUB( 201),
4EVEN,TSF,SPRAY,WATER,AXZ,TZ,UBL,F(3, 201),PI(3, 201),DELF(3, 201)
GO TO (1,2,3,4,5),L
1 WRITE(61,102) XD
102 FORMAT(*1*,* LIGUID WATER CONCENTRATION, G / CU M, AT THE IND
1 ICATED GRID POINTS FOR X =*,F8.4,* M*)
GO TO 4
2 WRITE(61,103) XD
103 FORMAT(*1*,* TEMPERATURE PROFILE, C, AT THE IND
1 ICATED GRID POINTS FOR X =*,F8.4,* M*)
GO TO 4
3 WRITE(61,104) XD
104 FORMAT(*1*,* WATER VAPOR CONCENTRATION, G / CU M, AT THE IND
1 ICATED GRID POINTS FOR X =*,F8.4,* M*)
4 WRITE(61,101)(J,Y(J),J=IB,IF)
101 FORMAT(* *,8(2X,I4,F10.4)1X)
RETURN
5 WRITE(61,105)(J,Y(J),J=IB,IE)
105 FORMAT(* *,8(2X,I4,F10.0)1X)
RETURN
END

FUNCTION FSUM (Y,IS,IF)
DIMENSION Y(201)
FSUM = 0.0
DO 10 I = IS,IF
10 FSUM = FSUM + Y(I)
RETURN
END

```

```

SUBROUTINE SOURCE
DIMENSION D(201)
COMMON XU,XD,XL,IX,INTG,ZMX,ZMN,ZZ,Z1,H,ROC,IZ,IZ1,IZ2,IZ3,NEQ,TI,
1Z2,Z3,AL,USTAR,VK,AC,IZM1,DOM,DDP,DX,DZ,TSTAR,USBK,DTLB,K,X1,ZTI,
2U( 201),UM( 201),IX1,RLH,OM( 201),Z( 201),AK( 201),AKM( 201),ZMS,
3DUDZ( 201),DUDZM( 201),AKBU( 201),AKBUM( 201),O( 201),ZUB( 201),
4EVEN,TSF,SPRAY,WATER,AXZ,TZ,UBL,F(3, 201),PI(3, 201),DELF(3, 201)
COMMON/SOBLK/ZB(201),M,ALRC,ALEV,EVAP,ES(201),Q(201),RHOMA,C1,J
COMMON/SATBLK/ P,RDA,RV,CP,CPV,EPS,CHISAT(201),CHISTAR,CHIZ,ITI
COMMON/COEBLK/ A(201),B(201),C(201),QBU(201),PDPF(201),ALPHAH
GO TO (1,2,3),K
1 IF (X1 .GT. 0.0 .AND. M .EQ. IX1+1) 25.11
11 DO 10 J=IZ1,IZ
CALL SATURAT (F(2,J),CHIS)
CHISAT(J) = CHIS
Q(J) = C1 * ( CHIS - F(3,J))
IF (F(1,J) .LE. Q(J))*DX/U(J) 4.5
4 Q(J) = -F(1,J)*U(J)/(DX*2.0)
GO TO 9
5 Q(J) = -Q(J)
9 QBU(J) = Q(J)/U(J)
10 CONTINUE
Q(IZ) = 0.0
CALL INTGRL (IZ1,IZ,Q,DZ,EVTOT)
EVAP = EVTOT * DX
IF (M .EQ. 2) 6.7
6 A1 = -C1*ALEV*P/(RHOMA*CP*RV*41.8684)
A2 = ALEV*0.0418684
A3 = 1.0 - EPS
7 CONTINUE
DO 15 J=IZ1,IZM1
D(J) = (A2*CHISAT(J)/(P-A3*ES(J)) + 1.0/A3)
PDPF(J) = (A1/(U(J))*(F(2,J)+273.16)**2)*D(J)
15 CONTINUE
GO TO 24

```

```

SUBROUTINE SOURCE (CONT'D)
C-----SOURCE TERM FOR HEAT
  2 IF (X1 .GT. 0.0 .AND. M .EQ. IX1+1) RETURN
    DO 20 J = IZ1, IZM1
      QBU(J) = QBU(J)*ALRC
      EVAP = EVAP + ALEV
    GO TO 24
C-----SOURCE TERM FOR WATER VAPOR DIFFUSION
  3 IF (X1 .GT. 0.0 .AND. M .EQ. IX1+1) RETURN
    DO 30 J = IZ1, IZM1
      PDPF(J) = -C1*A3*D(J)/U(J)
      QBU(J) = -QBU(J)/ALRC
    24 CONTINUE
      QBU(IZ1-1) = QBU(IZ1+1)
      PDPF(IZ1-1) = PDPF(IZ1+1)
    RETURN
  25 DO 26 J = IZ1, IZ
    26 QBU(J) = 0.0
      QBU(IZ1-1) = QBU(IZ1+1)
    RETURN
  END

```

```

SUBROUTINE COEFF
DIMENSION D(201),R(201),S(201),G1(201),G2(201),G3(201),G4(201)
COMMON XU,XD,XL,IX,INTG,ZMX,ZMN,ZZ,Z1,H,ROC,IZ,IZ1,IZ2,IZ3,NEQ,TI,
IZ2,Z3,AL,USTAR,VK,AC ,IZM1,DOM,DDP,DX,DZ,TSTAR,USBK,DTLB,K,X1,ZTI,
ZU( 201),UM( 201),IX1,RLH,OM( 201),Z( 201),AK( 201),AKM( 201),ZMS,
3DUDZ( 201),DUDZM( 201),AKBU( 201),AKBUM( 201),O( 201),ZUB( 201),
4EVEN,TSF,SPRAY,WATER,AXZ,TZ,UBL,F(3, 201),PI(3, 201),DELF(3, 201)
COMMON/SOBLK/ZB(201),M,ALRC,ALEV,EVAP,ES(201),Q(201),RHOMA,C1,J
COMMON/COEBLK/ A(201),B(201),C(201),QBU(201),PDPF(201),ALPHAH
GO TO (1,2,1),K
1 NS = 2
GO TO 25
2 NS = IZ1+1
25 CONTINUE
5 IF (M.EQ.2.AND.K.EQ.1) 5,11
5 T = 1.0/(DOM*DOM)
P1 = .125/DX
P2 = .75/DX
P3 = P1
DO 10 I = NS, IZM1
P4 = AC*AKBUM(I)*T*(1+DOM*DUDZM(I))/(6.*UM(I))
P5 = AC*AKBU(I)*DUDZ(I)/(3.*DOM*U(I))
P6 = AC*AKBUM(I-1)*T*(DOM*DUDZM(I-1))/(6.*UM(I-1))-1.)
D(I) = P2-P6+P4
R(I) = (P4+P5-P1)
S(I) = -(P3+P5+P6)
10 CONTINUE
11 IF (IX1 .GT. 0 .AND. M .GT. IX1+1) 30,12
12 CONTINUE
12 IF (IX1 .GT. 0 .AND. M .EQ. IX1+1) 13,14
13 DO 16 J = IZ1,IZM1
G1(J) = G2(J) = G3(J) = 0.0
G4(J) = 0.0
16 CONTINUE
GO TO 17
14 DO 15 J = IZ1,IZM1

```

```

SUBROUTINE COEFF (CONT'D)

  G1(J) = P1*DX*PDPF(J+1)
  G2(J) = P2*DX*PDPF(J)
  G3(J) = P3*DX*PDPF(J-1)
  G4(J) = (P1*(OBU(J+1)*F(K,J+1)) + P2*(OBU(J)-PDPF(J))*F(K
    1,J)) + P3*(OBU(J-1)-PDPF(J-1))*F(K,J-1))*DX
15 CONTINUE
17 IF (K.EQ. 2) GO TO 46
  IT = IZ1 - 1
  DO 45 J = 1,IT
    G1(IZ1-J) = G1(IZ1+J)
    G2(IZ1-J) = G2(IZ1+J)
    G3(IZ1-J) = G3(IZ1+J)
    G4(IZ1-J) = G4(IZ1+J)
45 CONTINUE
46 CONTINUE
  DO 20 I=NS,IZM1
    DEN = D(I) - G2(I)
    A(I) = (R(I) + G1(I))/DEN
    B(I) = (S(I) + G3(I))/DEN
    C(I) = (P1*(K,I+1) + P2*(K,I) + P3*(K,I-1) + G4(I))/DEN
20 CONTINUE
  RETURN
30 DO 35 I = NS,IZM1
  C(I) = (P1*(K,I+1) + P2*(K,I) + P3*(K,I-1) ) /D(I)
35 CONTINUE
  RETURN
  END

```

```

SUBROUTINE SOLVE
DIMENSION R( 201),S( 201)
COMMON XU,XD,XL,IX,INTG,ZMX,ZMN,ZZ,Z1,H,ROC,IZ,IZ1,IZ2,IZ3,NEQ,TI,
IZ2,Z3,AL,USTAR,VK,AC ,IZM1,DOM,DDP,DX,DZ,TSTAR,USBK,DTLB,K,X1,ZT1,
2U( 201),UM( 201),IX1,RLH,OM( 201),Z( 201),AK( 201),AKM( 201),ZMS,
3DUDZ( 201),DUDZM( 201),AKBU( 201),AKBUM( 201),O( 201),ZUB( 201),
4EVEN,TSF,SPRAY,WATER,AXZ,TZ,UBL,F(3, 201),PI(3, 201),DELF(3, 201)
COMMON/COEBLK/ A(201),B(201),C(201),QBU(201),PDPF(201),ALPHAH
C THIS SUBROUTINE SOLVES EQUATIONS OF THE FORM
C  $F(I) = A(I)*F(I+1) + B(I)*F(I-1) + C(I)$ 
C BY GAUSSIAN ELIMINATION
C R = A PRIME AND S = B PRIME
C GO TO (1,2,1), K
1 NS = 2
NT = IZM1
GO TO 20
2 NS = IZ1+1
NT = IZ1-1
20 NSP1 = NS + 1
R(NS) = A(NS)
S(NS) = B(NS)*F(K,NS-1) + C( NS)
DO 48 I = NSP1,IZM1
T = 1./((1.-B(I))*R(I-1))
R(I) = A(I)*T
S(I) = (B(I)*S(I-1))+C( I))*T
48 CONTINUE
DO 50 I = 2,NT
J = IZM1 - I + 2
50 F(K,J) = R(J)*F(K,J+1) + S(J)
IF (K .NE. 2) RETURN
12 F(K,IZ1) = F(K,IZ1+1) + TSTAR * (U(IZ1) - U(IZ1+1))/ USBK
RETURN
END

```

```

SUBROUTINE INTGRL (IL,IU,Y,DEL,TOTAL)
DIMENSION Y(IU)
TOTAL = 0.0
      C   INTEGRATION BY SIMPSONS RULE
      IF (IL.GT.IU) 7.8
7 WRITE(61,100)
100 FORMAT (*0*,*INTGRL WAS CALLED WITH THE LOWER LIMIT GREATER THAN
      !THE UPPER LIMIT*)
      RETURN
8 IF (IL.EQ.IU) 5.6
5 TOTAL = Y(IL)*DEL
      RETURN
6 IF((IU-IL).EQ.1) 1.2
1 TOTAL = (Y(IU) + Y(IL))*DEL/2.0
      RETURN
2 IF((IU-IL).EQ.2) 3.4
3 TOTAL =(Y(IL)+4.0*Y(IL+1) + Y(IU))*DEL/3.0
      RETURN
4 CALL ODDEVEN (IL,IU,EV)
      IF(EV .EQ. 2.0) 10.15
10 J = IU-3
      GO TO 20
15 J=IU-2
20 CONTINUE
      DO 200 I=IL,J,2
TOTAL = TOTAL + 2.0*Y(I+1) + Y(I+2)
200 CONTINUE
      IF(EV .EQ. 2.0) 30.31
30 TOTAL = (2.0*TOTAL+Y(IL) + Y(IU) + 4.0*Y(IU-1))*DEL/3.0
      RETURN
71 TOTAL = (2.0*TOTAL+Y(IL) + 5.0*Y(IU))*DEL/3.0-DEL*Y(IU)
      RETURN
      END
!RUN,3.00,3000
      G CAL

```

LIST OF REFERENCES

LIST OF REFERENCES

- Breasbois, L. and Nurnberger, F. V., (1970). Program GRAPHL Documentation, Michigan State University Computer Science Library Program No. 00000 494.
- Brooks, F. A., (1961). Need for Measuring Horizontal Gradients in Determining Vertical Eddy Transfers of Heat and Moisture. J. Meteorol. Vol. 18, 589-596.
- Brown, K. W. and Rosenberg, Norman J., (1971). Turbulent Transport and Energy Balance as Affected by a Windbreak in an Irrigated Sugar Beet (*Beta vulgaris*) Field. Agronomy Journal, Vol. 63, No. 3, 351-355.
- Calder, K. L., (1939). A Note on the Constancy of Horizontal Turbulent Shearing Stress in the Lower Layers of the Atmosphere. Quart J. Roy. Meteorol. Soc. v. of 65, 537-541.
- Carolus, R. L., (1965). Influence of Plant Water Stress Reduction by "Air-Conditioning" Irrigation on Seedling Survival, Flower Retention, Development, Yield, and Quality of Vegetables. Abs. of 62nd Annual Meeting of A.S.H.S. Paper No. 71.
- Carolus, R. L., (1969). Evaporating Cooling Techniques for Regulating Plant Water Stress. Proc. Symposium of the American Society Hort. Sci., Pullman Washington.
- Carolus, R. L., Erickson, A. E., Kidder, E. H., and Wheaton, R. F., (1965). Interaction of Climate and Soil Moisture on Water Use, Growth and Development of Tomatoes. Mich. Agr. Expt. Sta. Quart. Bul. 47, No. 4, pp. 542-581.
- Charnock, H., (1967). Comments on "An Examination of Three Wind-Profile Hypotheses," J. Appl. Meteor., Vol. 6, No. 1, 211-212.
- Crank, J., (1956). The Mathematics of Diffusion, Oxford Press, London.

- Deacon, E. L., (1959). The Measurements of Turbulent Transfer in the Lower Atmosphere, Adv. Geophys. Vol. 6 (Atmospheric Diffusion and Air Pollution), 211-288.
- deVries, D. A., (1959). The Influence of Irrigation on the Energy Balance and the Climate Near the Ground, J. Met., Vol. 16, 259.
- Dyer, A. J., (1962). The Adjustment of Profiles and Eddy Fluxes. Quar. J. Royal Meteorol. Soc. Vol. 89, 1963, pp. 276-280.
- Ellison, T. H., (1957). Turbulent Transfer of Heat and Momentum from an Infinite Rough Plane, J. Fluid Mech., Vol. 2, No. 5, 456-466.
- Geiger, R., (1965). The Climate Near the Ground, Harvard University Press, Cambridge, Mass.
- Gurvich, A. S., (1965). Vertical Wind-Velocity and Temperature Profiles in the Atmospheric Surface Layer, Izvestiya, Atmos. and Oceanic Phys. Vol. 1, No. 1., 55-65.
- Harrington, J. B., Jr., (1965). Final Report Atmospheric Pollution by Aeroallergens: Meteorological Phase (1 March 1962 to 28 February 1965) Vol. 11 Atmospheric Diffusion of Ragweed Pollen in Urban Areas: Test ORA project 06342, University of Michigan, Ann Arbor.
- Hess, S. L., (1959). Introduction to Theoretical Meteorology, Holt, Rinehart and Winston, New York.
- Himmelblau, D. M., (1970). Process Analysis by Statistical Methods, John Wiley & Sons Inc., New York-London-Sydney-Toronto.
- Huschke, R. E., (1959). Glossary of Meteorology, American Meteorological Society, Boston, Mass.
- Jaffe, S., (1967). A Three-Layer Diffusion Model as Applied to Unstable Atmospheric Conditions, Journal of Applied Meteorology, Vol. 6, No. 2, 297-302.
- Kazansky, A. B. and Monin, A. S., (1956). Turbulence in Surface Layer Inversions, Akademiia Nauk SSSR, Izves. Ser Geophys. No. 1, 86.

- Leichtmann, D. L. and Ponomareva, S. M., (1969). On the Ratio of the Turbulent Transfer Coefficients for Heat and Momentum in the Surface Layer of the Atmosphere, *Izvestiya, Atmos. and Oceanic Phys.*, Vol. 5, No. 12, 1245-1250.
- Lettau, H. and Davidson, B., (1957). Exploring the Atmosphere's First Mile, Vols. 1-2, Pergammon Press, London-New York-Paris.
- List, R. J., (1966). Smithsonian Meteorological Tables, 6th Rev. Ed. Smithsonian Miscellaneous Collections Vol. 114, Smithsonian Institution, Washington, D.C.
- Lumley, J. L. and Panofsky, H. A., (1964). The Structure of Atmospheric Turbulence, Interscience Publ., New York-London-Sydney.
- Milburn, R. H., (1957). Theory of Evaporating Water Clouds, *Jour. of Colloid Sci.*, Vol. 12, 378-388.
- Milburn, R. H., (1958). Theory of Turbulent Evaporating Clouds, *Jour. of Colloid Sci.*, Vol. 13, 114-124.
- Monin, A. S., (1956). Turbulent Diffusion in the Atmospheric Surface Layer, *Akademiia Nauk SSSR, Izves.*, Ser. Geophys. No. 12, 1461-1473.
- Monin, A. S. & Obukhov, A. M., (1954). Basic Laws of Turbulent Mixing in the Ground Layer of the Atmosphere. *Geophys. Inst. Acad. Sci. U.S.S.R.* Vol. 24, No. 151, 163-187 (English Translation From the Russian by Am. Meteorol. Soc. T-T-174, AF (19 (604)-1936).
- Monin, A. S. and Yaglom, A. M., (1971). Statistical Fluid Mechanics: Mechanics of Turbulence. Vol. 1, The MIT Press, Cambridge, Mass. and London, Eng.
- Munn, R. E., (1966). Descriptive Micrometeorology, Advances in Geophysics, Supplement 1, Academic Press, New York and London.
- Okuyama, M. and Zung, J. T., (1967). Evaporation-Condensation Coefficient for Small Droplets, *Jour. of Chem. Phys.* Vol. 46, No. 5, 1580-1585.

- Panofsky, H. A., (1961). An Alternative Derivation of the Diabatic Wind Profile, Quart. Jour. Roy. Meteor. Soc., Vol. 87, No. 374, 597-601.
- Panofsky, H. A., (1963). Determination of Stress from Wind and Temperature Measurements, Quart. Jour. Roy. Meteor. Soc., Vol. 89, No. 37, 85-93.
- Panofsky, H. A., Blackadar, A. K., and McVehil, G. E., (1960). The Diabatic Wind Profile, Quart. Jour. Roy. Meteor. Soc., Vol. 86, No. 369, 390-398.
- Panofsky, H. A. and Townsend, A. A., (1964). Change of Terrain Roughness and the Wind Profile, Quart. Jour. Roy. Meteor. Soc. Vol. 90, 1964, 147-155.
- Pasquill, F., (1962). Atmospheric Diffusion, D. Van Nostrand Publ., London-Toronto-New York-Princeton.
- Philip, J. R., (1959). The Theory of Local Advection, Jour. of Meteor., Vol. 16, No. 10, 535-547.
- Priestly, C. H. B., (1955). Free and Forced Convection in the Atmosphere near the Ground, Quart. Jour. Roy. Meteor. Soc., Vol. 81, No. 348, 139-143.
- Priestly, C. H. B., (1959). Turbulent Transfer in the Lower Atmosphere, 130 pp. University of Chicago Press, Chicago, Ill.
- Richtmyer, R. D. and Morton, K. W., (1967). Difference Methods for Initial-Value Problems, Interscience Tracts in Pure and Applied Mathematics, No. 4, 2nd ed., Interscience Publ., New York-London-Sydney.
- Rider, N. E., Philip, J. R. and Bradley, E. F., (1964). The Horizontal Transport of Heat and Moisture--A Micrometeorological Study, Quart. Jour. Roy. Meteor. Soc., Vol. 89, No. 382, 507-531.
- Seller, W. D., (1962). A Simplified Derivation of the Diabatic Wind Profile, Jour. of Atmosph. Sci. Vol. 19, No. 2, 180-184.
- Smith, G. D., (1965). Numerical Solution of Partial Differential Equations, Oxford University Press, New York and London.

- Spalding, D. B. and Patanker, S. V., (1968). Heat and Mass Transfer in Boundary Layers, 138 pp., C.R.C. Press: Cleveland.
- Stewart, D. W. and Lemon, E., (1969). The Energy Budget at the Earth's Surface: A Simulation of Net Photosynthesis of Field Corn. Ecom. US Army Elec. Com. Atmos. Sci. Lab., Fort Hauchuca, Ariz., p. 84.
- Sutton, O. G., (1953). Micrometeorology, McGraw-Hill, New York-Toronto-London.
- Swinbank, W. C., (1964). The Exponential Wind Profile, Quart. Jour. Roy. Meteor. Soc., Vol. 90, No. 384, 119-135. (1966) Discussion on the paper "Exponential Wind Profile," Quart. Jour. Roy. Meteor. Soc., Vol. 92, No. 393, 416-426.
- Swinbank, W. C., (1968). A Comparison between Predictions of Dimensional Analysis for the Constant Flux Layer and Observations in Unstable Conditions, Quart. Jour. Roy. Meteor. Soc., Vol. 94, No. 402, 460-467.
- Timofeev, M. P., (1954). The Change of the Meteorological Regime During Irrigation, IZV. Akad. Nauk. SSSR, Ser. Geophys., No. 2, pp. 108-113.
- Van Den Brink, C. and Carolus, R. L., (1965). Removal of Atmospheric Stresses from Plants by Overhead Sprinkler Irrigation, Quart. Bulletin of the Mich. Agr. Exp. Sta. Mich. State Univ., E. Lansing, Mich., Vol. 47, No. 3, 358-363.
- Waggoner, P. E., et al., (1965). Agricultural Meteorology, Meteorological Monographs Vol. 6, No. 28, American Meteor. Soc., Boston, Mass.
- Webb, E. K., (1960). An Investigation of the Evaporation from Lake Eucumbene, C.S.I.R.O., Div. Meteor. Phys., Techn. Pap. No. 10, Melbourne.
- Yamamoto, G., (1959). Theory of Turbulent Transfer in Non-neutral Conditions, Jour. Meteor. Soc. Japan, Vol. 37, No. 2, 60-69.
- Yordanov, D. L., (1966). On Diffusion from a Point Source in the Atmospheric Surface Layer, IZV., Atmos. and Ocean. Phys., Vol. 2, No. 6, 348-352.

- Yordanov, D. L., (1967). Diffusion in the Direction of the Wind and some Asymptotic Formulas of Diffusion in the Surface Layer of the Atmosphere, *Izv., Atmos. and Ocean. Phys.* Vol. 3, No. 8, 474-478.
- Yordanov, D. L., (1968). The Diffusion of a Contaminant from a Linear Source in the Layer close to the Ground Surface in the Case of an Unstable Stratification, *Izv., Atmos. and Ocean. Phys.*, Vol. 4, No. 6, 386-387.
- Zilitinkevich, S. S., Leichtmann, P. L., and Monin, A. S., (1967). Dynamics of the Atmospheric Boundary Layer, *Izv., Atmos. and Ocean. Phys.*, Vol. 3, No. 3, 170-191.
- Zung, J. T., (1967,a). Evaporation Rate and Lifetimes of Clouds and Sprays in Air--The Cellular Model, *Jour. of Chem. Phys.*, Vol. 46, No. 6, 2064-2070.
- Zung, J. T., (1967,b). Evaporation Rates and Lifetimes of Clouds and Sprays in Air, II. The Continuum Model, *Jour. of Chem. Phys.*, Vol. 47, No.9, 3578-3581.
- Zung, J. T., (1968). Evaporation Rates and Lifetimes of Clouds and Sprays in Air. III. The Effects of Cloud Expansion, *Jour. of Chem. Phys.*, Vol. 48, No. 11, 5181-5186.

MICHIGAN STATE UNIV. LIBRARIES



31293101186678